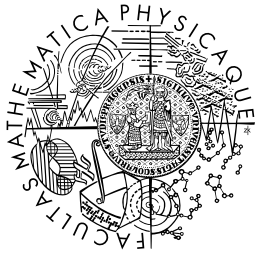

FACULTY
OF MATHEMATICS
AND PHYSICS
Charles University

DOCTORAL THESIS

Marek Radecki

Spectroscopic Study of the Dynamical Behavior and Interactions in Supramolecular and Macromolecular Systems

Department of Macromolecular Physics

Supervisor of the doctoral thesis:	Doc. RNDr. Lenka Hanyková, Dr.
Study programme:	Physics
Study branch:	Biophysics, Chemical and Macromolecular physics (4F4)

Prague 2018

I declare that I carried out this doctoral thesis independently, and only with the cited sources, literature and other professional sources.

I understand that my work relates to the rights and obligations under the Act No. 121/2000 Sb., the Copyright Act, as amended, in particular the fact that the Charles University has the right to conclude a license agreement on the use of this work as a school work pursuant to Section 60 subsection 1 of the Copyright Act.

In Prague, 20^{th} of August signature of the author

My greatest thanks belong to my supervisor, Lenka Hanyková, her endless patient, encouragement, understanding and support as well as leading, many advices, help and consultations on my sometimes too long way to understand how to look at the results, recognize the death-ends or what is important. Thanks to her I learnt how to write scientific articles, manuscripts, the thesis and present the results. I thank Jiří Spěváček for his ideas regarding the NMR measurements, Ivan Krakovský for his help with DSC measurements, my colleague and classmate Julie Šťastná and my dear friend David Píša for his help with LaTeXtables.

I would like to thank my mother Jindřiška and father Bruno for their support and also occasional pressure I needed to complete the tasks, but no less for them as my life role models and people who always believed I can success on the best university they know.

Love and warm thanks to my wife Beatka, my closest friend and superpower mother to our two children Majda and Rostík. Although sometimes tired because of them and me, she always has stayed by my side beside her own studies. Swear we are going to spend more time together.

Thanks God I have you. Cannot tell, how I appreciate all your help and patience!

Title: Spectroscopic Study of the Dynamical Behavior and Interactions

in Supramolecular

and Macromolecular Systems

Author: Marek Radecki

Department: Department of Macromolecular Physics

Supervisor: Doc. RNDr. Lenka Hanyková, Dr., Department of Macromolecular Physics

Abstract: In this thesis, the temperature-induced phase transition in liner polymer solutins and hydrogels of semi-interpenetrating (SIPNs) and interpenetrating (IPNs) polymer networks was studied with respect to various composition, network architecture and procedure. Thermoresponsive linear polymers based on poly(vinyl methyl ether) (PVME) in water and with terc-buthyl based additives, IPNs of polyacrylamide (PAAm), poly(*N*–isopropylacrylamide) (PNIPAm), poly(*N*–vinylcaprolactam) (PVCL) and IPNs and SIPNs of poly(*N,N*–diethylacrylamide) (PDEAAm) were investigated by the methods of nuclear magnetic resonance spectroscopy (NMR), differential scanning calorimetry (DSC), optical microscopy (OM) and swelling experiments. The effect of polymer concentration and presence of additives on the dynamics during the phase separation as well as interactions between the water and the polymer in aqueous solutions of PVME and PVME/additives were established. The increasing content of hydrophilic PAAm component in SIPNs and IPNs shifts the transition toward higher temperatures and fraction of polymer units with significantly reduced mobility as well as the enthalpy change, are reduced. The macroscopic transition parameters such as critical temperature, temperature range and transition extent and microscopic behavior of individual polymer groups are influenced by the architecture and reverse sequence in the preparation of IPNs and SIPNs. For the most of studied hydrogels, a part of water molecules bound to collapsed structures was detected showing restricted mobility.

Keywords: polymer hydrogel, interpenetrating networks, polymer solution, phase transition, NMR

Contents

Introduction

In the last years polymer networks swollen in water, so called smart hydrogels, have been widely studied for their attractive properties. They exhibit drastic changes in their properties in response to the external parameters like solvent composition, temperature, pH etc., as a consequence of the volume phase transition. Due to stimuli–responsive properties of smart hydrogels, several potential applications in drug delivery systems, bioseparation, artifical muscles, microfluidics, tissue engineering and micro/nanoactuators, etc., were suggested. The phenomenon of phase transition in hydrogels is on molecular level similar with phase separation in aqueous solutions of linear polymers which exhibit lower critical solution temperature.

This thesis deals with phase separation of linear poly(vinyl methyl ether) (PVME) in water and of the phase transition of semi- (SIPNs) and fully interpenetrating networks (IPNs) hydrogels based on poly(*N*–isopropylacrylamide) (PNIPAm), polyacrylamide (PAAm), poly(*N,N*–diethylacrylamide) (PDEAAm) and poly(*N*–vinylcaprolactam) (PVCL) swollen in water. The aim of our work is to characterize influence of structures and interactions in aqueous solutions and hydrogels on the parameters of their phase transition and physical properties. This study can improve the understanding of the phase transition on molecular level which can be useful in designing materials with specific properties for applications.

Basic introduction of this theme is presented in the chapter 1 as well as of the main experimental techniques used in this study. Chapter 2 summarizes the overview of publications on studied polymer solutions and hydrogels. Main aims are presented in chapter 3. Samples preparation and settings of experiments that we used is noted in chapter 4. Results and discussion are divided in four chapters, depending on the studied samples - PVME solutions with or without additives are studied in chapters 5 and 6, respectively, chapter 7 deals with IPNs of PNIPAm, PAAm and PVCL and chapter 8 describes IPNs and SIPNs of PDEAAm. The thesis is ended by the conclusions and the lists of cited bibliography, abbreviations and also by the list of publications and presentations of results related to this thesis and presented at various conferences.

1. Theory

1.1 Polymer Overview

1.1.1 Polymers

Polymeric materials are well known for a long time as the rubber was used by Olmec civilization 1600 BC and then Mayans in nowdays Latin America. It was even processed the sap by boiling to create the balls to play games. Then it was taken to Europe by French explorer in 1736 and got the name by Joseph Priestly, who tried to rubbing off pencil symbols writen on paper [1].

As rubber example shows, polymeric materials are flexible and easy moldable. They are consisting of many monomeric units, even up to 1010 for DNA molecule in human bodies. Their large molecular mass produces unique physical properties, including toughness, viscoelasticity, and a tendency to form glasses and semi-crystalline structures.

There are two terms to describe such a long molecules. Oldest term is "polymer" for the first time used by Berzelius in 1833, although it was not used in today meaning connected to the length. Second term "macro+molecules" was introduced by Nobel laureate Hermann Staudinger in 1920. He is so-called father of the polymer chemistry, because the era of the polymer science began by his article "Über Polymerization" in this year, although the first synthetic polymer bakelite was in 1907 made by Leo Baekeland [2].

From the origin point of view we distinguish:

1. natural polymers – as rubber, silk fibers, starch, cellulose, chitin, DNA or generally proteins, tissues, membranes

2. synthetic polymers – made artificially mostly in huge industrial amounts as polyvinyl chloride, polystyrene, polypropylene, polyethylene, teflon, nylon, etc.

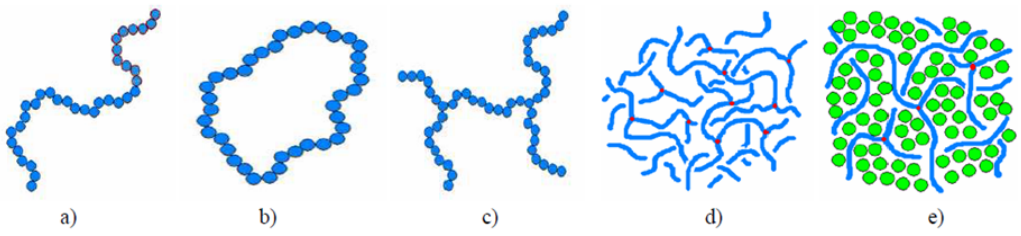

Figure 1.1: Different types of polymers: a) linear, b) cyclic, c) branching, d) polymer network, e) polymer hydrogel in water. Taken over from [3].

From the architekture point of view we can divide polymers as (see Fig. 1.1):

1. linear polymers – only main chain presented,

2. cyclical,

3. branching polymers – polymer chain has branch points that connect three or more polymer segments,

4. polymer networks – branching polymers form one molecule,

5. polymer hydrogel – polymer networks with solvent.

Copolymer consists of two or more different types of monomeric units. There are many ways to bind different types of monomers. Results can be then:

1. statistical and their special case – random, where the probability of finding a certain monomeric unit at any given place in the chain is independent of the origin of the neighboring units

2. n-blocked – when short blocks of each type/s are synthetized

3. grafted or comber as a special example

1.1.2 Polymer Hydrogels

Polymer hydrogels form three-dimensional structures with the ability to absorb large amounts of water while maintaining their dimensional stability [4]. They have a porous microstructure that holds a huge quantity of water, resulting in a wet and soft nature resembling biological tissues.. The integrity of hydrogels in their swollen state is maintained by either physical or chemical crosslinking [5]. Chemically crosslinked networks have permanent junctions, while physical networks have transient junctions that arise from either polymer chain entanglements or physical interactions such as ionic interactions, hydrogen bonds, or hydrophobic interactions [6]. Polymer hydrogels could consist of networks of linear homopolymers, linear copolymers, and block or graft copolymers; polyion–polyion or H-bonded complexes; hydrophilic networks stabilized by hydrophobic domains; and interpenetrating polymer networks (IPNs) or physical blends. Hydrogels can be separated into two groups on the basis of their natural or synthetic origins [7]. Hydrogel-forming natural polymers include proteins such as collagen and gelatin, and polysaccharides such as alginate and agarose. Synthetic polymer hydrogels are prepared using chemical polymerization methods.

Hydrogels have been of great interest to material scientists for many years since the pioneering work of Wichterle and Lim in [8] on crosslinked 2-hydroxyethyl methacrylate hydrogels. Lower interfacial tension, soft and tissue like physical properties, higher permeability to undersized molecules, and release of entrapped molecules have made hydrogels a focus of exploration in different fields [9], [10]. The so-called smart hydrogels are capable of responding to the changes in temperature, pH, humidity, light, specific ions or molecules, electrical fields, solvent and ionic strength. Smart hydrogels have been used in diverse applications, such as in making actuators [11] and valves [12], in the immobilization of enzymes and cells [13], in sensors [14], and in concentrating dilute solutions in bioseparation [15].

1.1.3 Stimuli–responsive Systems

Special type of polymeric system based on polyacrylamide (PAAm) was introduced by Toyoichi Tanaka [16] in 1978. Interesting physical properties of that so-called "smart hydrogel" began the wave of wider investigation theoretical, experimental and practical – oil spills cleaning, DNA separation, drug releasing. Beside the fact that various smart hydrogels can be swollen in polar solutions such as water [17]], there is also rapid and extensive volume reaction on the small changes in external parameters such as pH, temperature or/and solvent composition. The swelling ratio which indicates the relation between the original volume before the transition and after it could change in several magnitudes up to 1000. The change of swelling ratio depends on noncovalent interactions such as hydrogen bonds, hydrophilicity and hydrophobicity of the groups in polymer or its chemical structure, crosslinking density of the network. Volume change is accompanied with changes of other macroscopic quantities such as complex permittivity, mechanical modulus, conductivity or refraction changes.

Phenomenon called volume phase transition (with characteristic temperature VPTT) or collapse could be interpreted as a first-order transition [18], but also second-order transition interpretation could be found in some literature [19]. Temperature-induced volume phase transition in crosslinked hydrogels is similar phenomenon as the phase separation in polymer solutions exhibiting a lower critical solution temperature (LCST). On the molecular level, both phase separation in solutions and volume phase transition (collapse) in crosslinked hydrogels are assumed to be a macroscopic manifestation of a coil-globule transition (graphical scheme see Fig. 1.2), as was shown for poly(*N*–isopropylacrylamide) (PNIPAm) in water by light scattering [20] or [21].

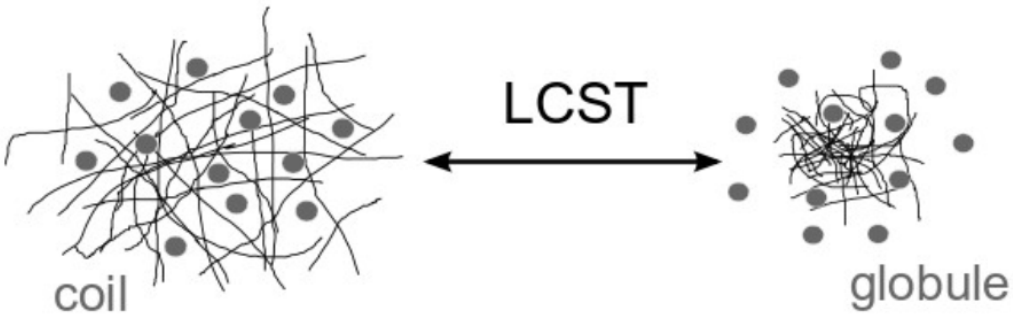

Figure 1.2: Schematic description of phase separation of polymer in aqueous solution.

Temperature as a stimuli was found for poly(*N,N*–diethylacrylamid) (PDEAAm) [22] or poly(*N*–isopropylmethacrylamid) (PNIPMAm) [23], and subsequently also for other amphiphilic polymers like poly(vinyl methyl ether) (PVME) [24], [25] and poly(*N*–vinylcaprolactam) (PVCL) [26], [27], [28]. This transition is followed by further aggregation and formation of so-called mesoglobules [27]. This reversible process is probably associated with a changed balance between various types of interactions, mainly hydrogen bonds and hydrophobic interactions,

when above the LCST, the hydrophobic interactions prevail over polymer–water hydrogen bonds with occurrence of the phase separation by milk-white turbidity of solutions [21], [27], [29]. There can be upper critical solution temperature for closer group of materials, for example nitrobenzene in hexane or aniline in water. There are LCST and UCST schematically described as critical points on the Fig. 1.3 where system is mixable (one phase system) only for some composition and/or certain temperatures in the middle of the picture between the two binodal or coexistence curves. Inside the so-called spinodal curve, there are always two phases and between each spinodal and binodal curve, there could one or two phases coexist depending on set of parameters which are thermodynamically more favourable.

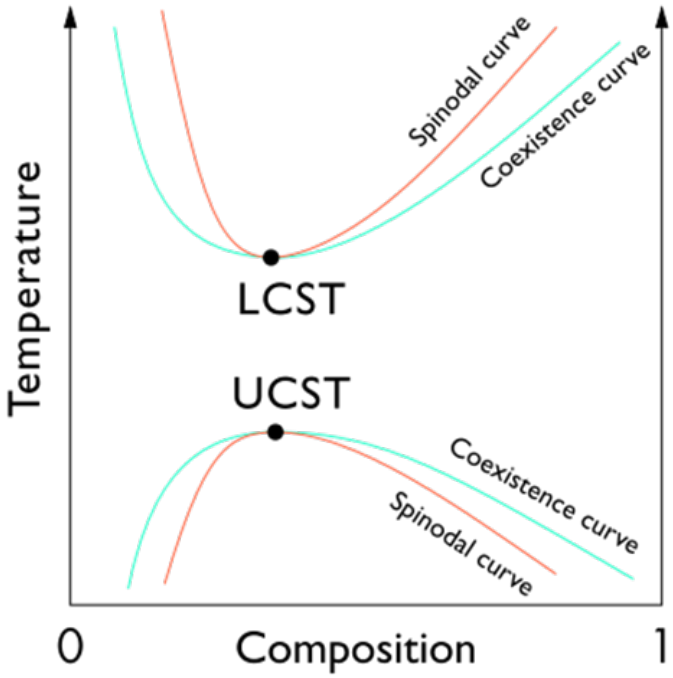

Figure 1.3: Temperature composition diagram for system manifesting both LCST and UCST [30].

1.1.4 Phase Separation Theory

Experiments with PAAm hydrogels in binary solutions of water and acetone done by Tanaka [31] shows how small change in composition ratio influences the polymer-solvent interactions. Water is good solvent for PAAm, while acetone is a bad one. With an acetone concentration over the 42 *vol.*% (see Fig. 1.4) the network collapses suddenly and volume shrinks 20 times. As later experiments confirmed the charges on the chains are inevitable to implicate collapse occurrence [32].

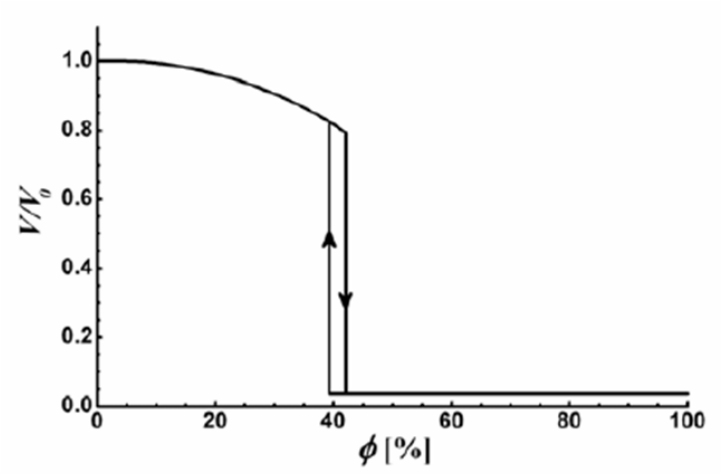

Figure 1.4: Change in volume of a polyacrylamide network depended on the volume percentage of the acetone in water. V_0 is the original volume during the preparation. Taken over from [33].

These experiments confirmed the previous theoretical predictions [34] and [35] that collapse is similar to the first-order phase transition. A small change in the polymer-solvent interactions, which may be given by a change in the external parameters, for example, by temperature or composition of solvent, then leads to a pronounced change in the degree of swelling of the gel. When two phases in the system occurs they must have different segment concentrations and conformations of the chains. Possible coexistence of two polymeric phases under the suitable conditions and chosen parameters is based on a Flory-Huggins equation swelling equilibrium.

The connection between collapse in hydrogels and phase transition in polymer solutions originates from the same phenomenon – coil–globule transition. During the coil–globule transition, polymer chains undergo an intramolecular phase transition from expanded coil state to the compact globular structure and there is a change in interactions between polymer and solvent characterized as shift from good–solvent behavior to poor–solvent behaviour. Good-solvent behavior occurs when polymer segment–solvent contacts are more favoured than segment–segment contacts. If the attraction between the segments becomes sufficiently large the polymer will separate to a globule whose density is close to that of dry polymer [36]. For lower concentrated solutions where mean quadratic radii of each polymer do not overlap the globules are formed intramolecularly and it is the only mechanism which assures the phase transition. With increasing concentration the different chains are closer to each other and intermolecular condensation is going to be competitive and more dominant to the accumulation of individual chains globules.

In real samples both mechanisms occur and phase separation is their combined result. The temperature at which this occurs is close to the Θ temperature – the temperature at which the attractive forces just balance the excluded volume forces. A more precise definition of the Θ temperature is the temperature at which the second virial coefficient of the osmotic pressure vanishes [37]. Another Flory–type approach is described in [38]. Both approaches are based on minimalization

of total Gibbs free energy between polymer stretching contribution derived from Gaussian statistics assumption and the van der Waals real gases assumption for monomer–solvent and monomer–monomer interactions.

Second fundamentally different model was 10 years later introduced by Lifshitz [39]. Using the model of spherically symmetric globule they we able to solve nonlinear Schrödinger–type equation and determine the inside density distribution of monomers. Equilibrium value of the transition point could be derived from both approaches. Equilibrium is defined by length and rigidity or flexibility of the molecular segments of the taught polymer, solvent affability in relation to the polymer and temperature. Type of the transition depends only on rigidity of the polymer. For rigidity below certain value we observe smoother second order transition, for more rigid chains the first order transition occurs with two minimums near the transition point.

1.2 Experimental Methods

A variety of techniques for characterizing temperature sensitive polymer solutions and hydrogels have been reported in the literature [4, 21]. The rather simple method of determining the LCST is the cloud point method determination using UV–VIS spectrophotometer. Thermodynamic parameters of the transition could be obtained from differential scanning calorimetry (DSC). Light scattering experiments using light as a probe offer information on the size, shape, and interactions of macromolecules. Change of viscosity could be also followed during the phase separation in polymer solutions.

The physical behavior of hydrogels is dependent on their equilibrium and dynamic swelling behavior in water and from this point of view the most important parameters that define the structure and properties of swollen hydrogels is the polymer volume fraction in the swollen state which could be determined from swelling experiments. Change of mechanical properties, mainly Young's modulus of hydrogels, during the phase transition is often investigated. Combination of NMR spectroscopy and DSC, swelling experiments and optical microscopy was used in the thesis to investigate polymer solutions and hydrogels. Basic description of these methods is introduced in this subchapter.

1.2.1 Nuclear Magnetic Resonance

This chapter has been constructed with help of the following books: [40, 41].

Nuclear magnetic resonance (NMR) used permanent strong magnetic field to study the response of the specific nuclear spin of the investigated atom. Pulse NMR is also used to measure the energy emission or absorption. Although quantum-mechanical description is used to determine the theoretical spectrum shape, experiments are mainly characterized by classical physics. Hydrogen ^{1}H and carbon ^{13}C are two most often examined nuclei, their spin $I = 1/2$. Two energetic levels of the Zeeman dublet are created when atom is inserted into the magnetic field. The energy gap between them is determined by the equation:

$$\Delta E = \hbar \gamma B_0, \tag{1.1}$$

where γ is gyromagnetic ratio specific for each nucleus, $\hbar$ is reduced Planc or Dirac constant and B_0 is an absolute value of the permanent magnetic field $\boldsymbol{B_0}$.

If there is no magnetic field, spins are in the equilibrium. But spin starts to precess after turning the field on along the axis parallel to the direction of the magnetic field $\boldsymbol{B_0}$. The frequency of that motion $\boldsymbol{\omega_0}$ is called Larmor as a result of solving the evolution operator from Schrödinger equation with Hamiltonian derived for the free particle in the magnetic field and the gap between its eigenvalues defined by eq. 1.1:

$$\boldsymbol{\omega_0} = -\gamma \boldsymbol{B_0}. \tag{1.2}$$

Macroscopic magnetization $\boldsymbol{M}$ is then sum of all the spin vectors. When the external field is off there is none macroscopic magnetization, although when field is applied Boltzman statistics for basic and excited levels change and nonzero magnetization $\boldsymbol{M}_0$ occurs (Fig. 1.5a).

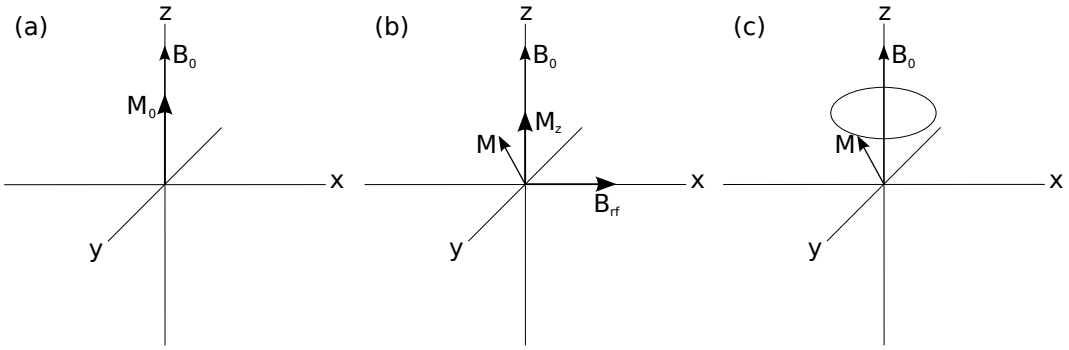

Figure 1.5: Magnetization $\boldsymbol{M}$: (a) in equilibrium – parallel to the external field $\|\boldsymbol{B_0}$; (b) after rf pulz $\boldsymbol{B_{rf}}$ applied in x axis – folding $\boldsymbol{M}$ into the zy plane; (c) final situation – precession around the external field $\boldsymbol{B_0}$.

Beside the permanent magnetic field $\boldsymbol{B_0}$ there is application of the radiofrequency (rf) pulse $\boldsymbol{B_{rf}}$ as another fundamental part of the NMR spectroscopy. $\boldsymbol{B_{rf}}$ has very small intensity in comparison to the $\boldsymbol{B_0}$, with $\pi/2$ angle, often in the x or y axis, but with the same Larmor frequency as the investigated nucleus (Fig. 1.5b).

Then so-called Bloch equations [42] describe the time dependence of the magnetization projections to the Cartesian coordinates of the precession (Fig. 1.5c) and its return to the equilibrium along the z axis because of the spin interactions in the magnetic field and the energy dissipation into the ambient. Component M_z is maximal in the equilibrium, minimal right after the rf pulse and then increasing back to the maximum value at the equilibrium. Component projection to the xz plane M_{xy} is inversely zero in the equilibrium, then maximal and decreasing back. Oscillating current – free induction decay (FID) on the receiver coils is produced by the precession motion of the magnetization. If we transform time FID intensity by the Fourier Transformation, so-called NMR spectrum, where x axis is in *ppm*. Solving the Bloch equations for magnetization components we get longitudinal relaxation time T_1 and transversal T_2. When we change to the rotation coordinates, Lorentz absorption and dispersion curve, in phase, out of phase, respectively, could be investigated. Resonance frequency changes due to

the surrounding and structure of the molecule by the electron shell when inserted to the magnetic field. Molecule bond changes the local magnetic field for the nuclei. The Larmor frequency is then changed by the shielding constant $\overleftrightarrow{\boldsymbol{\sigma}}$:

$$\boldsymbol{\omega} = -\gamma(1- \overleftrightarrow{\boldsymbol{\sigma}})\boldsymbol{B_0}. \tag{1.3}$$

Generally the shielding constant is a tensor in the crystalline matter, although in liquids there is a fast molecular isotropic rotation connected to the thermal movement and tensor is reduced to scalar which is between 0 and 1. More the nucleus is surrounded by electron shielding, means higher electronegativity, is rotated at lower frequencies. The shielding is weaker and frequencies higher for the light or/and isolated nuclei. If we relatively compare the original and shielding influenced frequencies and the result multiply by several orders, we obtain chemical shift δ in units ppm (parts per million):

$$\delta = \frac{\omega - \omega_0}{\omega_0} 10^6, \tag{1.4}$$

where ω_0 is a Larmor frequency of no interactive, concentration independent standard.

Relaxation is a process by which the spin system returns to the equilibrium state and interchanges the excess energy with its surroundings. NMR relaxation depends on the mobility of the NMR active species. As the molecule undergoes random thermal motion, there arise uctuating magnetic fields from interactions with the lattice and from mutual interactions between spins. The fluctuation is mainly caused by the following processes [41]:

1. Direct dipole–dipole interaction between two spins in one molecule,
2. Chemical shift anisotropy,
3. Spin–rotation interaction.

In liquids, dipole–dipole interaction is averaged by the rotation molecular motion to zero, but its influence on the relaxation is the most significant.

After switching magnetic field on, the system goes to the new equilibrium state. The magnetization M_0, which is given by the sum of magnetic moments of individual spins, is not zero anymore. After applying radiofrequency field the z–component of magnetization relaxes to the new equilibrium state and its time dependency $M_z(t)$ will be

$$M_z(t) = M_0 \left(1 - 2e^{-\frac{t}{T_1}} \right). \tag{1.5}$$

The constant T_1 is called the longitudial (spin–lattice) relaxation time.

Transverze (spin-spin) relaxation corresponds to a decoherence of the transverse nuclear spin magnetization. Random fluctuations of the local magnetic field lead to random variations in the instantaneous NMR precession frequency of different spins. As a result, the initial phase coherence of the nuclear spins is lost,

until eventually the phases are disordered and magnetization M_{xy} is decreasing as:

$$M_{xy}(t) = M_0 e^{-\frac{t}{T_2}}, \tag{1.6}$$

where the constant T_2 is called the transverse (spin–spin) relaxation time.

1.2.2 Differential Scanning Calorimetry

Technique to determine thermodynamical parameters such as heating capacities, enthalpies or latent heats of the transitions which occur when we heat up or cool investigated sample is called differential scanning calorimetry (DSC). On the so-called thermograms (heat flow Q dependent on temperature T) we see amount of heat required to increase the temperature, starting and finishing points and type of the phase transition as glass transition, melting points, etc. DSC has two chambers as we can see in Fig. 1.6, where reference and investigated sample are and we measure the difference of the added heat to each other. Proper heat rate has to be chosen, pan space maintained clean and several gases which create environment to get proper results needs to be controlled.

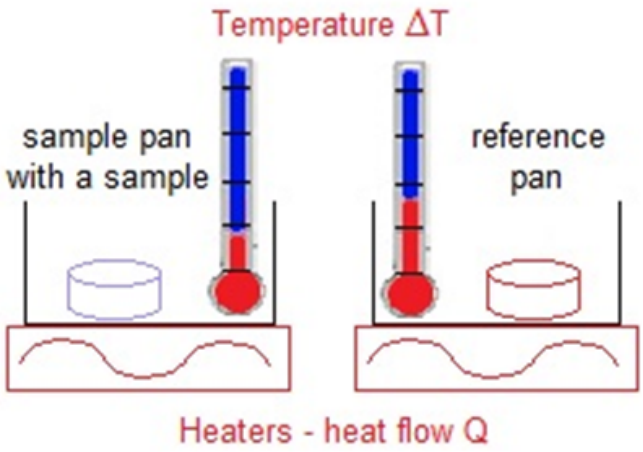

Figure 1.6: DSC working scheme.

1.2.3 Optical Microscopy

Magnifying objects using optical principles when light comes through at least one lens are basics of optical microscopy (OM). In the modern science compound microscopes are fundamental. They have two lens as is depicted in Fig. 1.7, first objective lens very close to the examined object and produce the real image ("image 1" in Fig. 1.7) inside the body of the microscope. Second ocular/eyepiece lens then produce virtual and inverted image ("image 2" in Fig. 1.7). Object could be typically magnified 10-200 times. For better automation and processing CCD and CMOS cameras are placed on the top of the ocular and connected to the computer.

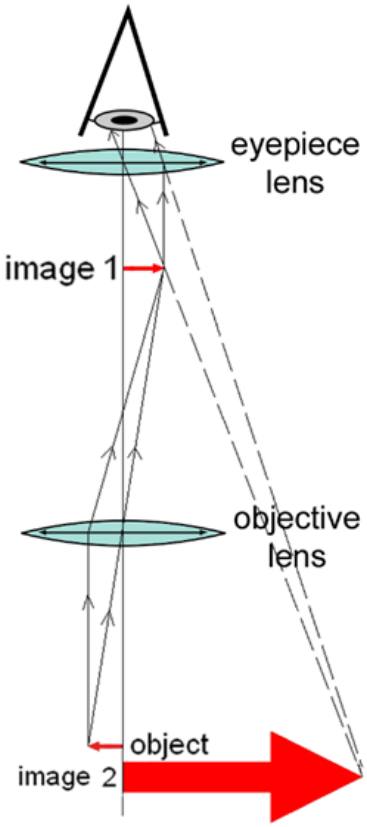

Figure 1.7: Schematic diagram of the compound microscope.

1.2.4 Swelling experiments

Hydrogels can contain the multiple times more water than is their own volume. Chains are swelling water and want to expand, but the crosslink structure produce counteractive force to keep the chains inside. After some time these forces are tending to equilibrium and the network become fully swollen. That weight ratio between the swollen polymer and dry polymer is called swelling degree or ratio. Beside volume fraction between dry and swollen state the dynamic growing parameters or degree of crosslinking could be determined.

2. State of Art

Temperature as a stimuli was found for poly(*N*–isopropylacrylamid) (PNIPAm) [21, 23], poly(*N*,*N*–diethylacrylamid) (PDEAAm) [22, 23] or poly(*N*–isopropylmethacrylamid) [23] and subsequently also for other amphiphilic polymers like poly(vinyl methyl ether) (PVME) [24, 26, 25] and poly(*N*–vinylcaprolactam) (PVCL) [27, 28]. Following subchapter deals with review of studies on solutions or hydrogels based on these polymers.

2.1 Linear poly(vinyl methyl ether)

As a representative of the water–soluble non–ionic linear polymers we have been interested in poly(vinyl methyl ether) (PVME). It has useful properties, such as biocompatibility, non-toxicity, low glass transition temperature and thermoresponsive behavior. Pure PVME in water (H_2O or D_2O) has low critical solution temperature (LCST) around 308 K. Below LCST there is one homogeneous phase in the solution and above LCST the solution is turbid and separates into two phases [43, 44]. A study of phase separation in PVME solutions using various methods is widespread. The overview is presented in following text.

Maeda [45] determined three PVME concentration regions differing in water behavior. Region-III (at highest polymer concentrations) is characterized by a cooperative polymer-water complex, involving hydrogen bonding of water to oxygen atoms of the polymer. The region-II (intermediate concentrations) also appears to be formed a hydrogen-bonded water clusters around hydrophobic groups. Free water appears only in region-I at the lowest polymer concentrations. This can be interpreted as a cooperative collapse of the hydrogen-bonded water structure to free water, resulting in the aggregation of the polymer chains due to the exposure of their hydrophobic groups at the cloud point.

In IR spectroscopic study of PVME aqueous solution done by Y. Maeda [46] it was found that below LCST, the hydrophilic ether oxygens on the polymer makes hydrogen bonds with water molecules, which overcomes the unfavorable decrease in entropy of water due to a formation of an iceberg structure around the hydrophobic moiety and stabilizes the solution. With increasing temperature, the hydrogen bonds of the ether oxygens are broken and apolar groups are concomitanly dehydrated in the transition region from ca. 33 to 40 °C. Above the temperature region, the hydrophobic interaction between apolar moieties becomes dominant and induces separation of polymer chains from solvent (water). PVME concentration dependence of the position of IR bands shows that the methyl groups are more dehydrated than the ether oxygen at higher water/monomer ratios.

Aseyev et al. [47] were investigating the PVME in dilute aqueous solutions above LCST using several methods such as dynamic and static light scattering and differential scanning calorimetry. They found that particles (globules) are spherical and have very narrow size distribution. The size of formed particles depends on the initial concentration and the heating rate of the solution and it is not significantly affected by the molar mass of individual macromolecules. Once being formed, the particles neither precipitate nor disintegrate upon dilution. The

size of globules did not change at least for several weeks, showing the absence of any significant association of globules. Narrow size distribution of the globules also suggests entropic origin of the intermolecular association. The stability of the dispersion upon dilution at 50°C and zero value of the osmotic second virial coefficient indicate that the surface of the particles at temperatures above the LCST may possess a hydrophilic character. The macromolecules self-organize and build up particles with the polar groups turned towards the surrounding aqueous phase.

DSC and IR spectroscopy measurements on PVME/water systems [48, 49, 50] revealed that solutions with high PVME concentration ($> 60wt.\%$) do not show crystallization and melting of water. This abrupt change in crystallization and melting behavior is related to the vicinity of the glass transition temperature (ca. -25°C) generating a dramatic slowing down of the nucleation rate. Below -20°C, in solution with $30wt.\%$ of PVME, two types of ice was found. One is formed by free water and the other is formed by frozen bound water. IR data show that there are no hydrogen bonds between water molecules and polymer groups.

The phase diagram was revealed for PVME aqueous solutions from modulated temperature differential scanning calorimetry (DSC) experiments [48, 49, 51]. Evolution of morphology pattern and reversibility during heating–cooling cycle in PVME/water/ethanol solutions was observed using optical microscopy [52]. ^{1}H NMR spectroscopy was applied to investigate structural, dynamical changes and dynamics during temperature-induced phase separation in PVME/D_2O solutions [53, 54, 55, 56, 57, 58]. Formation of rather compact globular-like structures caused by the phase separation above the LCST is viewed as marked line broadening of the corresponding units of the PVME molecule [53, 54]. Above the phase separation, the fraction of PVME units involved in collapsed globular-like structures was stable at approximately 0.85 for solutions in the range of concentrations 0.1 – 30wt.% [54].

The data as obtained from NMR spectroscopy were used to construct van't Hoff plot and thermodynamical parameters of the transition in polymer solutions and hydrogels were determined [59, 60, 61]. On the basis of phenomenological model of the rigid sphere with variable diameter in which macromolecule is viewed as consisting of independent cooperative units, cooperativity of the transition can be related to comparison of the effective (van't Hoff) enthalpy and the calorimetric enthalpy of a polymer molecule and also determined the approximate the diameter [62].

There are different ways to influence the transition temperature or modify the length the transition parameters of the thermoresponsive polymers. As the polymer character above the transition is switched from hydrophilic to hydrophobic, we can influence that behavior by the composition of the polymer itself e.g. by co-polymerization, grafting with hydrophilic parts or side-chains. Behavior could be also influenced by changes of the solvent composition through the adding additives to the water/polymer solution. Additives are often small molecules which alter interactions between water and polymer, examples mentioned [43, 52, 63].

Horne et al [43] investigated the effect of different types of alcohols on the cloud point temperature of PVME. It was found that propanol has little effect on cloud point whereas lower molecular weight alcohols (methanol, ethanol) stabilize the hydrogen bonds and shift slightly the cloud point towards higher tempera-

ture. Higher molecular weight alcohol, n-buthanol, destabilize the interactions in system and decreases strongly the cloud point temperature.

Additive molecules can sometimes be used as a crude model of a medical drug for examining drug delivery systems [3], [64]. The ability of an additive compound to interact with the polymer chain on the one hand and to bind water molecules on the other hand plays an important role in its influence on the transition mechanism [65]. In particular, the ability of the additive to be embedded into the polymer globules affects the mechanism of their formation and the kinetics of water release and, possibly, also the additive release from the globular structures. Based on their influence on polymer structure, it is possible to distinguish two types of additives, namely those that either stabilize or destabilize the hydration structure surrounding the polymer chain [66].

Micro-Raman spectroscopic investigation [67] of PVME/water/alcohol ternary mixtures showed that transition temperature monotonically increase with increasing fraction of alcohol (methanol and ethanol). The obtained results suggest that association between the alcohols and PVME is mainly driven by hydrophobic interaction. More hydrophobic alcohols associate with PVME easier, raise the hydrophobicity of PVME, and finally reduce the transition temperature to a larger extent.

2.2 Hydrogels based on poly(*N*–isopropylacrylamide)

One of the most frequently used thermoresponsive polymer is poly(*N*–isopropylacrylamide) (PNIPAm) which undergo a volume phase transition around $307\,K$ [20, 27]. Temperature-induced phase transition in PNIPAm hydrogels was investigated by various techniques such as dynamic light scattering [68], differential scanning calorimetry (DSC) [69], rheology [70] or nuclear magnetic resonance (NMR) [71], [72]. Due to attractive stimuli-responsive properties of smart hydrogels, several potential applications in drug delivery systems [73], bio-separation [74], artificial muscles [75], microfluidics [12], tissue engineering [76] and micro/nanoactuators [77], etc., were suggested. In connection with application of PNIPAm however some concerns appeared about potential release of toxic low-molecular-weight amines due to hydrolysis and other thermoresponsive polymers have been proposed as alternatives for bio-applications [78]. On the molecular level, PNIPAM has been used in many forms including single chains, macroscopic hydrogels, microgels, latexes, thin films, membranes, coatings, and fibers [21].

With respect to possible applications, control of the swelling properties and parameters of phase transition in hydrogels is desired. Conventional single network (SN) hydrogels prepared with one polymer component exhibit limited thermosensitivity and possibility to tune transition parameters. They usually fail at poor tensile properties they show very low resistance against crack propagation. SNs hydrogels have been thus limited in the usage such as controlled drug delivery devices or water–absorber. The reasons for lack in mechanical strength of a hydrogel are its solution-like nature, i.e., low density of polymer chains and small friction between the polymer chains, and heterogeneity of the network structure of the hydrogel formed during the gelation. When a force is applied to a gel with

heterogeneous structure, stress is concentrated around the shortest chain, and this leads to a failure of the sample at a very low force.

Responsive rate of the transition or swelling capacities of PNIPAm and other thermoresponsible hydrogels can be affected by copolymerization of two monomers [79, 80]. Formation of interpenetrating polymer networks (IPNs) could be another strategy. IPNs are defined as a combination of two or more polymers in network form where at least one component is synthetized in the presence of the other component. Compositions in which one or more polymers are crosslinked and one or more polymers are linear or branched are semi-interpenetrating networks (SIPNs) [81]. First attempt for interpenetrating network was done by Aylsworth, who combined sulfur and rubber with phenol-formaldehyde in 1914 [82].

In literature, there are several investigations of IPNs and SIPNs containing PNIPAm and temperature insensitive network which significantly influences the final macroscopic properties. Kim et al. have synthesized IPN poly(vinyl alcohol)/PNIPAm, and they studied the swelling kinetics [83], electroactive characteristics [84], and thermal properties [85]. IPNs composed of poly(vinyl alcohol) and PNIPAAm-co-acrylamide copolymers that were also investigated by cloud point measurement and differential scanning calorimetry [86], and significant differences in volume phase transition enthalpies of PNIPAm were found. Here, acrylamide increases the hydrophilicity of PNIPAm and therefore shifts the LCST of the copolymer network to higher values.

Thermo and pH sensitivity were besides the PNIPAm/PAAm systems investigated also on the IPN systems PNIPAm with polyurethane (PU) [87]. The swelling transition temperatures of PNIPAAm gels were little affected by the incorporation of PU networks in IPN structures. The swelling and drug releasing behavior of PNIPAAm/PAA IPNs was significantly affected by the variation of PAA compositions. Drug release process rate decreased in the solution with pH 7.4, but increased with increasing PAAm content for pH 5.0 due to the decreasing swelling power of PAAm with decreasing pH. Zhang et al. [88] studied IPN of two PNIPAm hydrogels with different compositions. Although transition temperature is similar as for ordinary neat PNIPAm hydrogel, mechanical properties improved (compression modulus increased 1.9 to 3.5 times, tensile modulus 1.5 to 16.8 times), drug is being released for longer time and deswelling kinetics can be tuned with the composition of the IPN. The reason of these changes are higher polymer mass per unit volume and changes in morphology. Unlike normal PNIPAAm hydrogel, the IPN-PNIPAm gels are not homogenously porous, but they have a fibrillar-like structure with non-uniform mass distribution.

There are virtually no studies how polymer architecture affects transition behavior of IPNs where both chemically different networks are thermoresponsive except the Šťastná et al. [89] used the combination of NMR spectroscopy, DSC, dynamic mechanical spectroscopy and optical microscopy to investigate temperature-induced volume phase transition in hydrogels of IPN poly(*N*–isopropylmethacrylamide) (PNIPMAm)/PNIPAm with various PNIPAm contents where both components are thermosensitive. The behavior of the hydrogels (one or two transitions) was found to depend on the ratio of the two IPN components. Separate transitions for the two components were revealed in hydrogels of IPNs containing around 50 *mol*% of PNIPAm monomer units. A certain portion of

spatially restricted bound water was established from NMR relaxation measurements for all studied copolymer solutions and IPNs at temperature above the phase transition.

Gutowska et al. [90] were one of the first investigators, who described networks with one component cross-linked and one linear, so called semi-interpenetrating networks (SIPNs). In this case it was long studied PNIPAm with linear poly-(ether(urethane-urea)) as a representative of biomers. The deswelling rates were unchanged for concentrations under the 2.5% of biomer compared to the cross-linked PNIPAAm. Above the 2.5% biomer helped deswelling process by preventing the skin-type layer formation on the surface of the gel. The goal was use it as a drug delivery system in this case heparine. Increasing temperature and biomer content decrease amount of drug which could be loaded into the swollen polymer.

Temperature-induced collapse was studied on SIPNs composed of PNIPAm and various hydrophilic polymers [91]. Due to hydrogen bonding in the hydrogel network, critical collapse temperatures of SIPNs were shifted to lower values in comparison with neat PNIPAm network. Hydrogels of SIPN based on crosslinked PAAm with linear PNIPAm were synthesized and their properties, such as swelling ratio and compressing elastic moduli, were studied at several temperatures [70]. Equilibrium swelling ratios of SIPNs markedly decreased due to the presence of less hydrophilic PNIPAm chains. SIPN hydrogels present better mechanical properties than PAAm hydrogel, mainly when the PNIPAm chains are in a collapsed state. The effect was explained as being an additional contribution of the PNIPAm chains, which collapsed around the PAAm networks.

SIPNs based on crosslinked PNIPAm and nonionic or ionic linear polyacrylamide PAAm were synthesized and effects of crosslinking density and incorporation of linear polymers into networks on the temperature-induced transition, swelling behavior and mechanical properties were studied [92]. The introduction of cationic and anionic linear hydrophilic PAAm into PNIPAm networks increased the rate of swelling, whereas the presence of nonionic PAAm diminished it. Transition temperatures were significantly affected by both the crosslinking density and the presence of linear PAAm in the hydrogel networks. SIPNs reinforced with cationic and nonionic PAAm exhibited higher tensile strengths and elongations at break than PNIPAm hydrogels, whereas the presence of anionic PAAm caused a reduction in the mechanical properties.

2.3 Hydrogels based on poly(*N,N*–diethylacrylamide)

Poly(*N,N*–diethylacrylamide) (PDEAAAm) is another *N*–substituted thermosensitive polymer with VPTT values 304 – 307 K [93, 94, 95]. PNIPAm and PDEAAm share the same backbone structure, except for the *N*–substituted groups, two ethyl groups for PDEAm, and one isopropyl group for PNIPAm (cf. Fig. 4.3 in chapter 4). Owing to the absence of NH in the amide group, PDEAAm can only act as hydrogen bond acceptor and thus disable the formation of intra- or interchain hydrogen bonds. Therefore, PDEAAm is a suitable candidate for comparative study with PNIPAM to check the role of NH moiety [96, 97].

Baltes [93] investigated PDEAAm also with PNIPAm in various solutions by

photometry and high sensitivity DSC with the result that the salt effect influence PNIPAm and PDEAAm in the same way by decreasing the LCST temperature. Others also saw the PDEAAm capacity to store and release active agents, meaning that PDEAAm is attractive candidate for biomedical applications, particularly drug delivery [94]. Effect of the chemical composition on the phase separations of the aqueous solutions of the copolymers of *N,N*–dimethylacrylamide and other *N*–substituted acrylamides including *N*–ethylacrylamide, *N,N*–diethylacrylamide or *N*–tert-butylacrylamide was studied [95]. The copolymers exhibit systematic changes in their LCSTs as a function of their comonomer composition, for which an empirical equation was established.

The cytotoxicity of PDEAAm hydrogels was found to be less pronounced than for PNIPAm ones, though there are no short time effects (less than 4h) and is rather low in both cases for higher temperatures and longer time of explosion determined by the WST-1 viability and the LDH cytotoxicity [98] – there are also shown TEM pictures of so-called microgels. PDEAAm is often compared to the PNIPAm and it has been found that swelling properties of both hydrogels can be considerably influenced by the crosslinking density, on the other hand swelling ratio of PDEAAm hydrogels below VPTT is much lower than that of PNIPAm hydrogels which is attributed to the different chemical structure of monomeric side chains [99, 100]. PDEAAm has more significant dependency on the crosslinking agent, slower reswelling kinetics and also broader temperature phase transition region.

Besides investigation of the neat PDEAAm hydrogels, copolymerization of DEAAm with a hydrophilic (hydrophobic) monomer or introducing another polymer into PDEAAm hydrogel to form IPN were also used to control phase transition behavior. The effect of copolymerization of DEAAm with various hydrophilic co-monomers on the swelling properties and parameters of the phase transition were studied using nuclear magnetic resonance (NMR), Fourier transform infrared spectroscopy (FTIR) and modulated differential scanning calorimetry (DSC) [101]. Crosslinking density and the nature of the incorporated hydrophilic component were found to impact hydrogel structure, mechanical properties and swelling kinetics. Aminophylline was selected as a model solute for drug loading and release studies by thermal deswelling in HCl buffer and phosphate buffer media.

Temperature-dependent FTIR was employed to study the phase transition process in random copolymers and microgels based on NIPAm and DEAAm and the transition mechanism by the difference of various hydrogen bonds was explained [102]. The thermo- and pH-sensitive behavior of SIPN hydrogels based on poly((2-dimethylamino)ethyl methacrylate) and PDEAAm were investigated for various compositions by scanning electron microscopy (SEM) and DSC [103]. SIPNs showed mutative values in reaction to the temperature and pH change with faster de/swelling rates compared to the neat cross-linked PDEA.

2.4 Hydrogels based on poly(*N*–vinylcaprolactam)

Poly(*N*–vinylcaprolactam) (PVCL) is another important example of the thermosensitive amphiphilic water-soluble polymer [27]. PVCL hydrogels and solutions have attracted much attention, as they are biocompatible and reversibly thermoresponsive near physiological temperature (LCST $\approx$ 303–311 K, depending on the concentration and molecular weight) [26, 104, 105]. Some important differences were found for PVCL in comparison with acrylamide-based polymers, especially a much lower level of dehydration of PVCL segments at temperatures above the phase transition [105, 106]. The origin of these differences can be in different structures of respective monomer units. IR spectroscopy results showed that PVCL mesoglobules might forma sponge-like structure in contrast to PNIPAm cotton-like globules [107]. Slightly crosslinked hydrogels of PVCLwas studied as a function of temperature [108]. In water, PVCL hydrogels showed a sharp volume transition on heating. In water/alcohol mixtures, the hydrogel first shrank and then expanded as the temperature was raised. The swelling behavior of PVCL hydrogel in surfactant solution depended on kind and concentration of the surfactant. High-sensitivity microcalorimetry studies have revealed that PVCL hydrogels undergo two heat-induced cooperative transitions: at 304.5 and 310.5 K [109]. The low-temperature transition is proposed to be associated with the microsegregation resulting in formation of hydrophobic domains in the gel whereas the high-temperature transition is due to the gel volume collapse. The transition temperatures decrease in the presence of NaCl and increase with increasing sodium dodecyl sulfate concentration.

3. The Main Goals of the Thesis

The main aim of this thesis is to characterize structures and interactions in aqueous solutions and hydrogels of responsive interpenetrating (IPNs) and semi–interpenetrating (SIPNs) polymer networks. Information how the architecture of the polymer system affects the phase-separated globular structures on various level should be obtained. This includes information on the sizes and shape of these structures, on the fraction of monomeric units directly involved in these structures, on changes in hydrogen bonding of specific funtional groups, on changes in the arrangement and order of water molecules as well as on changes in the dynamics both of polymer segments and water molecules due to the phase transition. As main method, NMR spectroscopy will be used in these investigations and combined with swelling, DSC and optical microscopy experiments.

In the thesis we will focus on the following systems:

1. Aqueous solutions of linear poly(vinyl methyl ether). The NMR and DSC parameters will be analyzed to determine thermodynamical parameters of the phase transition for various polymer concentrations. Reversibility during heating and cooling cycles will be studied as well. The effect of small molecular additives on the appearance and extent of the phase transition will be determined.

2. Hydrogels of IPNs of poly(*N*–isopropylacrylamide)/polyacrylamide and poly(*N*–vinylcaprolactam)/poly(*N*–isopropylacrylamide). The influence of IPNs composition and reverse sequence in the preparation procedure on the phase transition will be examined.

3. Hydrogels of SIPNs and IPNs of poly(*N,N*–diethylacrylamide)/polyacrylamide. Besides the effect of network composition on the volume phase transition, we will investigate SIPNs and IPNs with a reversed sequence of the two components in the preparation procedure, i.e., SIPNs of crosslinked PDEAAm and linear PAAm and inversely SIPNs of crosslinked PAAm and linear PDEAAm, and both types of IPNs PDEAAm/PAAm and PAAm/PDEAAm, as there are virtually no studies of this aspect in the literature. The behavior of prepared networks will be compared with aqueous solution of linear PDEAAm and neat hydrogel of crosslinked PDEAAm.

4. Experiments

4.1 Samples

4.1.1 PVME Solutions

PVME (purchased from Sigma-Aldrich (St. Louis, MO, USA), supplied directly as 50$wt.\%$ aqueous solution with average molecular weight $M_w = 60.500$ and index of polydispersity $M_w/M_n \cong 3$) was used after drying to prepare PVME/D2O (99.9$vol.\%$ of deuterium) solutions of desired concentration in the range c = 0.1 – 90 $wt.\%$. Samples for NMR measurements were prepared for 5 mm tubes, a small droplet of highly diluted NMR standard tetramethylsilane (TMS) was added. Then the tube was degassed and sealed under argon. Structural formula is shown on the Fig. 4.1.

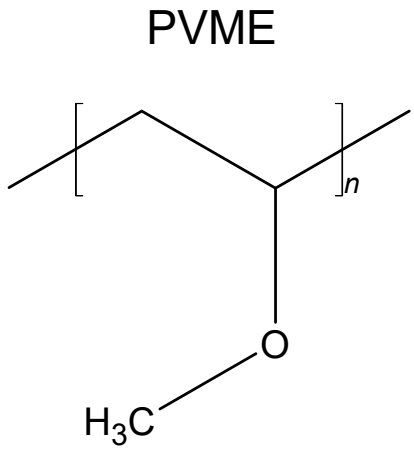

Figure 4.1: Structural formula of PVME repeating units.

4.1.2 Additives

There were added t-butyl methyl ketone (TBMK or 3,3-Dimethyl-2-butanone), t-butyl methyl ether (TBMe), t-butylamine (TBAm), and t-butanol (TBOH) into the PMVE/water solutions. All these substances were purchased from Sigma-Aldrich with the purity 99$vol.\%$, 99,8$vol.\%$, 98$vol.\%$, 99,5$vol.\%$ for TBMK, TBMe, TBAm, TBOH, respectively, and has not been mixed or changed in other way. The same PVME was dried and prepared qualitatively as previously in the subsection 4.1.1. Solutions in the concentration range c_P = 0.5-10$wt.\%$ were prepared, 0,5, 1, 5, 10$wt.\%$, concretly. Then additives were carefully mixed into the PVME/water solutions with the concentrations c_{ad} = 1, 2, 5, 7, 10$wt.\%$. Most of the additives were highly volatile and so we estimate concentration error at about 0,5$wt.\%$. All the PVME/D_2O samples for NMR measurements were prepared for 5 mm tubes, a small droplet of highly diluted NMR standard sodium 2,2-dimethyl-2-silapentane-5-sulfonate (DSS) was added, then degassed

and sealed in the argon atmosphere. In the Fig. 4.2, there are formulas of all the additives used.

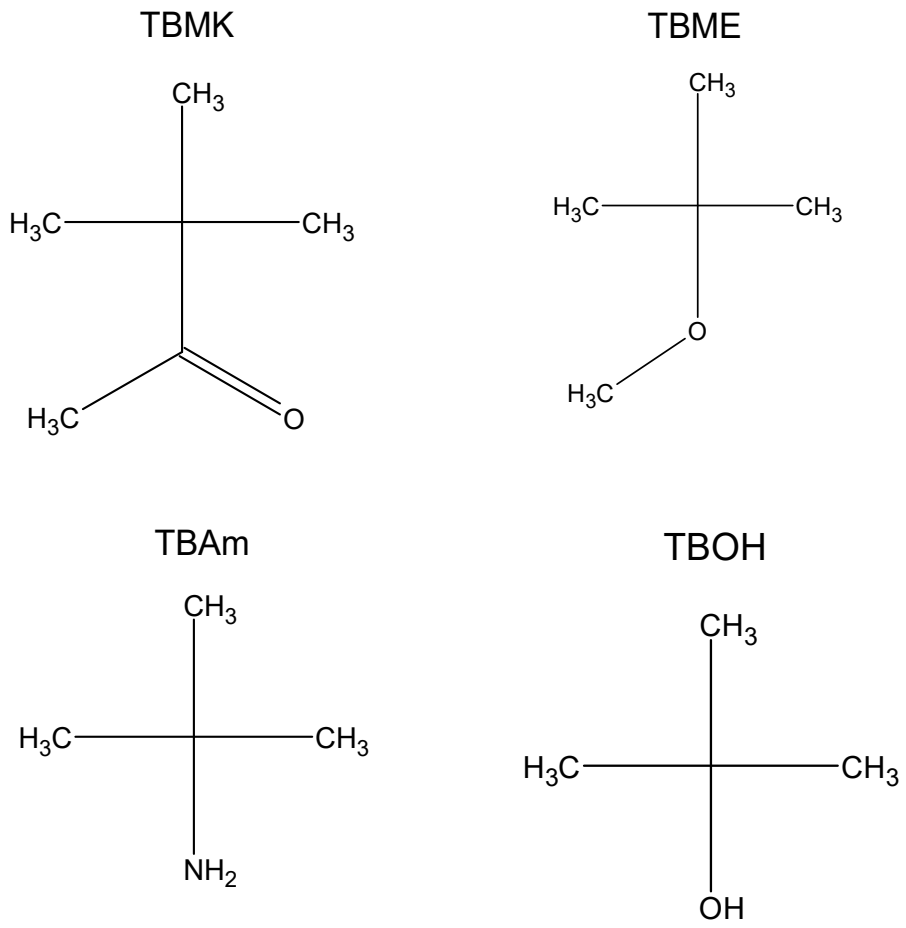

Figure 4.2: Structural formulas for methyl ketone, t-butyl methyl ether, t-butylamine, and t-butanol additives.

4.1.3 IPNs Based on PNIPAm and PVCL

There were group of samples containing *N*–vinylcaprolactam (VCL; Sigma-Aldrich, ≥97.5% GS), *N*–isopropylacrylamide (NIPAm; Sigma-Aldrich, 97%) as well as NIPAm (Fluka/Honeywell, 98% by HPLC) and acrylamide (AAm; Fluka/Honeywell, 99% by HPLC). They have been further purified by sublimation.

Following chemicals as *N,N'*–methylenebisacrylamide (MBAAm; Fluka), 2,2'-azobis(2-methylpropionitrile) (ABIN; Fluka), and 2-hydroxy- 2-methylpropiophenone (Darocur 1173; Fluka), 4,4'azobis(4-cyanovaleric acid), diethylether, *N,N,-N',N*–tetramethylenediamine (TEMED, Sigma-Aldrich) were used as obtained.

Ethylidene-bis-3(*N*–vinyl-2-pyrrolidone) (EBVP) was synthesized using the procedure given in ref. [57].

Two types of interpenetrating networks of PAAm and PNIPAm were prepared in reversed order, i.e. both PNIPAm/PAAm and PAAm/PNIPAm. IPNs were synthesized in water using redox initiating system ammonium persulfate TEMED

and crosslinking agent MBAAm. 20$wt.$% solution of NIPAm with 0.06$wt.$% of MBAAm and 5$wt.$% solution of AAm with 0.135$wt.$% of MBAAm were used for IPN preparation. In the synthesis of interpenetrating network PNIPAm/PAAm the PNIPAm network was prepared first at 277 K. Unreacted monomer was repeatedly washed out by water and PNIPAm networks were pre-dried for subsequent swelling. The first network was then swollen in aqueous solution of AAm monomer, redox initiating system and MBAAm in refrigerator for 24 hours, and polymerization was carried out at room temperature. The interpenetrating network PAAm/PNIPAm was prepared in a similar way but the PAAm network was prepared first. The final interpenetrating networks were repeatedly washed and reswollen by distilled water and finally reswollen in D_2O.

For the linear PNIPAm Darocur 1173 has been used as photoinitiator for the UV polymerization of NIPAm in ethanol at 278 K. Linear PAAm was prepared by radical polymerization of AAm in ethanol/water mixture (85/15 by volume) at 333 K with 4,4'-azobis(4-cyanovaleric acid) as initiator. Polymer was isolated by precipitation with diethylether and purified by reprecipitation from water to ethanol. After subsequent drying of all samples to constant weight under low pressure, the D_2O solutions (2$wt.$% and 8$wt.$% for NMR and DSC measurements, respectively) of PNIPAm/PAAm mixtures were mixed in molar ratio of variour monomeric units with respect to the real compositions of the corresponded IPNs.

In the synthesis of IPN PVCL/PNIPAm, the PVCL network was prepared first, thermally from reaction mixture containing 10$wt.$% solution of VCL and with cross-linking agent EBVP (2$mol.$% related to monomer) and initiator ABIN. The polymerization was carried out in ethanol under nitrogen atmosphere at 333 K for 24 h in sealed glass capsules. Unreacted monomer was repeatedly washed out by ethanol. Subsequently, the PVCL network was swollen in the ethanol solution of monomer NIPAm (20$wt.$%), with photo initiator Darocur 1173 and cross-linking agent MBAAm (1$mol.$% related to monomer) in a refrigerator with no access of air and light. Then, the samples were purged with nitrogen, sealed, and exposed to UV light with a wavelength of 254 nm at room temperature.

Structural formulas of the repeated units are shown on the Fig. 4.3. PVCL and PNIPAm are hydrophobic in water solutions and undergo phase separation, on the other hand hydrophilic PAAm does not. PVCL has two transitions at 304.5 K and 310.5 K and PNIPAm only one at 307 K as was mentioned in chapter 2.

4.1.4 IPNs and SIPNs Based on PDEAAm

PDEAAm and PAAm homopolymers were prepared by free radical polymerization of DEAAm (Sigma-Aldrich, 98,5% GC) and AAm (Fluka, 98% HPLC) monomers in ethanol (96$vol.$%) at 343 K for 24 h using 2,2'-azobis(2-methylpropionitrile) (ABIN, Fluka) as initiator. For the preparation of PDEAAm/PAAm (and reverse PAAm/PDEAAm) SIPNs of various composition DEAAm (or AAm) monomer and crosslinker, *N,N'*–methylene bisacrylamide (MBAAm, Fluka), were dissolved in aqueous solution of PAAm (or PDEAAm). Hydrogels were prepared using the redox initiating system ammonium persulfate – *N,N,N',N'*–tetramethylenediamine (TEMED). In the synthesis of IPNs PDEAAm/PAAm

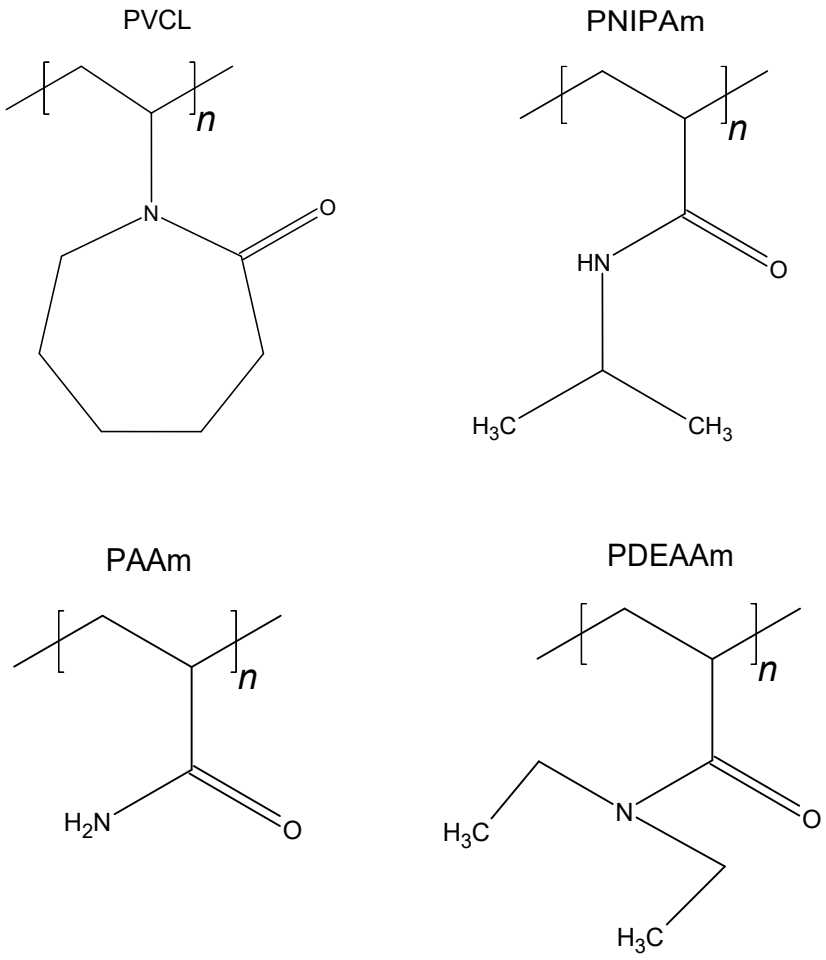

Figure 4.3: Structural formulas for PVCL, PNIPAm, PAAm and PDEAAm repeating units.

the PDEAAm network was prepared first in water at 277 K using the redox initiating system [$(NH_4)_2S_2O_8$-TEMED] and crosslinking agent MBAAm. Subsequently, the first network was swollen in aqueous solution of AAm monomer, redox initiating system and MBAAm, polymerization was then carried out at room temperature. The IPNs PAAm/PDEAAm were prepared in a similar way but the PAAm network was prepared as the first one. For that hydrophobic polymer with transition between 304-307 K (see chapter 2) there is structural formula on Fig. 4.3.

4.2 Experimental Settings

4.2.1 DSC

DSC measurements were performed with a Pyris 1 apparatus (Perkin-Elmer). Nitrogen was used as the temperature control gas. Helium gas was passed through the DSC cell at a flow rate of 20 ml/min. Into the pan (max. 40 ml) there were 8 – 16 mg of the material – no matter if solution or solid sample. All enthalpy peaks

were recounted to the element (most often per gram) of the polymer. DSC thermograms were recorded by Pyris apparatus (Perkin-Elmer). Qualitative scheme of the cycles you can see on the Fig. 4.4. There are full 2 heating cycles, 2 cooling cycles and 3 waiting periods.

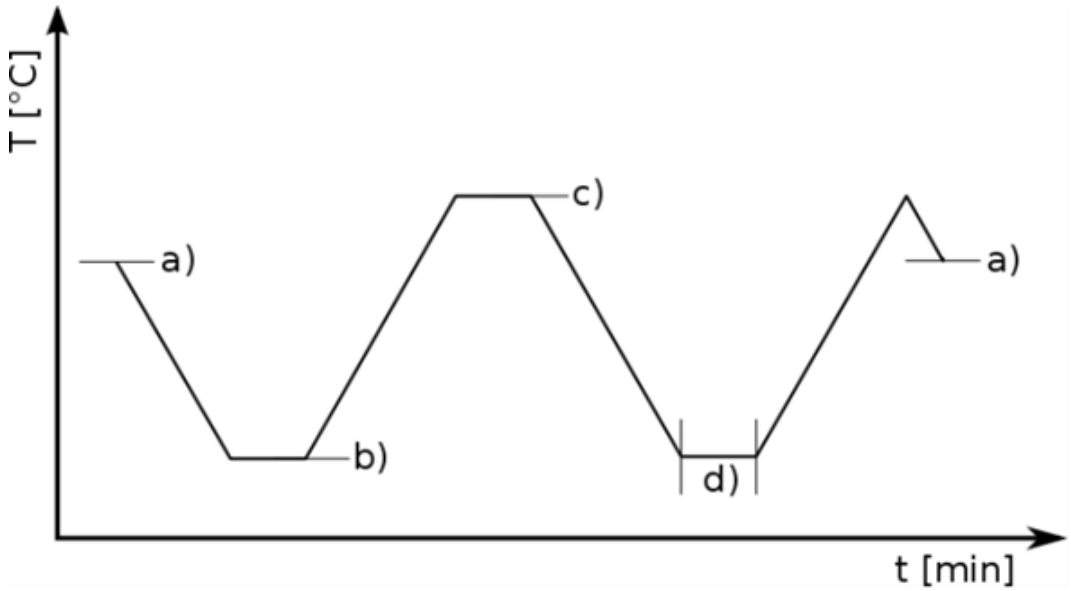

Figure 4.4: Schema of the DSC cycles used to carry out the measurements.

Samples were heated within the range 298 – 318 K (b) and d) points on the y axis on the Fig. 4.4) and carried out at the heating and cooling rate (slope of the line between the b) and c) or c) and d), respectively, on the Fig.4.4) 10 K/min for samples with PVME without additives. There were heating and cooling rates of 5 K/min over a range of 275 – 325 K for PVME with additives and 295 – 335 K range with rate 5 K/min for IPNs and SIPNs, respectively. Delay between next step was 2 min for all samples. In the aluminum pan there were 8.9 – 18.4 mg of samples. The transition was characterized by calculation of the enthalpy changes per unit mass of polymer through integration of the experimental DSC thermograms.

4.2.2 NMR

High-resolution ^{1}H NMR spectra were obtained with a Bruker Avance 500 and Bruker 600 MHz Avance III spectrometers (Billerica, MA, USA). 5 mm NMR tubes were always used for all samples. Before each NMR experiment, the samples were kept at the final experimental temperature always for at least 15 min. Temperature was maintained constant within ±0.2 K using a BVT 3000 temperature unit. The integrated signal intensities were determined with the spectrometer integration software Topspin with an accuracy of 1%. All the obtained T_2 relaxation curves had the monoexponential character and relative error for then discussed T_2 values did not exceed ±5%.

Typical conditions for ^{1}H NMR spectra detection were as follows:

- spectral width 5 kHz

- pulse width 10 s (Π/2 pulse)
- length of the Π/2 pulse between 12.5 μs
- relaxation delay 20 s
- relaxation delay of 100 s in quantitative measurements of HDO signals
- 8 scans or 16 scans

The ^{1}H spin-spin relaxation times T_2 were detected with parameters:

- CPMG pulse sequence $90^{\circ}_{x} - (t_d - 180^{\circ}_{x} - t_d)_n$
- acquisition width td = 0.5 ms
- acquisition time 1.64 s
- D1 delay between two scans 100 s
- 8 scans
- an array of ∼35 values

Conditions for ^{13}C to determine the real compositions of the IPNs:

- frequency 125.7 MHz
- spectral width of 30 kHz
- Π/2 pulse width 9.5 or 10.5 μs
- relaxation delay 80 s
- full proton decoupling

4.2.3 OM

Optical Microscope sample were prepared by tapping a 10 μl droplet of the sample on the microscope support slide with 75 by 25 mm and were covered by standardized cover slips. Thanks to that thin layer was produced. Edge were sealed by nail-polish to unable the external air go inside or the sample go outside or so-called "flow" during the measurements. Optical microscope photography was performed under nitrogen atmosphere using a Nikon eclipse 80i with camera PixeLINK PL-A662 and temperature-controlled cell Linkam LTS350, blow through with vapours of liquide nitrogen to ensure the proper temperature. Development of the morphology was observed with 50-fold magnification. The heating rate was 1 K/min, and before each temperature step, the samples were always maintained at the experimental temperature at least for 1 min.

4.3 Processing Methods

4.3.1 *p*-fraction

From the temperature dependent integral intensity of the ^{1}H NMR spectra for one of the peaks, parameter p could be obtained as:

$$p = 1 - \frac{I}{I_0}, \tag{4.1}$$

where I and I_0 are in general terms integrated intensities of polymer signal in the partly phase-separated(collapsed) system and if no phase separation (transition) occurs, respectively, and variable quantity p determines the fraction of the phase separated (collapsed) polymer units with reduced mobility above LCST (VPTT). For I_0, we took values based on integrated intensities as obtained at temperature T_0 below transition and taking into account the fact that the integrated intensities should decrease with absolute temperature as $1/T$, i.e., $I_0(T) = I_0(T_0/T)$ [57].

4.3.2 Van‘t Hoff Equation

Considering the phase separation as the competition between non-phase separated (coil) and phase separated (globule) states governed by the Gibbs free energy than the equilibrium constant K is given by the ratio [59]:

$$K = \frac{p}{1-p}. \tag{4.2}$$

Van't Hoff equation describes temperature changes of the equilibrium constant K of the coil–globule transition as follows:

$$lnK = \frac{-\Delta H}{RT}\frac{\Delta S}{R}, \tag{4.3}$$

where ΔH and ΔS are the changes in enthalpy and entropy, respectively, and R is the gas constant. If we apply eq. 4.2 into the eq. 4.3, the dependences of $Rln(p/(1-p))$ on $-1/T$ could be obtained.

4.3.3 Swelling ratio

As was described in subsection 1.2.4 the swelling ratio can be defined as:

$$SR = \frac{m_T - m_d}{m_d}, \tag{4.4}$$

where m_d is identified as weight for dry polymer and m_T as polymer swollen in the solution at certain temperature T.

5. Results – PVME water solutions

^{1}H NMR techniques combined with DSC experiments are employed to study dynamical and structural changes during the temperature-induced phase transition in aqueous poly(vinyl methyl ether) solutions. NMR data were used to construct van't Hoff plots and changes of the enthalpy and entropy characterizing the phase transition were determined.

This section is prepared from the results done by author and published in articles 1. and 2. from the List of publications. Text below use quotes or is inspired by these articles.

5.1 DSC

Thermal characteristics were examined by DSC for different PVME concentrations. Heating thermograms are seen in the Fig. 5.1.

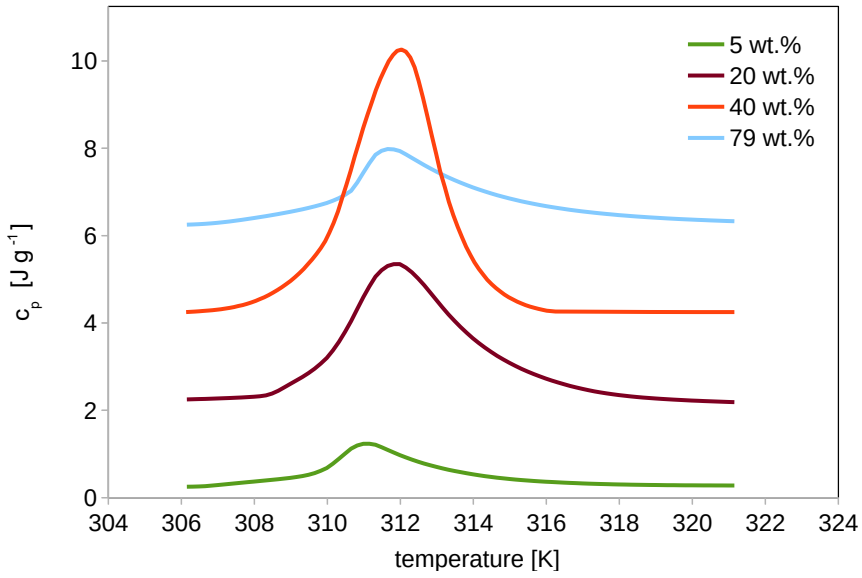

Figure 5.1: Heating DSC thermograms for various polymer concentrations. Curves are shifted vertically for clarity by the step of 2 Jg^{-1}.

It is obvious that the shape of the DSC peaks depends on polymer concentration. While temperature onset (which defines the origin of the transition) is not practically influenced by PVME concentration ($\sim 308\,\mathrm{K}$), the enthalpy values given as the peak area show maximum for polymer concentration $\approx 40wt.\%$ and this is in accord with literature [44], [45].

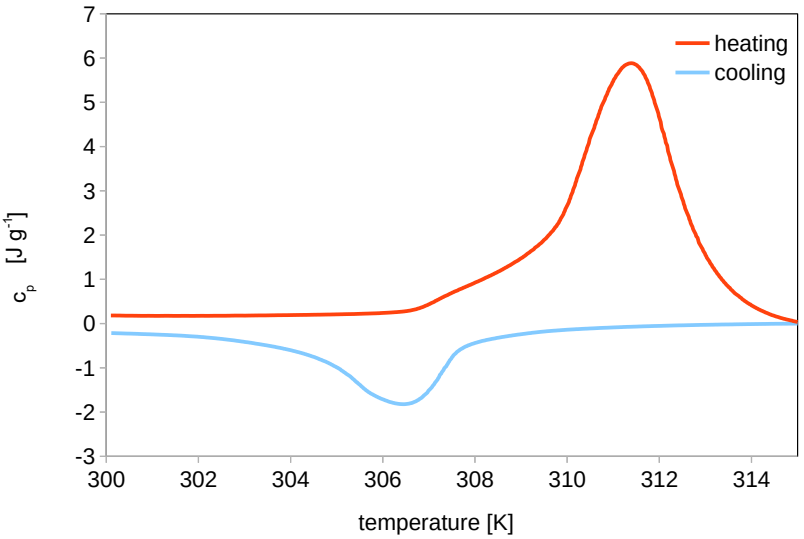

Figure 5.2: DSC thermogram for one complete cycle for $50wt.\%$ of PVME.

On the Fig. 5.2 we can see the cooling branch (bottom of the figure) and heating branch (upper part) of one cycle. It is clearly seen that during cooling the peak is shifted to lower temperatures and shows smaller enthalpy values in comparison with heating process. Cooling branch also has longer low-temperature "tail". The same behavior is observed for all the other samples if transition occurs. Different shape of DSC curves corresponds to different time scale of processes during formation (heating) and dissolving (cooling) of mesoglobules. This effect is also seen in concentration dependence of the enthalpy changes (per gram of polymer) as obtained from DSC heating and cooling branches (Fig. 5.2). The values of the exothermic enthalpy for cooling process is smaller in comparison with the values from heating and this difference strongly depends on the polymer concentration. In the case of cooling, a remixing transition from locally heterogeneous to homogenous state takes place. Here, the compact globules with low or almost no water content are available for hydrogen bonding but the water molecules must penetrate the globules interior. Moreover as it will be shown in the section 5.3, optical microscopy experiments revealed, that the size of globules in PVME solutions with $c = 20 - 50wt\%$ is approximately $5 - 10$ times larger than size of mesoglobules in PVME solution with $c = 5wt\%$, so penetration of large agglomerates takes much longer than in the case of small globules. When the concentration c is increasing over $60wt\%$, a molecular complex between water and PVME is composed of maximum two water molecules per monomer unit [26] and the enthalpies corresponding to formation and dissolution of globules become smaller and equivalent.

On the Fig. 5.4 we draw the differences of the onset temperature corresponding to heating and cooling branches. The solutions with polymer concentrations $50 - 60wt.\%$ show maximum differences and it corresponds to the middle region where enthalpies of separation and remixing diverges. Samples with low ($0 - 20wt.\%$) and high ($75 - 90wt.\%$) PVME concentrations show no divergence in onset temperatures.

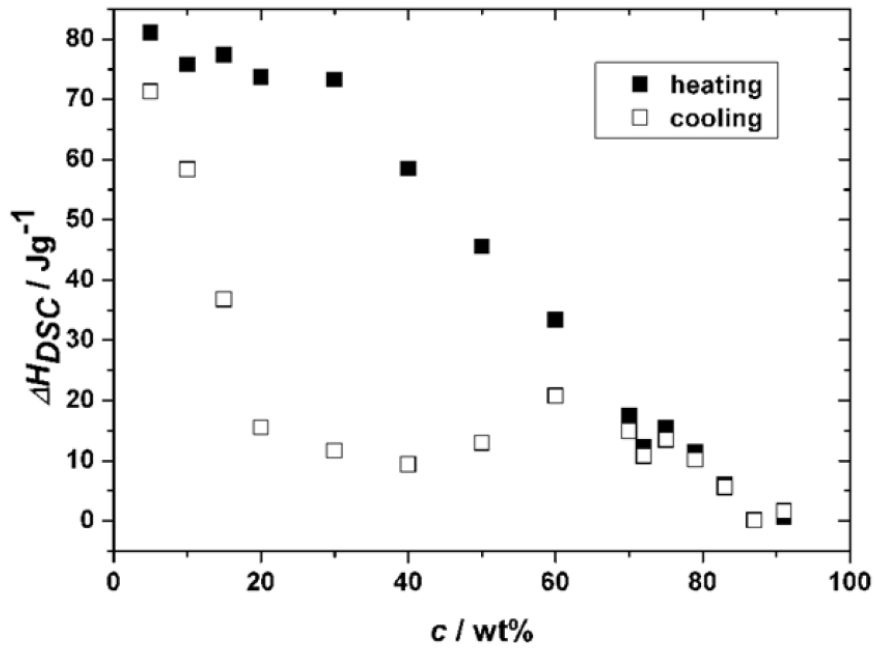

Figure 5.3: Concentration dependence of the enthalpy change per gram of polymer for DSC heating and cooling scans.

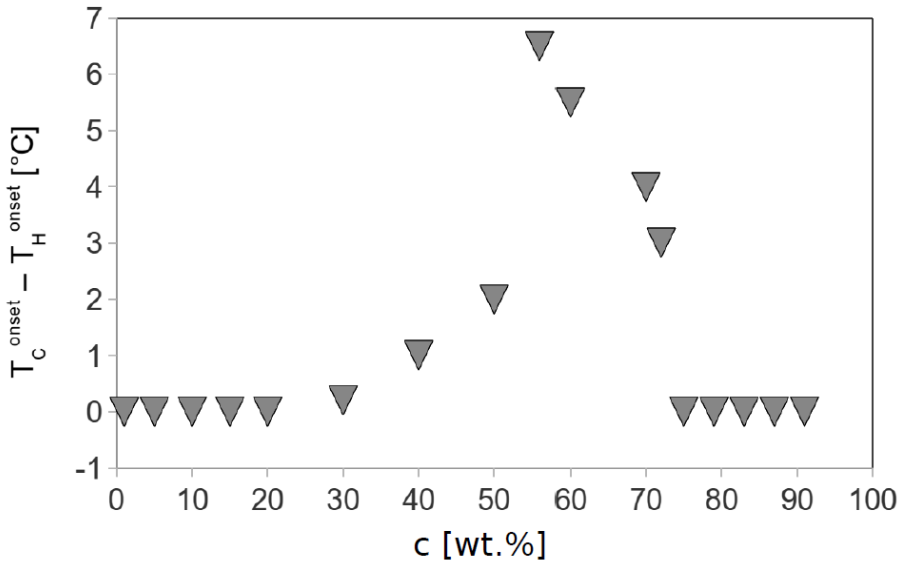

Figure 5.4: Polymer concentration dependence of the onset temperature differences as obtained from heating and cooling process.

5.2 NMR

High-resolution ^{1}H NMR spectra of $30wt.\%$ solution of PVME in D_2O solution for two different temperatures are shown in Fig. 5.5. Substantial decrease of integrated intensity for CH, CH_2 and CH_3 units of PVME bands is the most observable effect. Mobility of polymer units involved in compact globular structures

is extremely reduced and this is manifested in the NMR spectra by marked line broadening for major part of PVME units.

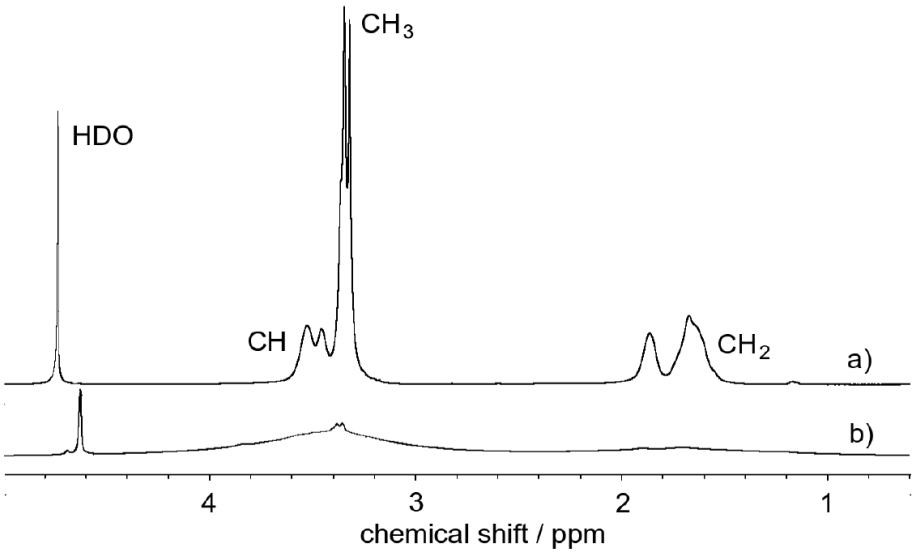

Figure 5.5: ^{1}H NMR spectra of 30$wt.\%$ PVME solution a) 298 K b) 310 K.

From the temperature dependent integral intensity, parameter p and equilibrium constant K were calculated using the eq. 4.1 and the eq. 4.2 (section 4.3), respectively. If eq. 4.2 is applied to the eq. 4.3 dependences of $Rln(p/(1-p))$ on $-1/T$ in so-called van't Hoff plot could be obtained for the solutions PVME with various polymer concentrations (Fig. 5.6).

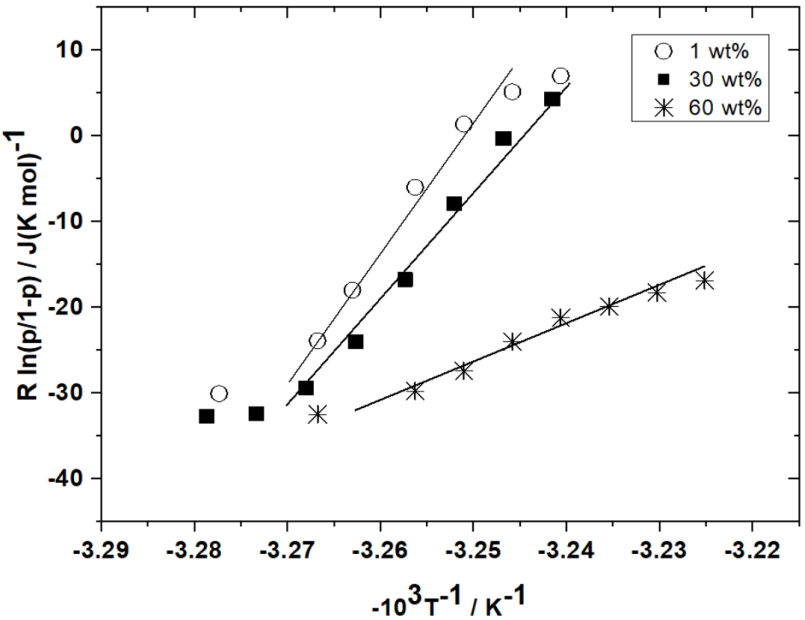

Figure 5.6: The van't Hoff plot for the phase transition in PVME solutions with various polymer concentrations. Solid lines are fits according to eq. 4.2 and 4.3.

The parameters ΔH_{NMR} and ΔS_{NMR} from the fitted dependences for PVME solutions are summarized in Table 5.1. From this Table it follows that both

ΔH_{NMR} and ΔS_{NMR} are positive and their values correspond to breakdown of hydrogen bonds between polymer and water and disruption of hydrophobic hydration [110]. Assuming that the phase transition is a cooperative process and the polymer chain consists of cooperative units (domains) which undergo transition as a whole [62], the values ΔH_{NMR} are thus related to mol of cooperative units.

Table 5.1 contains also enthalpy changes ΔH_{DSC} as obtained from DSC measurements. These values can be recalculated to mol of monomer units and compared with those determined from NMR. From the ratios $\Delta H_{NMR}/\Delta H_{DSC}$ the number of monomer units in one domain can be determined (cf. Table 5.1). For PVME solutions with c = 1–30$wt.\%$ the size of domains agrees quite well with average degree of polymerization (DP ∼348) so showing that in this case the cooperative unit is the whole polymer chain. From Table 5.1 it follows that the size of domain decreases for solutions with higher $c = 50$ and 60$wt.\%$. This tendency to form smaller domains could follow from more significant influence of interchain interactions as well as from the occurrence of non-hydrated PVME units in solutions with higher polymer concentrations.

c [$wt.\%$]	ΔH_{NMR} [MJ mol^{-1}]	ΔS_{NMR} [kJ (Kmol)$^{-1}$]	ΔH_{DSC} [J g^{-1}] of polymer	number of mon.u. in domain
1	1.56	5.10	82	328
6	1.69	5.59	81	360
10	1.46	4.75	76	331
30	1.34	4.35	73	316
50	0.55	1.77	46	206
60	0.42	1.40	34	213

Table 5.1: Thermodynamic parameters determined by using NMR and DSC data and number of monomer units in the domain for PVME solutions of various concentrations.

5.3 Optical Microscopy

Optical micrographs as obtained for PVME solutions with various concentrations are depicted in Fig. 5.7. For lower concentration $c = 5wt.\%$, formation of rather spherical globular structures with the radii in the range 1 – 3μm is seen. As the polymer concentration is increasing up to $c = 50wt.\%$, globular structures are increasing in their size ($\sim 10\mu m$) similarly as it was observed for PVME/water/ethanol solutions [52]. Globular structures formed in the highly concentrated PVME solutions ($c > 50wt.\%$) are then smaller as the water content in solution is not sufficient to form complex with PVME, water-polymer hydrogen bonds are thus less frequent and the phase separation becomes less pronounced. This corresponds to smaller values of the transition enthalpies as it was shown in the section 5.2.

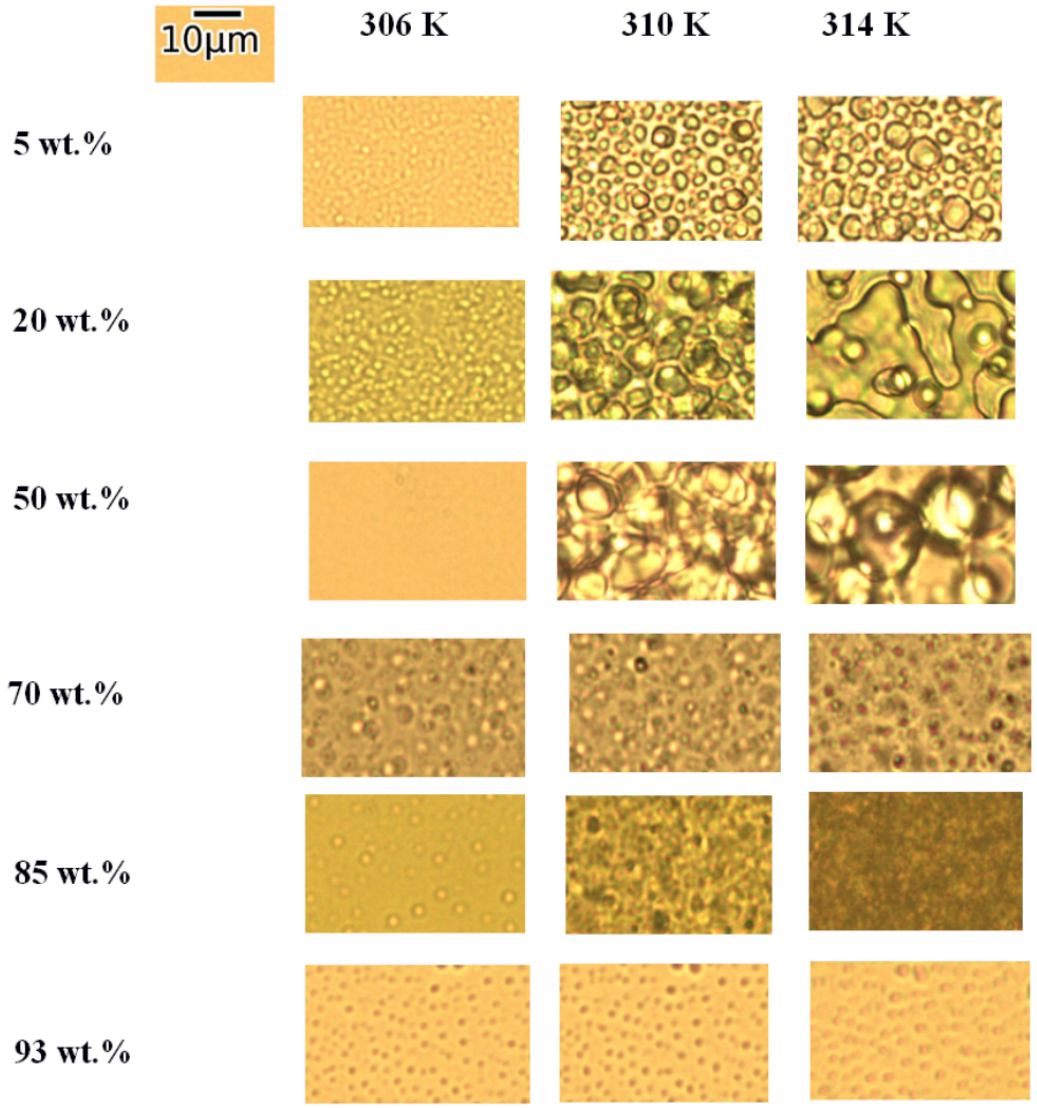

Figure 5.7: OM images during the heating for various PVME concentrations at different temperatures.

6. Results – PVME water solutions with additives

In this chapter we perform a comparative analysis of the phase separation of PVME in the presence of structurally similar additives, *t*–Butyl methyl ketone (TBMK), *t*–Butyl methyl ether (TBME), *t*–Butylamine (TBAm) and *t*–Butanol (TBOH) differing in individual chemical groups (carbonyl, ether, amine and hydroxyl group, respectively). Several experimental techniques is used in this investigation. NMR spectroscopy was applied to individually analyze the additive, water and polymer segments and analyze their mobility and interactions during the transition. DSC and optical microscopy were used to characterize the macroscopic behavior. Differences in the mechanism of transition because of the presence of these additives are discussed.

This section is prepared from the results published in article 5. from the List of publications. Text below use quotes or is inspired by this article.

6.1 NMR

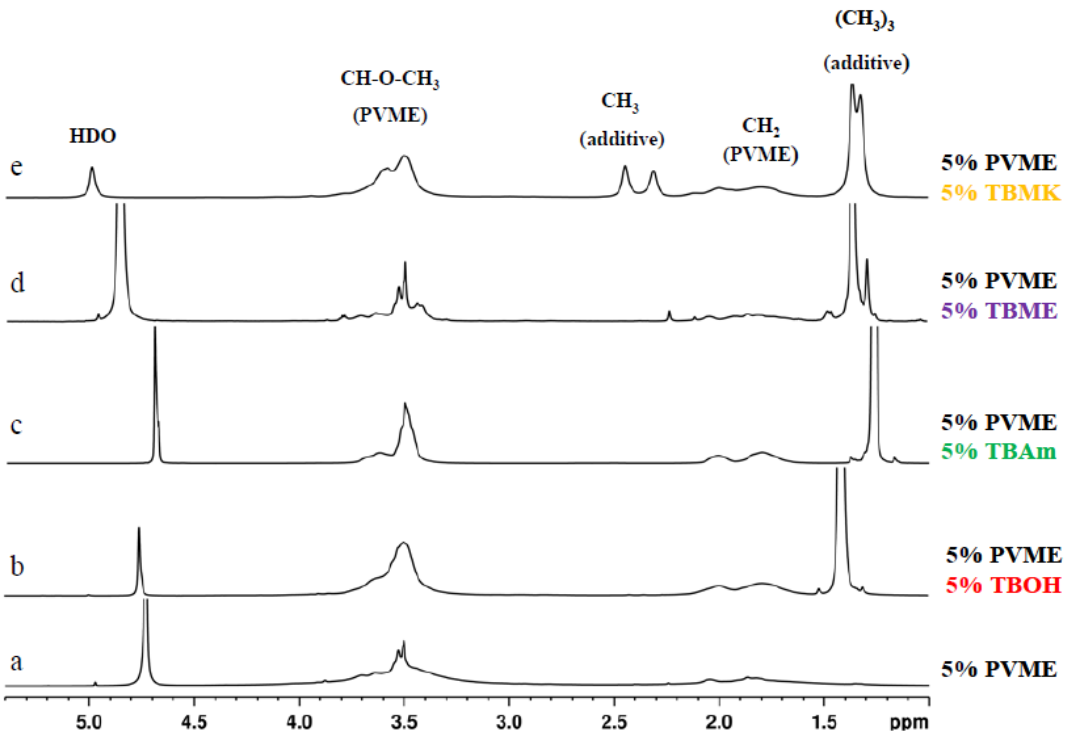

Figure 6.1: High-resolution ^{1}H NMR spectra of D_2O solutions of neat PVME ($c = 5wt.\%$) (a); and solutions with additives TBOH (b); TBAm (c); TBME (d); and TBMK (e) ($c = 5wt.\%$, $c_{ad} = 5wt.\%$) measured at temperatures above the transition of each particular system.

Fig. 6.1 shows ^{1}H NMR spectra as detected for the neat aqueous PVME solution and solutions of PVME with additives at temperatures above the transition of each particular system. The shapes of the peaks in the spectra are different for individual additives and for the pure PVME solution. Similarly as in the aqueous PVME solutions, the intensity and shape of the polymer, additive, and water HDO signals in NMR spectra vary with temperature. The polymer signal vanishes from the high-resolution NMR spectra because of broadening (often extreme) of the polymer peak due to the restriction in the mobility of polymer chains upon formation of the solid-like globules [54].

In Fig. 6.1 we can distinguish two types of polymer peaks. The first type corresponds to flexible polymer segments which are not involved in compact globular structures (the narrow part of the CH_3O peak at 3.5 ppm in spectrum a, Fig. 6.1). The second type is assigned to the major part of polymer units which form solid-like globular structures (the broad part of the same peak from 4 to 5 ppm). The presence of additives strongly influences the shape of both polymer band components. As it follows from Fig. 6.1, the signal of the globular units is extremely broadened, so it is no longer visible in the spectra (spectra in Fig. 6.1 b–e); this disappearance indicates that the polymer units involved in globules formed in solutions with additives show higher immobilization in comparison with collapsed units in the solution of neat PVME. Further, it is seen in Fig. 6.1 that the shape of NMR signal corresponding to PVME group $CHOCH_3$ depends on the type of additive. The solution with TBME shows quite narrow $CHOCH_3$ peak whereas, for solutions with others additives, this peak broadens.

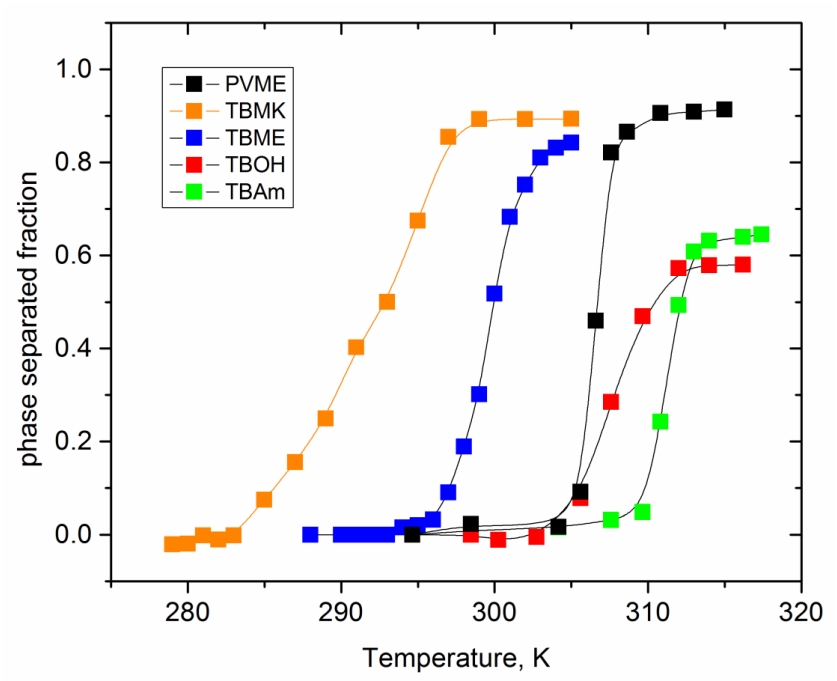

Figure 6.2: Temperature dependences of the fraction p as obtained from integrated intensities of $CHOCH_3$ protons of PVME in neat PVME solution ($c = 5wt.\%$ in D_2O) and PVME/additives solutions ($c = 5wt.\%$, $c_{ad} = 5wt.\%$ in in D_2O).

For further analysis, we determined the fraction of PVME units in concen-

trated, polymer-rich phase (fraction p) using the eq. 4.1 (section 4.3). Fig. 6.2 shows temperature dependences of the fraction p as obtained from integrated intensities of $CHOCH_3$ protons of PVME in neat PVME solution ($c = 5wt.\%$) and PVME solutions with additives ($c_{ad} = 5wt.\%$). It follows that all solutions with additives exhibit broader transition region than the solution with neat PVME; this effect is the most significant in PVME/TBMK solution where the transition is ∼12 K broad. For all polymer and additive concentrations investigated, the solutions show a qualitatively similar behavior of the polymer $CHOCH_3$ proton intensities.

From temperature dependences of the fraction p the transition temperature was detected as the temperature in the middle of the transition, i.e., where the signal has decreased by 50%. Fig. 6.3 shows the dependence of transition temperature on additive concentration for solutions with $c = 5wt.\%$. It is seen that increasing the concentration of the additives TBMK and TBME in the solutions significantly decreases the transition temperature. It indicates that TBMK and TBME promotes destabilization of the hydration structure surrounding the polymer chain. As it is shown in Fig. 6.3, this effect is more pronounced for TBMK. The presence of the ether additive only results in changes of the transition temperature, and no broadening of the transition region was observed. Similarly as TBMK and TBME, higher alcohols, and simple inorganic salts tend to destabilize the structure, i.e., lead to lower transition temperatures in aqueous solutions of PVME [43]. The values of fraction p above the transition in PVME/TBMK and PVME/TBME solutions reach ∼0.9 similarly as the values in neat PVME solution. We assume that the remaining minority mobile component (∼ 10%), which does not take part in the phase transition, comes from low-moleuclar weight oligomers as it was shown for PVME/D_2O solutions [55].

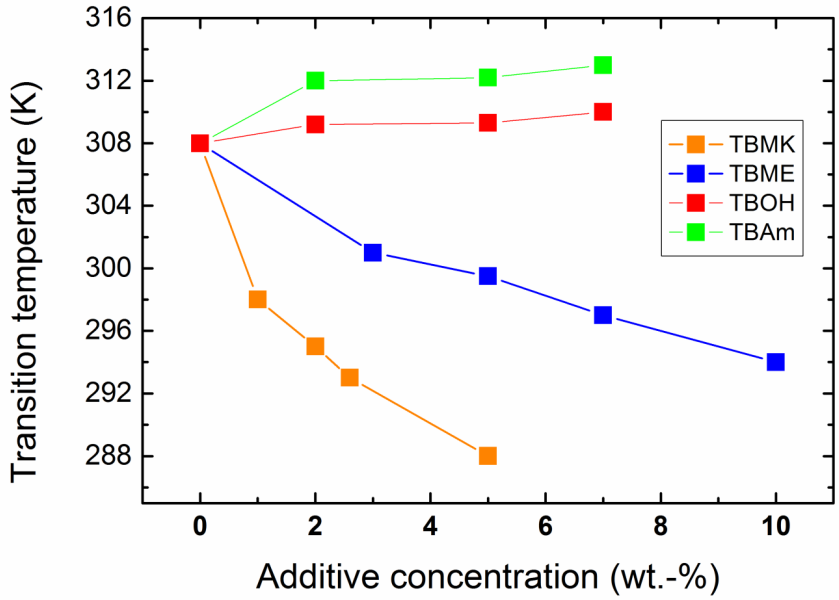

Figure 6.3: Concentration dependence of the transition temperature for PVME/-additives solutions ($c = 5wt.\%$ PVME in D_2O).

On the other hand for TBAm and TBOH, increasing concentration was observed to lead to a slight shift of transition temperature to higher values; at the

same time the transition extent (maximum values of fraction p above the transition in Fig. 6.2) decreases as compared with the neat PVME. TBAm and TBOH molecules obviously stabilize polymer-solvent interactions and prevent hydrophobic polymer-polymer interactions. Such stabilizing effect was detected in aqueous solutions of PVME and lower molecular weight alcohols [43, 52, 67].

The effect of polymer concentration on the phase transition of solutions with hydrophilic and hydrophobic additives (TBAm and TBME, respectively) is seen in Fig. 6.4. For higher PVME concentrations ($c = 10wt.\%$) in PVME/TBAm solution, the dependence is shifted by $\sim$4 K to lower values. This shift of the transition is probably a consequence of the preferred polymer-polymer contacts at higher concentration, allowing hydrophobic interactions to predominate at lower temperatures. More complicated behavior was detected for solutions with hydrophobic TBME. An increase of the transition temperature is observed for additive concentration $c_{ad} = 3wt.\%$ and higher polymer concentration, apparently since the number of hydrophobic additive molecules per polymer segment decreases and, thus, hydrophobic interactions of the additive with the chain are reduced. Subsequently, for more concentrated polymer solutions and $c_{ad} > 5wt.\%$, the transition temperature decreases by $\sim$4 K. The solvent quality for such high TBME concentrations is probably reduced and the phase transition occurs already at lower temperatures. These two different mechanisms controlling LCST shift were described for aqueous solutions of poly(N–isopropylacrylamide) and hydrophobic benzaldehydes [3].

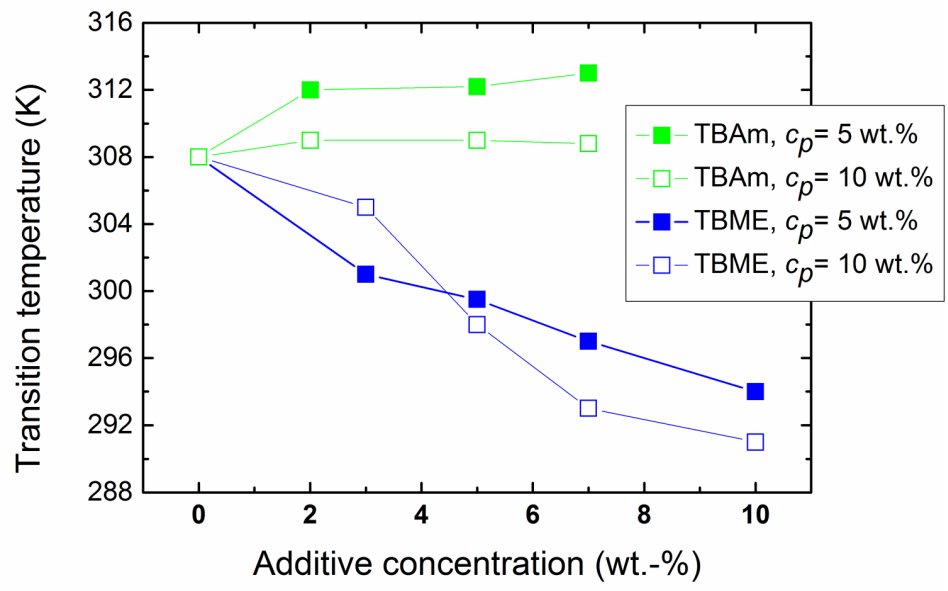

Figure 6.4: Concentration dependence of the transition temperature for PVME/-TBME and PVME/TBAm solutions for two various polymer concentrations $c = 5$ and $10wt.\%$ PVME in D_2O.

6.2 Mobility of Water and Additives

A comparative analysis of T_2 of water and additive molecules was performed at temperatures below and above the transition to follow the changes in the dynami-

cal behavior of these molecules in the presence of the polymer. In this respect it is useful to introduce T_{2r} as the ratio of T_2 values measured in the polymer-additive system $T_2(pvme + additive)$ and in the corresponding additive/D_2O solution $T_2(additive)$ at the same temperature ($T_{2r} = T_2(pvme + additive)/T_2(additive)$) [3]. The value of T_{2r} gives temperature-independent information about the extent of the immobilization of the water and additive molecules caused by the presence of the polymer. The comparison of these quantities for HDO molecules and for the *t*–butyl group of the additives is given in Table 6.1. If no interaction with the polymer occurs, the value of T_{2r} should be equal to 1 (if the effects of viscosity can be neglected).

The lower the resulting value T_{2r} the higher the immobilization effect caused by the polymer–water or polymer–additive interaction.

	TBMK		**TBME**		**TBOH**		**TBAm**	
LCST	HDO	$(CH_3)_3$	HDO	$(CH_3)_3$	HDO	$(CH_3)_3$	HDO	$(CH_3)_3$
below	0.16	0.42	0.78	0.78	0.65	0.92	0.60	0.88
above	0.14	0.32	0.60	0.54	0.34	0.30	0.83	0.79

Table 6.1: T_{2r} parameters for the PVME/additive solutions ($c = 5wt.\%$, $c_{ad} = 5wt.\%$).

It follows from Table 6.1 that, for the solution with TBMK, T_{2r} of water and *t*–butyl group reach substantially lower values indicating that water and additive molecules are strongly involved in interactions with the polymer at temperatures both below and above LCST. For TBME, the solvent and additive molecules are only slightly affected by the presence of the polymer. Relaxation parameters T_{2r} detected in PVME/TBOH and PVME/TBAm solutions below LCST reach similar values. T_{2r} values of the additive *t*–butyl group are almost equal to 1, values as obtained for water molecules are somewhat lower which could indicate a slight interaction with the polymer as well as the influence of chemical exchange. Different relaxation behavior of molecules in solutions with hydrophilic additives was found at elevated temperatures above LCST.T_{2r} values of molecules in PVME/TBAm solution remain high even above the transition while a reduction of T_{2r} values was observed for water and additive molecules in PVME/TBOH solution. The greater immobilization above the transition temperature for TBOH and water can be attributed to the effect of incorporation of a certain portion of these molecules into the globular structures.

6.3 Cooperativity of the Transition

The temperature dependences of p fraction shown in Fig. 6.2 can be used for determining the enthalpy and entropy changes during phase transition, considering this process as the competition between non-phase separated (coil) and phase separated (globule) states governed by the Gibbs free energy. The van't Hoff equation then describes temperature changes of the equilibrium constant K (Chapter 4.3). Fig. 6.5 exemplifies Van't Hoff plot for PVME/TBMK and PVME/TBME solutions ($c = 5wt.\%$, $c_{ad} = 5wt.\%$).

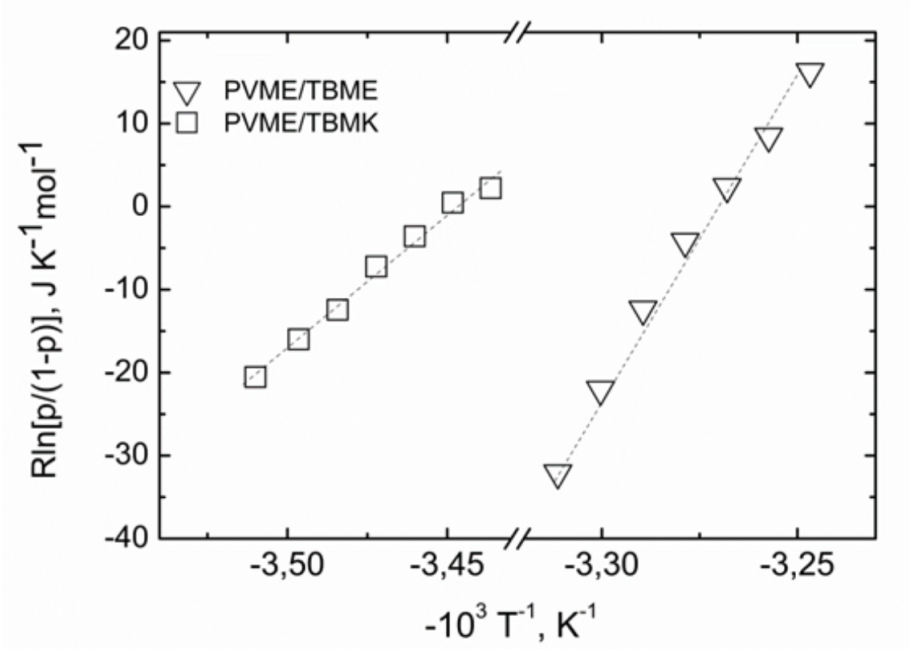

Figure 6.5: Van't Hoff plot for the phase transition in PVME/TBMK and PVME/TBME solutions ($c = 5wt.\%$, $c_{ad} = 5wt.\%$). Dot lines are fits according to eq. 4.2 and 4.3.

The parameters ΔH_{NMR} fitted from the eq. 4.3 are summarized in Table 6.2. Table 6.2 contains also enthalpy changes ΔH_{DSC} as obtained from DSC measurements and recalculated to the mol of monomer units. Similarly as in the case of neat PVME solutions (Chapter 5), enthalpy values ΔH_{DSC} can be compared with those determined from NMR. The ratio $\Delta H_{NMR}/\Delta H_{DSC}$ corresponding to the average number of monomer units in one cooperative domain are summarized in Table 6.2. For the $5wt.\%$ solution of neat PVME and solutions of PVME with TBME and TBAm ($c_{ad} = 5wt.\%$), the size of the domains agrees quite well with the average degree of polymerization (DP of PVME $\sim$348), thus showing that, in this case, the cooperative unit is the whole polymer chain. For solutions with TBMK and TBOH ($c_{ad} = 5wt.\%$), these domains are smaller and consist of only 140 and 170 monomer units, respectively. As follows from relaxation experiments, a certain amount of water and additive molecules is incorporated into the globules formed in these two solutions. This process is obviously time-consuming and disrupts the cooperativity of the transition; cooperative units are smaller and the phase transition is broader.

6.4 Optical Microscopy

The difference in the structure and size of the polymer globules in the presence of the additives can be demonstrated by the optical microscopy images shown in Fig. 6.6. This figure shows that globular stuctures formed above LCST transition in aqueous PVME/TBMK and PVME/TBOH are somewhat smaller than those observed for solutions PVME/TBAm, PVME/TBME and neat PVME.

This finding corresponds to the data in Table 6.2 where size of cooperative domains as calculated for PVME/TBOH and PVME/TBMK solutions is about

	ΔH_{NMR}	ΔH_{DSC}	Number of monomer units
	MJ/mol	kJ/mol	in domain
neat PVME	1.32	4.05	326
PVME + TBMK	0.32	2.23	143
PVME + TBME	0.78	2.32	336
PVME + TBOH	0.40	2.30	174
PVME + TBAm	0.58	1.98	293

Table 6.2: Thermodynamic parameters determined by NMR and DSC and the number of monomer units in the domain for mixtures of $5wt.\%$ PVME.

twice smaller in comparison with domains formed in other solutions and this is obviously macroscopically manifested in smaller polymer aggregations. Interestingly enough, polymer agglomerates formed in PVME/TBME solutions show strong separation and well-defined surfaces. This could be the consequence of the fact that 90% of polymer chains are involved in the collapsed structures, as follows from the fraction p above the transition, and at the same time these structures do not contain any bound water or additive.

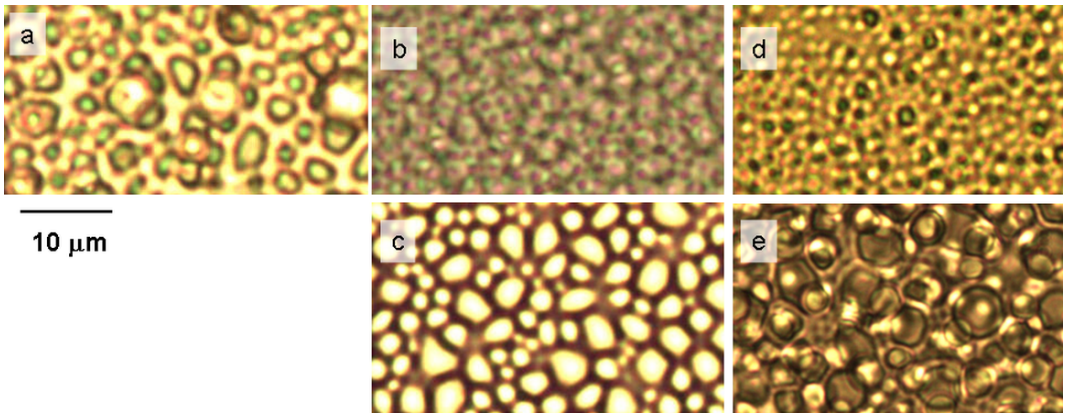

Figure 6.6: Photomicrographs of the neat PVME solution ($c = 5wt.\%$ PVME in D_2O) (a) and solutions with additives TBMK (b); TBME (c); TBOH (d); and TBAm (e) ($c = 5wt.\%$, $c_{ad} = 5wt.\%$) recorded at temperatures above the transitions of the particular systems.

7. Results - IPNs of PNIPAm, PVCL, PAAm

In this section, collapse transition in hydrogels of IPNs of thermoresponsive PNIPAm and PVCL and hydrophilic PAAm was studied by a combination of NMR spectroscopy, swelling and DSC experiments. Besides the effect of IPN composition on the volume phase transition we investigated IPNs with a reversed sequence of the two components in the preparation procedure, i.e., both PNIPAm/PAAm and PAAm/PNIPAm IPNs. The behavior of prepared IPNs was compared with aqueous mixtures of linear PNIPAm and PAAm which were considered as model systems for corresponding IPN hydrogels. IPNs PVCL/PNIPAm where both components are thermoresponsive were studied as well.

This section is prepared from the results published in articles 3. and 4. from the List of publications. Text below use quotes or is inspired by these articles.

7.1 Characterization

The IPNS consisting of PNIPAm, PAAm or PVC are two-component systems. The real ratios of these components in IPNs were determined from the integrated intensities of the respective C=O peaks in ^{13}C NMR spectra using the fact that chemical shifts of C=O carbons in PNIPAm, PAAm and PVCL units are somewhat different. The values of the real composition (the molar ratio of respective monomer units) of investigated IPNs obtained in this way are shown in Table 7.1. For the PNIPAm/PAAm samples the obtained real ratios were confirmed by values obtained from ^{1}H NMR integral intensities of the signal C corresponding to isopropyl CH protons of NIPAm units and signal G corresponding to CH_2 protons of NIPAm and AAm units (cf. Fig. 7.3). The molar ratios as obtained from ^{13}C and ^{1}H spectra were determined with relative errors 6% and 3%, respectively. Compositions (the molar ratio of respective monomer units) of investigated IPNs obtained from ^{13}C and ^{1}H NMR spectra are virtually the same as shown in Table 7.1. In the case of PVCL/PNIPAm samples, the real composition was not determined from ^{1}H spectra due to strong overlapping of signals. From Table 7.1 it follows that the real content of the component prepared as the first is in the IPN always somewhat higher than the content of the respective monomer. Evidently, polymerization of the second component did not proceed to full conversion and remaining monomer was washed out. In further text we used for designation of samples values determined from ^{13}C NMR spectra. Sample PNIPAm/PAAm sol in Table 7.1 denotes D_2O solution of the mixture of PNIPAm and PAAm homopolymers in the ratio which is identical to the composition of PAAm/PNIPAm IPN 42/58.

	composition monomer ratio in synthesis	molar ratio from ^{13}C NMR spectra	molar ratio from ^{1}H NMR spectra
PNIPAm	100/0	100/0	100/0
PNIPAm/PAAm	80/20	82/18	83/17
PNIPAm/PAAm	70/30	78/22	79/21
PNIPAm/PAAm	60/40	69/31	68/32
PNIPAm/PAAm	50/50	60/40	60/40
PAAm/PNIPAm	30/70	42/58	40/60
PAAm/PNIPAm	40/60	61/39	59/41
PNIPAm/PAAm sol	58/42	58/42	58/42
PVCL/PNIPAm	30/70	54/46	
PVCL/PNIPAm	30/70	50/50	
		rel. error 6%	rel. error 3%

Table 7.1: Theoretical and experimental compositions of PNIPAm/PAAm, PAAm/PNIPAm and PVCL/PNIPAm hydrogels and mixed solution of linear PNIPAm/PAAm. The experimental compositions were determined from ^{13}C and ^{1}H NMR spectra.

The swelling ratio was determined at two temperatures 300 K (below VPTT) and 320 K (above VPTT) and it is summarized in the Table 7.2. To obtain m_T (cf. eq. 4.4 in section 4.3) values for 320 K, the samples were immersed in water for 3 days (measurement of the time dependences showed that such time is sufficient for attaining an equilibrium swelling ratio). As we can see hydrogels containing hydrophilic PAAm show higher swelling ratios at both temperatures than other IPNs.

	components molar ratio	swelling ratio 300K	swelling ratio 320K
PNIPAm	100/0	13.3	1.3
PNIPAm	100/0	13.3	1.3
PNIPAm/PAAm	82/18	19.1	3.6
PNIPAm/PAAm	78/22	18.1	3.6
PNIPAm/PAAm	69/31	15.8	3.5
PAAm/PNIPAm	42/58	26.6	5.2
PVCL/PNIPAm	54/46	13.2	0.91
PVCL/PNIPAm	50/50	12.9	0.78
		rel. error 8%	rel. error 8%

Table 7.2: Swelling ratios below and above the phase transition of PNIPAm/-PAAm, PAAm/PNIPAm and PVCL/PNIPAm hydrogels.

7.2 DSC

DSC thermograms were measured for all IPN hydrogels, and the peak corresponding to endothermic transition was observed upon heating in most cases.

as it is seen for PNIPAm/PAAm and PAAm/PNIPAm IPNs samples and solution of their mixture are shown in Fig. 7.1. The DSC thermograms of the PVCL/PNIPAm hydrogels are shown in Fig. 7.2. The thermogram of the PVCL/PNIPAm (50/50) sample is virtually the same.

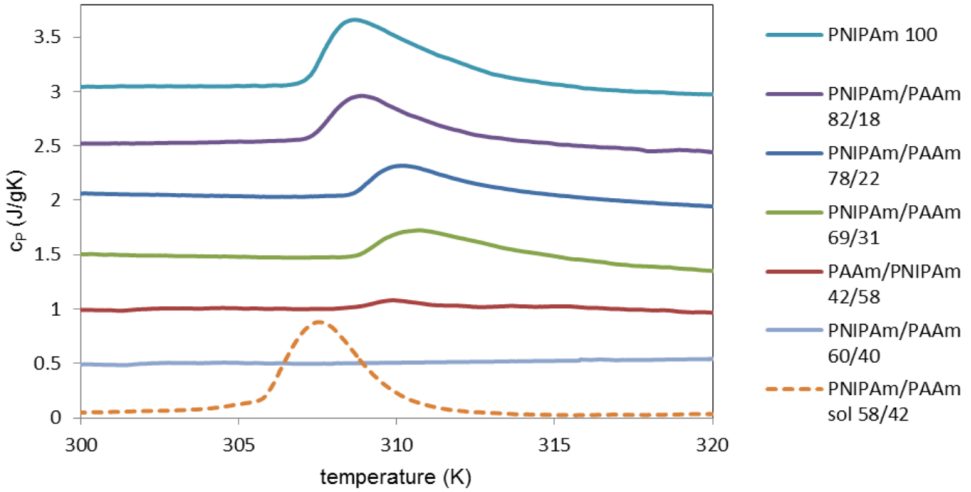

Figure 7.1: DSC thermograms of PNIPAm/PAAm and PAAm/PNIPAm hydrogels and mixed solution of linear PNIPAm/PAAm.

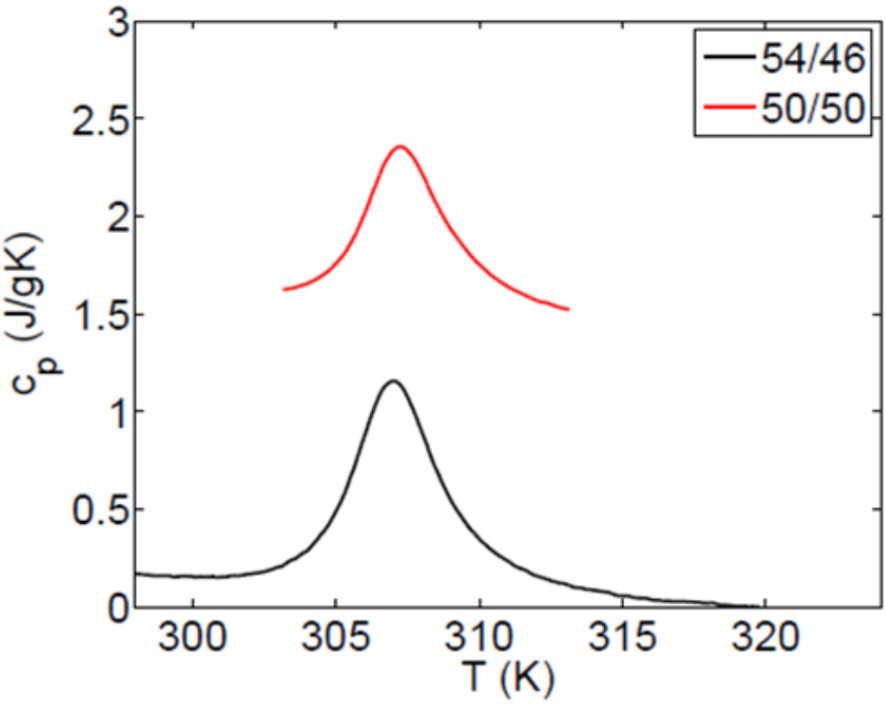

Figure 7.2: DSC thermograms of PVCL/PNIPAm hydrogels.

As it is obvious from Fig. 7.1 and 7.2 the DSC peak is rather symmetric for the PNIPAm/PAAm solution as well as for PVCL/PNIPAm networks. On the other hand, for PNIPAm/PAAm and PAAm/PNIPAm IPNs, it is asymmetrically

broaden in higher temperature side in contrast as a consequence of heterogeneity character of collapsed structures [49].

Samples		T_{on} [K]	T_{peak} [K]	ΔH [J/g of hydrogel or sol.]	ΔH [J/g of dry polym.]	ΔH [kJ/mol of polym. u. in d.p.
PNIPAm	100/0	306.7	308.6	2.8	39	4.5^a
PNIPAm/PAAm	82/18	306.9	308.9	1.5	29	4.1^a
PNIPAm/PAAm	78/22	308.4	310.1	1.4	27	4^a
PNIPAm/PAAm	69/31	308.9	310.6	1.2	20	3.3^a
PAAm/PNIPAm	42/58	308.6	310	0.2	6	1.1^a
PNIPAm/PAAm sol	58/42	305.7	307.5	2.4	30	5.9^a
PVCL/PNIPAm	54/46	304.1	307.0	2.3	31	4.0^b
PVCL/PNIPAm	50/50	305.0	307.1	2.2	29	3.7^b

Table 7.3: DSC parameters (see Fig. 7.1 and 7.2), where T_{on} is the onset temperature, T_{peak} is the peak temperature and ΔH is the enthalpy of the transition. (Values were calculated per mol of: ^{a} PNIPAm units in dry polymer; ^{b} PVCL and PNIPAm units in dry polymer.)

The onset and peak temperatures T_{on} and T_{peak} as well as the enthalpy ΔH of the transition were extracted in Fig. 7.1 and 7.2 (Table 7.3).

Critical transition temperature of PNIPAm/PAAm solution ($T_{on} \approx 305.7K$, $T_{peak} \approx 307.5K$) corresponds to critical temperature of neat PNIPAm [47, 111] and it is not affected by the presence of PAAm similarly as it was previously found for mixtures of PNIPAm and PNIPMAm [111]. In comparison with solution PNIPAm/PAAm and hydrogel of neat PNIPAm, IPNs show shift of the critical temperature to higher values with increasing content of PAAm. Together with the fact that hydrogels of IPNs PNIPAm/PAAm 60/40 and PAAm/PNIPAm 61/39 did not show any phase transition, these results are in accord with results which were found for aqueous solutions of random copolymers P(NIPMAm/AAm) where also increase of critical temperature with higher content of AAm units was observed [112, 113]. On the other hand, these results are opposite to finding of Shin et al. [91] for semi-interpenetrating networks PNIPAm/PAAm who by using DSC reported that VPTT decreased with the incorporation of PAAm. Critical transition temperature of PVCL depends on the molecular weight and polymer concentration [26, 105], and it is in the range 303–311 K which is closed to critical temperature of PNIPAm; therefore, for PVCL/PNIPAm networks, the transition temperatures of individual components are practically the same which leads to single DSC transition.

From Table 7.3 it follows that the enthalpy values recalculated per gram of dry polymer significantly depend on IPNs composition as well as on the order of components during preparation for PNIPAm/PAAm and PAAm/PNIPAm samples. ΔH values for IPN PNIPAm/PAAm 69/31 sample are three times larger than values for IPN PAAm/PNIPAm 42/58 with similar composition but reversed order in the synthesis procedure. Last column in Table 7.3 shows ΔH values calculated per mol PNIPAm units for hydrogels of PNIPAm/PAAm and

PAAm/ PNIPAm. These values are similar to those reported for gels of NIPAm copolymers [69], with exception of PAAm/PNIPAm 42/58 sample.

It follows from the literature that enthalpy ΔH values as obtained by DSC for cross-linked PVCL are somewhat lower than those for PVCL solutions, e.g., 1.9 kJ/mol [109] and 4.4 kJ/mol [114] for PVCL hydrogels and solutions, respectively. Higher ΔH values for IPN PVCL/PNIPAm as obtained by us in comparison with neat PVCL hydrogels according Mikheeva et al. [109] indicate that both PVCL and PNIPAm units are mutually involved in the collapse transition. The other attribute concerning to DSC thermograms of IPN PVCL/PNIPAm should be mentioned: as reported, neat PVCL hydrogels have shown two endothermic transitions: at 304.5 K, attributed to a microsegregation of hydrophobic domains, and at 310.6 K, corresponding to the gel volume collapse itself [109]. To the contrary, two-component IPNs containing PVCL show one endothermic peak at 307 K and this transition obviously covers all the interaction and volume changes.

7.3 NMR

In Figure 7.3 there are ^{1}H NMR spectra of PAAm/PNIPAm 42/58 hydrogel below the transition temperature at 298 K and above it at 315 K. The assignment of resonances to various proton types is shown directly in the spectrum measured at 298 K. The strong peak A corresponds to HDO, peaks C and H to isopropyl CH and CH_3 groups of PNIPAm, respectively. Main chain CH and CH_2 groups from both components have signals F and G, respectively.

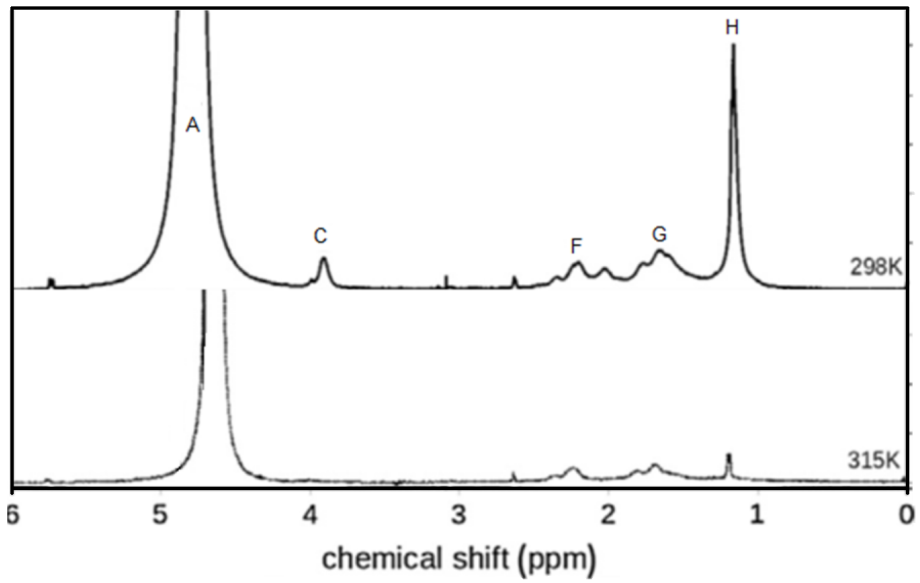

Figure 7.3: 500.1 MHz ^{1}H spectra of IPN hydrogel PAAm/PNIPAm (42/58) in D_2O recorded at 298 K and 315 K under the same instrumental conditions. Peak assignments are explained in the text.

Fig. 7.5 shows high-resolution ^{1}H NMR spectra of IPN PVCL/PNIPAm (50/50) measured under the same instrumental conditions at three temperatures. The assignment of resonances to various proton types is shown directly in the

spectrum measured at 300 K, i.e., below the VPTT of both polymeric components (cf. Fig. 7.5). The strong peak A corresponds to HDO. The signal marked by an asterisk at 3.6 *ppm* corresponds to CH_2 protons of residual ethanol (from sample preparation), and the signal of ethanol CH_3 protons overlaps with that of methyl protons of PNIPAm in the peak H.

The most important effect observed in the spectra measured at higher temperatures as shown in Figs. 7.3 and 7.5 is the marked decrease in the integrated intensity of all polymer signals. Evidently, at temperatures above the VPTT, the mobility of most PVCL and PNIPAm units in polymer chains is reduced to such an extent that the corresponding lines become too broad to be detected in high-resolution NMR spectra.

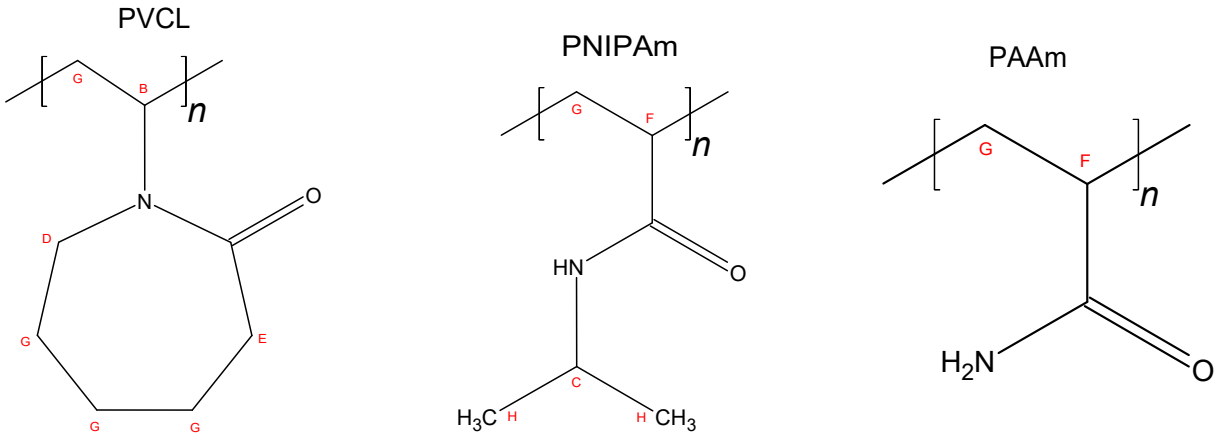

Figure 7.4: Structural formula of PVCL, PNIPAm, and PAAm repeating monomer units with marked groups from B to G.

To quantitatively characterize the phase transition, we have used the values of the collapsed p fraction obtained as in eq. 4.1 in section 4.3. Temperature T_0 used to obtain the integrated intensity I_0 of the signals for samples with PAAm was 298 K and for these with PVCL was 300 K, both low enough to be sure that samples are below the VPTT region. From Fig. 7.3 it follows that there are two types of polymer signals in NMR spectrum: PNIPAm signals (C and H) and mixed PNIPAm and PAAm signals (F and G).

In ^{1}H NMR spectrum for the PVLC samples in the Fig. 7.5 there are three types of polymer signals: PVCL signals (B, D, and E), PNIPAm signals (C, F, and H), and mixed PVCL and PNIPAm signal (G) which is predominantly determined by PVCL component (eight protons of PVCL monomer units and two protons of PNIPAm monomer units contribute to this signal, cf. Fig. 7.4). PVCL signals B, D, and E show significant broadening even at temperatures below VPTT (cf. Fig. 7.5), which makes their temperature analysis unfeasible.

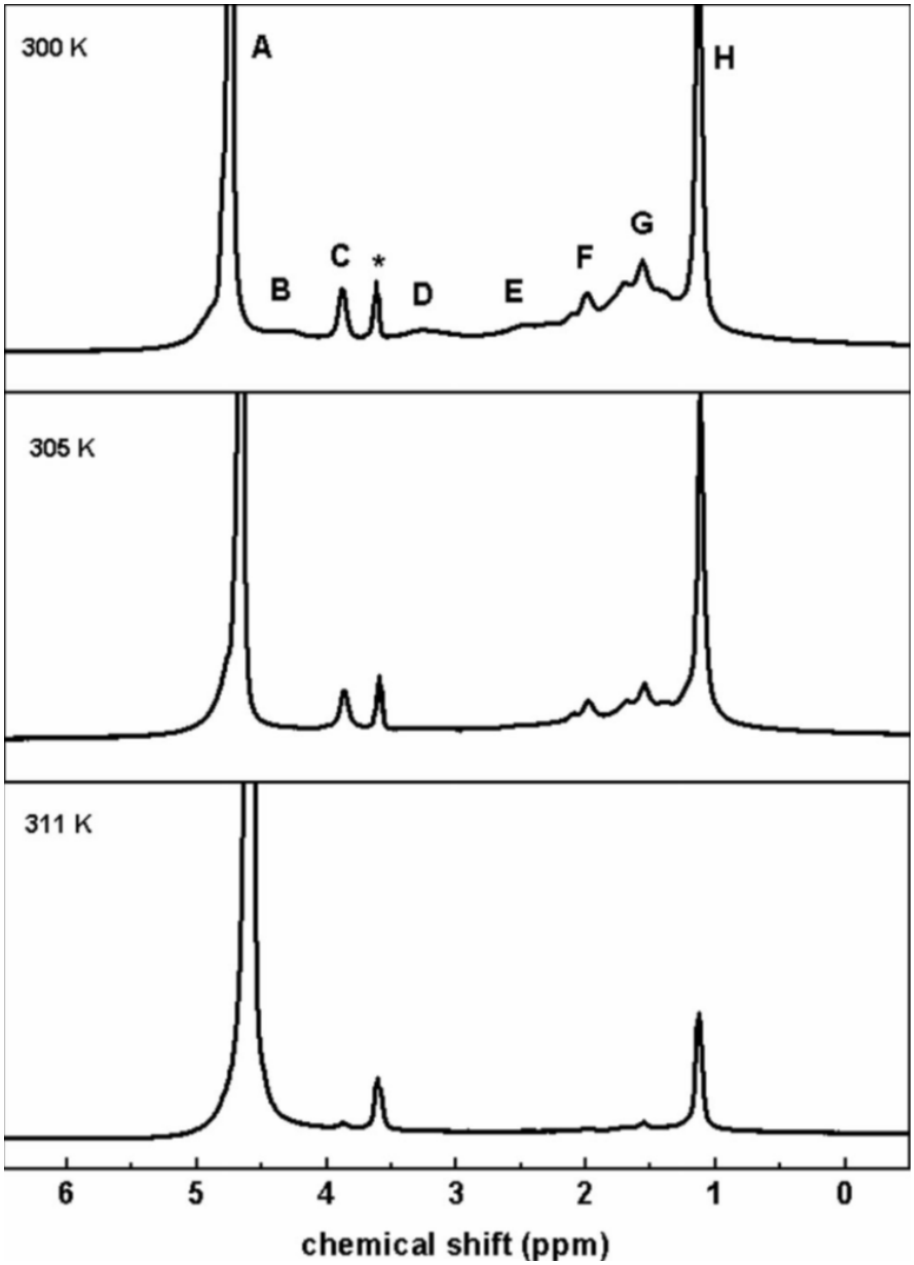

Figure 7.5: ^{1}H spectra (500.1MHz) of PVCL/PNIPAm (50/50) IPN hydrogel in D_2O recorded at 300, 305, and 311 K at the same instrumentál conditions. Peak assignments are explained in the text and in Fig. 7.4.

Temperature dependences of the p fraction, determined from the integrated intensities of the methyl signal of PNIPAm (signal H) are depicted in Fig. 7.6a; virtually same dependences were obtained from the PNIPAm isopropyl CH signal (signal C). In addition to PNIPAm/PAAm and PAAm/PNIPAm hydrogels ^{1}H NMR spectra were also measured for hydrogel of PNIPAm and for D_2O solution of the mixture of homopolymers PNIPAm/PAAm 58/42; temperature dependence of p-fraction for this solution is also presented in Fig. 7.6a. Analogously to DSC results, PNIPAm/PAAm mixed solution undergoes the phase separation in temperature region corresponding to the LCST of neat linear PNIPAm. Maximum values of p-fraction p_{max} is equal to 1 meaning that all PNIPAm units are involved in phase separated globular structures. From Fig. 7.6a it follows that the

transition temperature of PNIPAm hydrogel (temperature in the middle of the transition interval) is 307 K and the transition is relatively sharp (transition width 2.5 K). Introduction of the second hydrophilic component PAAm into networks PNIPAm/PAAm shifts VPTT to ∼310 K, transition interval is broader and maximum values p_{max} of PNIPAm methyl group are between 0.61 and 0.74 depending on composition of the network. From Fig. 7.6a it further follows that there is a marked effect of the process of IPNs preparation on the phase transition. Phase transition of IPN sample PAAm/PNIPAm 42/58 is shifted to ∼312 K and it is ca. 4 K broad. In accord with DSC results no phase transition was detected for PNIPAm/PAAm 60/40 and PAAm/PNIPAm 61/39 hydrogels.

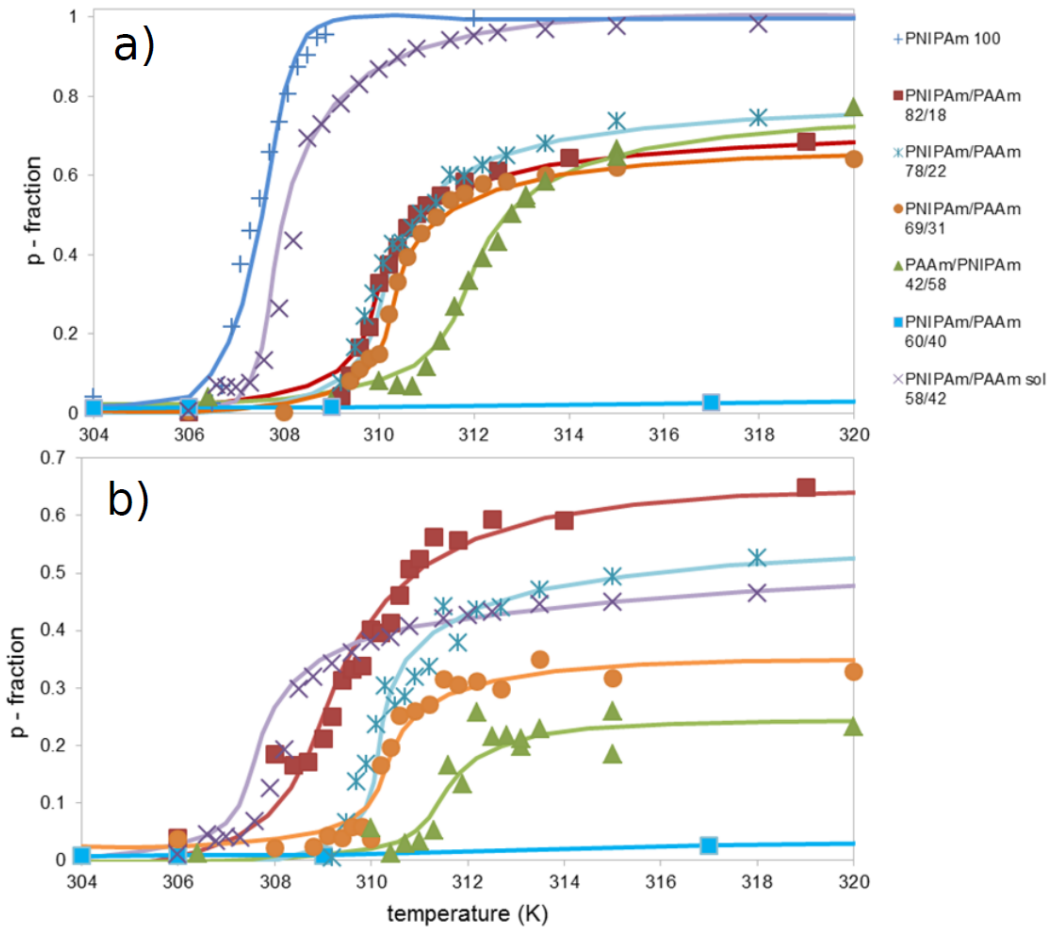

Figure 7.6: Temperature dependences of p fraction determined from PNIPAm CH_3 signal (a) and mixed main chain CH signal (b) in PNIPAm/PAAm solution and hydrogels with various composition..

Temperature dependences of the p-fractions as obtained from the integrated intensities of main chain CH signal of PNIPAm and PAAm units (signal F) are plotted in Fig. 7.6b. The second mixed signal of main chain CH_2 protons (signal G) showed similar dependences. Maximum values of p-fraction p_{max} for the PNIPAm/PAAm solution is approximately 0.5 which roughly corresponds to the molar ration of PNIPAm units in the solution and thus to contribution to the F signal. p_{max} values as obtained for PNIPAm/PAAm IPNs approximately cor-

respond to p_{max} values of PNIPAm signals. For example for PNIPAm/PAAm 78/22 IPN p_{max} value of the PNIPAm CH_3 signal is 0.75 (cf. Fig. 7.4) meaning that 75% of CH_3 protons in NIPAm units participate in collapsed structures. Comparing value of mixed main chain CH signal with $p_{max} = 0.55$ (cf. Fig. 7.6b) and taking acount IPN composition, we have found that 71% of main chain CH protons are incorporated in collapsed structures if we assume that AAm units do not participate in collapse transition at all.

Distinct behaviour can be observed for IPN PAAm/PNIPAm 42/58 hydrogel. Analysis of p_{max} values showed that although 77% of methyl groups are not visible in NMR spectra, there are only 45% of the main chain CH groups of NIPAm units which are not detected in NMR spectra due to significantly restricted mobility. This behaviour can be in connection with the fact that in PAAm/PNIPAm 42/58 hydrogel some inhomogeneities were found in article 3. (List of publications) at temperatures below the VPTT, which might be, e.g., regions of higher crosslinking density. While isopropyl groups of PNIPAm units in these inhomogeneities retain relatively high mobile, mobility of respective main chain protons can be significantly reduced and this can result in reduced I_0 values in eq. 4.1 in section 4.3 and subsequently in smaller values of the p-fraction. This assumption is also supported by the fact that in contrast to other samples, the intensities of NMR bands in PAAm/PNIPAm 42/58 hydrogel at temperatures below VPTT are not in proportion to number of protons in respective groups; e.g., intensities of bands F (CH group) and G (CH_2 group) are in the ratio 1 : 1.5.

For the samples PVCL/PNIPAm where both components are temperature-sensitive we observed specific differences in behavior of PVCL and PNIPAm component. As far as the IPN PVCL/PNIPAm (54/46) results were practically the same, we depicted only temperature dependences of the p-fraction obtained for signals C, G, and H in IPN PVCL/PNIPAm 50/50 (Fig. 7.7). Mixed signal G which predominantly corresponds to PVCL component shows somewhat different temperature dependences of the p-fraction (open symbols in Fig. 7.7) in comparison with signals of PNIPAm component (filled symbols). In comparison with the transition of PNIPAm component which is centered (for $p = 0.5$) around 307 K, the transition of PVCL component is shifted at 2 K towards lower temperatures (~ 305 K). The transitions of both components are approximately 7 K broad. For PVCL component (signal G), the p_{max} value at higher temperatures is equal to 1, while for PNIPAm component (signals C and H), the somewhat lower values of $p_{max} \approx 0.9$ are caused by signals of residual ethanol partially affecting also the integrated intensity of signals C and H.

Different temperature dependences of the collapsed p-fraction as detected for PVCL and PNIPAm components in PVCL/PNIPAm IPNs can indicate certain imperfect mutual penetration of two IPN components which influences differently the dynamics of PVCL and PNIPAm chains at molecular level, and in this case, during the transition, both IPN components keep their individual character to a large extent. Nevertheless, as it was mentioned in section 2.4, only a single transition of PVCL/PNIPAm hydrogels was detected by DSC (cf. Fig. 7.2). We assume that this can be in connection with the fact that the difference in the transition temperatures of PVCL and PNIPAm components is only 2 K which is not sufficient for macroscopic detection. Therefore, for PVCL/PNIPAm hydrogels, the transitions of PVCL and PNIPAm components can merge in one DSC

peak.

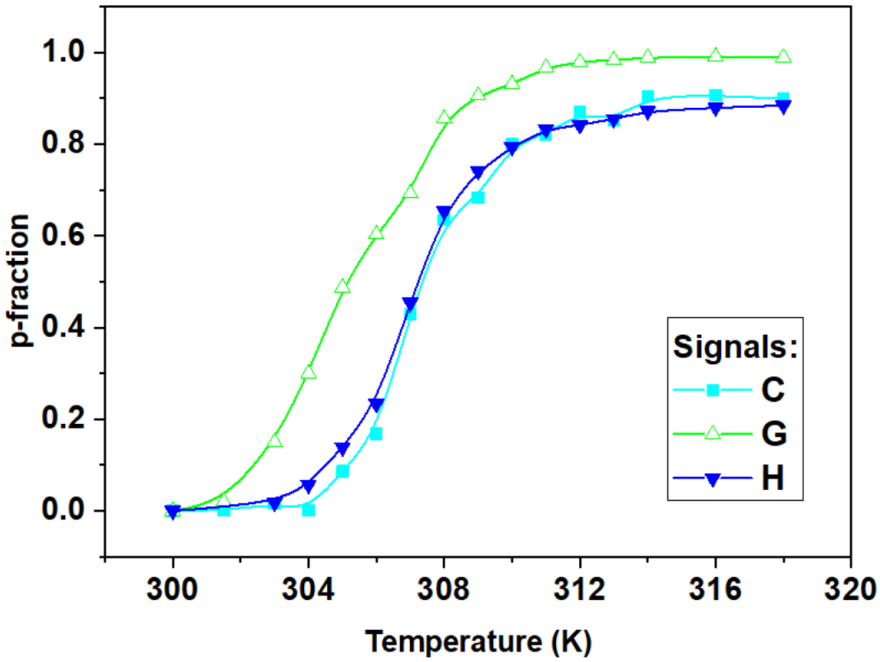

Figure 7.7: Temperature dependences of the p fraction as determined from various PVCL and PNIPAm NMR signals for PVCL/PNIPAm (50/50) IPN hydrogel.

Fig. 7.8 shows part of ^{1}H NMR spectra with signals of water (HDO) for PNIPAm/PAAm 78/22 hydrogel measured at various temperatures.There is second HDO signal which suddenly occurs at higher temperatures at the phase transition with ∼0.015 – 0.05 ppm smaller chemical shift in comparison to the main HDO peak. The observed change in the HDO region is fully reversible, after cooling from 317 K to 303 K there is again a single HDO signal (cf. blue spectrum in Fig. 7.8 which was recorded ∼1 h after cooling from 317 K). This new HDO signal which appears in NMR spectra detected in transition region at temperatures above the VPPT evidently corresponds to water molecules bound in collapsed hydrogel globular structures. The correctness of this assignment is also supported by spin-spin relaxation measurements (see further text below). The existence of two separate HDO signals then means that in the studied IPN hydrogels, there is a slow exchange of water molecules between bound and free sites. The additional HDO peak occurs for hydrogels of neat PNIPAm, PNIPAm/PAAm 82/18 and 78/22 and the both PVCL/PNIPAm hydrogels. Samples of hydrogels of IPNs with PNIPAm content lower than 78 *mol.*% and the mixed solution PNIPAm/PAAm showed at all measured temperatures a single HDO peak.

Similar behavior was previously found for bound and free water or ethanol (EtOH) in highly concentrated poly(vinylmethyl ether) (PVME)/D_2O [56] and PVME/D_2O/EtOH [115] solutions, respectively. Assuming that the exchange between free and bound water is associated with diffusion proces of water molecules through mesoglobules, the direct correlation between the rate of exchange process (slow or fast) and the size of phase-separated mesoglobules was shown for concentrated and semidiluted PVME/D_2O solutions [58].

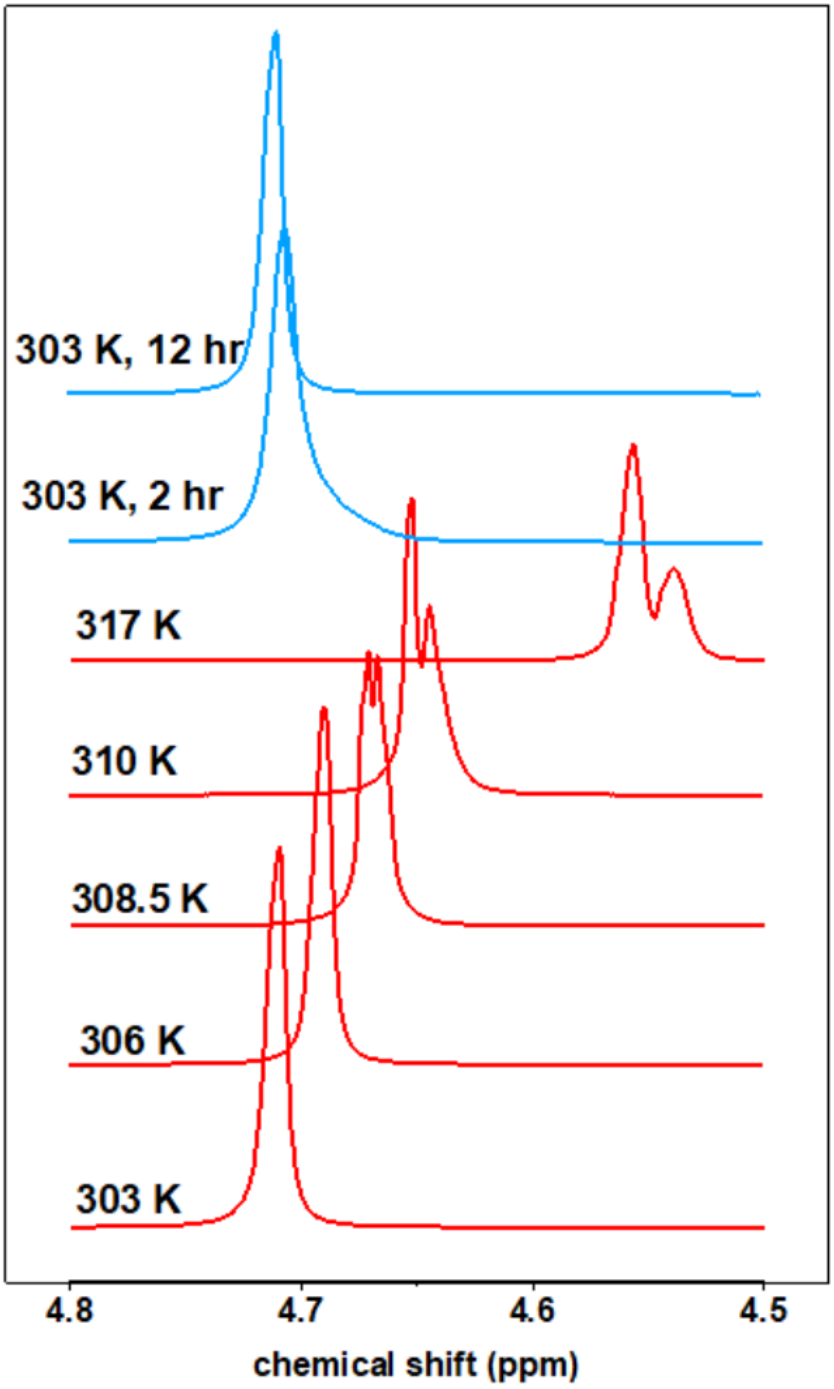

Figure 7.8: HDO signals in ^{1}H NMR spectra of PNIPAm/PAAm 78/22 hydrogel in D_2O measured at various temperatures during gradual heating (five spectra from the bottom) and after subsequent cooling (two spectra at the top).

Two separate signals of water were also found in PVME and PNIPAm hydrogels [54, 116, 117] and in homo- and copolymer microgels of NIPAm and *N,N*–diethylacrylamide in water/methanol mixtures [118]. On the other hand, a decrease in the temperature dependence of spin–spin relaxation time (T_2) of water observed in the transition region for PNIPAm microgels by Sierra-Martin et al. [119] indicates a fast exchange between bound and free water. We assume that similarly as in PVME aqueous solutions [58], also in hydrogel samples, the rate

of the exchange process can depend on the size of collapsed globular structures. From the condition [120] $1/\tau \ll \Delta\nu$, where τ is the residence time and $\Delta\nu$ is the difference of the respective chemical shifts in Hz, it follows that for the residence time of bound HDO molecules it holds $\tau \gg 70$ ms.

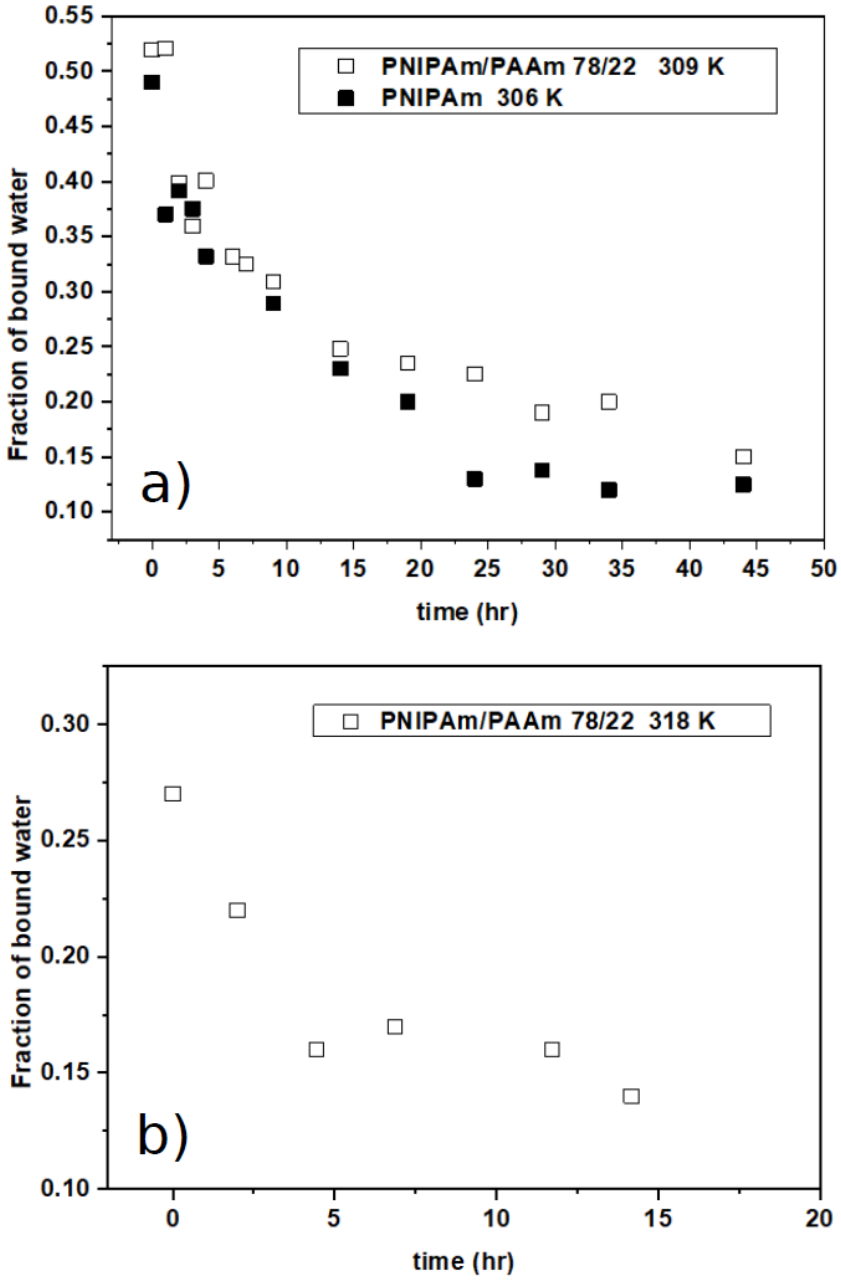

Figure 7.9: Time dependence of the fraction of bound water as detected for PNIPAm hydrogel and IPN hydrogel PNIPAm/PAAm 78/22 at 306 and 309 K, respectively (a) and in the latter case also at 318 K (b).

Interestingly enough, it follows from comparison with temperature dependences of p-fraction (Fig. 7.6) that bound water appears already at ≈306 K and 309.5 K for PNIPAm and PNIPAm/PAAm 78/22 hydrogels, respectively, i.e. at temperatures when polymer segments just begin to form collapsed structures

and p-fraction starts to increase above zero value. This behavior is probably connected with self-organization process which includes water molecules and which begins in the early stage of the phase transition in hydrogels. Fig. 7.9a shows time dependences of the fraction of bound water in PNIPAm hydrogel and IPN hydrogel PNIPAm/PAAm 78/22 at 306 and 309 K, respectively, i.e., just below the phase transition (cf. Fig. 7.6). For PNIPAm/PAAm 78/22 IPN hydrogel Fig. 7.9b also shows the time dependence of the content of bound water at 318 K, i.e., well above the phase transition (cf. Fig. 7.6), for PNIPAm/PAAm 78/22 IPN hydrogel. From Fig. 7.9 it follows that both in PNIPAm hydrogel and in PNIPAm/PAAm 78/22 IPN hydrogel the fraction of bound water slowly decreases with time. After 45h the fraction of bound water is ∼0.15, i.e., ∼30% of the original value. At the same time the rate of this decrease is not significantly affected by the temperature (cf. Fig. 7.9b).

samples	components molar ratio	T_2[s]		
		T <VPPT	T >VPPT	
PNIPAm	100/0	4.3	6.8[a]	0.8[b]
PNIPAm/PAAm	82/18	4.2	5.5[a]	1.3[b]
PNIPAm/PAAm	78/22	4.2	4.7[a]	0.6[b]
PNIPAm/PAAm	69/31	4.9	2.0[c]	
PAAm/PNIPAm	42/58	3.5	3.6[c]	
PAAm	0/100	3.7	3.8[c]	
PVCL/PNIPAm	54/46	1.9	2.8[a]	0.15[b]
PVCL/PNIPAm	50/50	1.3	1.9[a]	0.17[b]

[a] "Free" water signal. Samples showed two water signals (cf. Fig. 7.8)
[b] "Bound" water signal. Samples showed two water signals (cf. Fig. 7.8)
[c] Samples showed a single water signal

Table 7.4: ^1H spin–spin relaxation times T_2 of HDO molecules in hydrogels based on PNIPAm at temperatures below and above the phase transition.

Substantial differences between bound and free water were found from measurements of spin-spin relaxation time T_2 of HDO molecules in hydrogels of neat PNIPAm and PAAm and IPNs of PNIPAm/PAAm, PAAm/PNIPAm and PVCL/PNIPAm as we can see in Table 7.4. From this Table it follows that T_2 values in hydrogels of neat PNIPAm and IPNs PNIPAm/PAAm 82/18, 78/22 and the both PVCL/PNIPAm are for bound water substantially smaller in comparison with free water molecules - up to 2 orders of magnitude shorter. The main source of these differences is evidently the fact that the motion of bound water is spatially restricted and anisotropic [56].

IPN hydrogels PNIPAm/PAAm 69/31 and PAAm/PNIPAm 42/58 above VPTT did not show the second additional peak corresponding to bound HDO molecules. T_2 value of HDO obtained for IPN PNIPAm/PAAm 69/31 declines substantially as hydrogel passes over VPTT (Table 7.4). Such decrease of water relaxation time T_2 was previously observed in the transition region for PNIPAm microgels by Sierra-Martin et al. [119] and it is consistent with a fast exchange between bound and free water. Significant differences in T_2 values in dependence on temperature were not found for PAAm/PNIPAm 42/58 hydrogel and for neat PAAm hydrogel which does not show phase transition (Table 7.4).

As described above, investigated systems show in principle three types of water behaviour during phase transition. The fact that no bound water was detected by NMR in PAAm/PNIPAm 42/58 hydrogel can be in connection with the DSC finding that enthalpy of the transition is for PAAm/PNIPAm 42/58 hydrogel substantially smaller in comparison with PNIPAm/PAAm hydrogels (cf. Table 7.2). Relatively small p_{max} values obtained for main chain protons in PAAm/PNIPAm 42/58 hydrogel in Fig. 7.6b) can be also relevant in this respect. In this sample probably because of non-perfect chain interpenetration during network preparation heterogeneous regions with higher crosslinking density appear already at temperature below VPTT. Above VPTT PAAm/PNIPAm network can form globular regions which are extensively hydrated. Rather insignificant interaction changes during transition are thus in this case accompanied with a small change of enthalpy.

8. Results - IPNs and SIPNs of PDEAAm and PAAm

Temperature-induced phase transition in hydrogels of semi-interpenetrating (SIPNs) and fully interpenetrating (IPNs) polymer networks of thermoresponsive poly(*N,N*–diethylacrylamide) (PDEAAm) and hydrophilic polyacrylamide (PAAm) was studied by a combination of ^{1}H NMR spectroscopy, swelling and DSC experiments. We investigated the effect of network composition on the volume phase transition of SIPNs and IPNs. Networks were prepared with a reversed sequence of the two components, i.e., SIPNs of crosslinked PDEAAm and linear PAAm and inversely SIPNs of crosslinked PAAm and linear PDEAAm, and both types of IPNs PDEAAm/PAAm and PAAm/PDEAAm. The behavior of prepared networks was compared with aqueous solution of linear PDEAAm and neat hydrogel of crosslinked PDEAAm.

This section is prepared from the results published in article 6. from the List of publications. Text below use quotes or is inspired by this article.

8.1 Characterization and swelling ratios

The real molar ratios of components PDEAAm and PAAm in hydrogels of SIPNs and IPNs were determined from integrated intensities of ^{1}H NMR signals C and D of the main chain CH protons of DEAAm and AAm units, respectively (cf. Figs. 8.1 and 8.2). The molar ratio of respective monomer units established from NMR spectra are shown in Table 8.1. The samples D sol and D in Table 8.1 denotes 5*wt.*% D_2O solution of linear PDEAAm and the hydrogel of PDEAAm network.

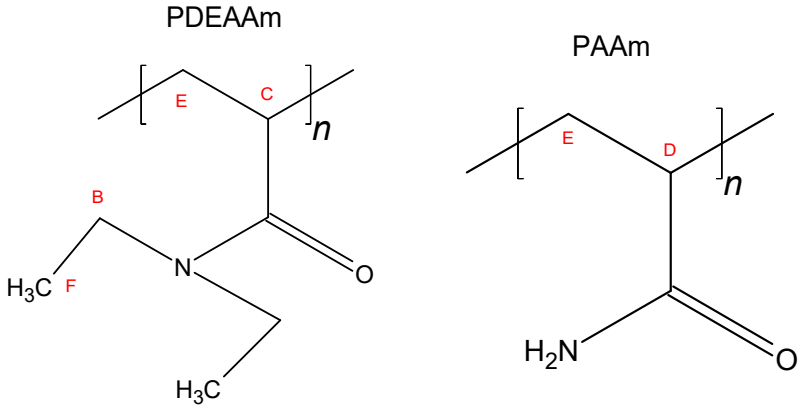

Figure 8.1: Structural formula of PDEAAm, and PAAm repeating monomer units with marked groups from B to F.

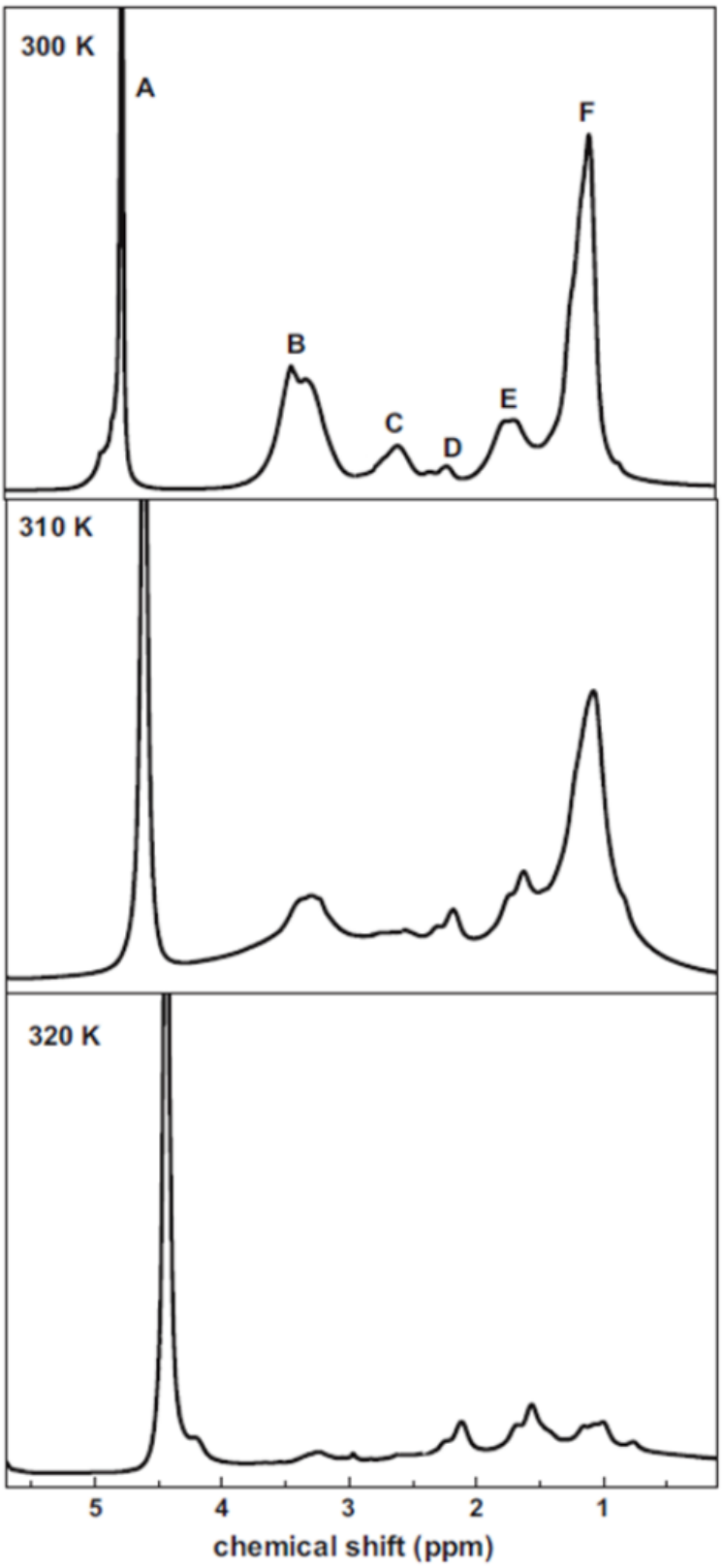

Figure 8.2: ^{1}H NMR spectra (500.1 MHz) of SIPN A/D 56/44 in D_2O recorded at 300 K, 310 K, and 320 K at the same instrumental conditions. Peak assignments are explained in the text and in Fig. 8.1.

The equilibrium swelling ratio was determined at 300 K (below VPTT) after 3

days as the ratio $SR\ (m_T - m_d)/m_d$ (as defined in section 4.3 eq. 4.4) similarly as for IPNs (Chapter 7). The values are given in Table 8.2. It should be emphasized that with the exception of IPNs A/D 20/80 and 30/70, all hydrogels of SIPNs and IPNs show lower swelling ratios in comparison with hydrogel of the neat PDEAAm. Relatively high swelling ratio observed for IPNs A/D is obviously a consequence of preparation procedure used for these samples when hydrogel of neat hydrophilic PAAm with high swelling ratio is prepared as the first component and subsequently immersed into solution of DEAAm monomer.

sample description	sample description	composition	
		monomer ratio in the synthesis	molar ratio from ^{1}H NMR spectra
PDEAm solution	D sol	100/0	100/0
PDEAm hydrogel	D	100/0	100/0
SIPN of crosslinked PDEAAm and linear PAAm	SIPN D/A 77/23	80/20	77/23
	SIPN D/A 64/36	70/30	64/36
	SIPN D/A 60/40	60/40	60/40
SIPN of crosslinked PAAm and linear PDEAAm	SIPN A/D 30/70	20/80	30/70
	SIPN A/D 32/68	30/70	32/68
	SIPN A/D 43/57	60/40	43/57
	SIPN A/D 56/44	70/30	56/44
IPN of PDEAAm (first component) and PAAm	IPN D/A 89/11	70/30	89/11
	IPN D/A 85/15	60/40	85/15
	IPN D/A 64/36	50/50	64/36
IPN of PAAm (first component) and PDEAAm	IPN A/D 15/85	20/80	15/85
	IPN A/D 20/80	30/70	20/80
	IPN A/D 30/70	40/60	30/70

rel. error 3%

Table 8.1: Theoretical and experimental compositions of SIPN and IPN hydrogels based on PDEAAm. The experimental compositions were determined from ^{1}H NMR spectra.

8.2 DSC

One rather broad endothermic transition was observed in all samples with PDEAAm as it illustrated in DSC thermograms obtained for PDEAAm hydrogel and the set of samples SIPN D/A (Fig. 8.3). Such broad DSC peaks were previously detected for PDEAAm solutions [121] and we suppose that a significant peak broadness ($\sim$10 K) is connected with chemical structure of the DEAAm side chains as it was observed for all samples, even for solution of linear PDEAAm.

Table 8.2 contains the onset and peak temperatures T_{on} and T_{peak}, and enthalpy ΔH of the transition as we obtained from DSC thermograms. Transition temperature of PDEAAm solution (T_{on} = 306.5 K) matches with the interval of LCST values 304–307 K determined from turbidimetric and microcalorimetric measurements of linear PDEAAm solutions [93, 94, 95].

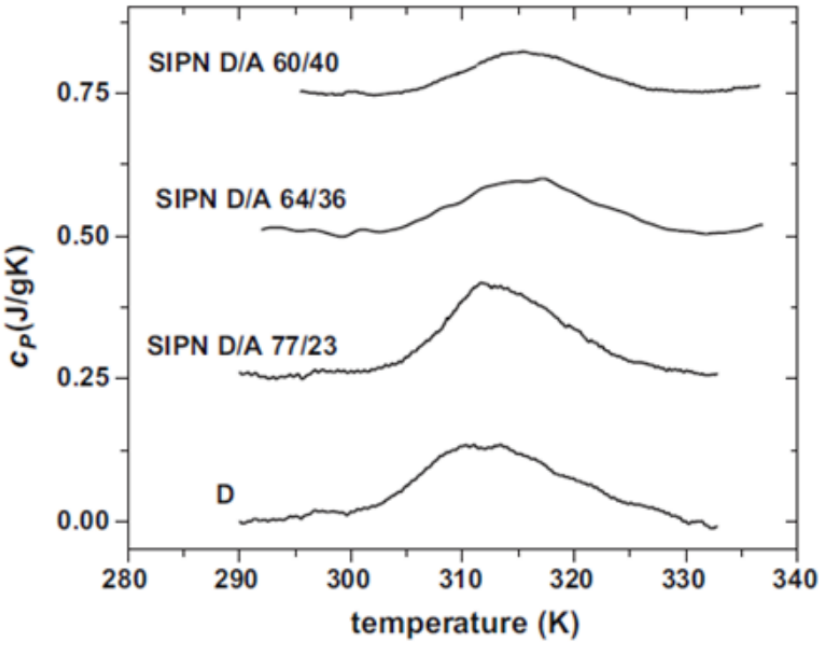

Figure 8.3: DSC thermograms of PDEAAm hydrogel (D) and hydrogels SIPNs D/A with various composition.

samples	swelling ratio	T_{on} [K]	T_{peak} [K]	ΔH [J/g of dry polymer	ΔH [kJ/mol of PDEAAm units in d.p.*
D sol	-	306.5	314.3	29.6	3.76
D	24.7	302.9	312.4	41.2	5.24
SIPN D/A 77/23	16.3	304.6	311.7	26.9	4.44
SIPN D/A 64/36	19.1	307.2	315	21.8	4.33
SIPN D/A 60/40	21.7	308.8	315.2	18.6	3.94
SIPN A/D 30/70	10.4	305	310.7	26.1	4.75
SIPN A/D 32/68	16.3	306.2	313.4	24.2	4.52
SIPN A/D 43/57	14.6	307.3	316.2	20	4.47
SIPN A/D 56/44	14.1	309.1	317.7	15.1	4.36
IPN D/A 89/11	13.7	302.3	310.4	27.7	3.95
IPN D/A 85/15	14.7	302.8	310.9	26.6	3.98
IPN D/A 64/36	14.2	305	315.4	19.8	3.93
IPN A/D 15/85	17.7	303.6	313.3	22.9	3.43
IPN A/D 20/80	35.6	306.4	313.5	16.7	2.67
IPN A/D 20/70	33.3	309.7	316.8	5.9	1.07
		rel. error 8%	rel. error 5%		

Table 8.2: Equilibrium swelling ratio at 300 K and parameters of the phase transition obtained from DSC measurements (see Fig. 8.3), where T_{on} is the onset temperature, T_{peak} is the peak temperature and ΔH is the enthalpy of the transition. (* dry polymer)

Neat PDEAAm hydrogel shows the transition temperature shifted to lower

value compared with PDEAAm solution. This effect was observed previously for linear and crosslinked PDEAAm by NMR [122] and it could be attributed to the restricted mobility of PDEAAm network segments due to crosslinking structure in hydrogel.

The increasing content of hydrophilic PAAm component in SIPNs or IPNs leads to higher critical temperatures of the transition. The dependences of critical temperatures on composition of hydrogels will be discussed in detail together with NMR results (section 8.3). The enthalpy values of the phase transition ΔH were recalculated to the weight of dry sample (J/g of dry polymer) and to PDEAAm monomer units (kJ/mol of PDEAAm units in dry polymer). SIPNs and IPNs hydrogels show somewhat lower enthalpy values in comparison with neat PDEAAm hydrogel and at the same time enthalpies slightly decrease with increasing content of AAm units in the hydrogel. Significant lowering of enthalpy values was detected for IPNs A/D 20/80 and 30/70, i.e., for samples which showed significantly higher swelling ratio.

8.3 NMR

High-resolution ^{1}H NMR spectra of SIPN A/D 56/44 detected under the same instrumental conditions at three various temperatures are shown in Fig. 8.2. The assignment of resonances to various proton types (from Fig. 8.1) in the spectrum measured at 300 K (i.e., below the VPTT of PDEAAm) is folowing – the strong peak A corresponds to HDO, peaks B and F to CH_2 and CH_3 groups of PDEAAm, respectively. Main chain CH_2 group from both components have signal E (means mixed signal G in chapter 7). Signals C and D corresponds to the backbone CH group of the PDEAAm and PAAm, respectively. The most important effect observed in the NMR spectra measured at higher temperatures is a marked decrease in the integrated intensity of all polymer signals. Evidently, the mobility of most polymer units is significantly reduced to such an extent that the corresponding signals are too broad to be detected in high resolution NMR spectra in the same way as in the case of hydrogels based on PNIPAm (Chapter 7).

The temperature dependences of the p-fraction as measured for all polymer signals in hydrogels of neat PDEAAm (D) (Fig. 8.4a), semi-interpenetrating networks SIPN A/D 56/44 (Fig. 8.4b) and D/A 64/36 (8.4d) and interpenetrating network D/A 37/64 (Fig. 8.4c) are depicted in Fig. 8.4. From Fig. 8.4a it follows that p-fraction of all groups in the neat PDEAAm hydrogel show virtually identical dependences on temperature and maximum value p_{max} is equal 1 which means that all PDEAAm units are involved in phase separated globular structures.

Figs. 8.4b–d depict various temperature dependences of p-fraction for particular polymer signals in the main and side chain of SIPNs and IPNs. In the case of SIPN A/D 56/44 (Fig. 8.4b), maximum values p_{max} approach 0.67 and 0.57 for the PDEAAm side diethyl group CH_2 and CH_3 (signals B and F) and PDEAAm main chain group CH, respectively. Signal E corresponding to the main chain groups CH_2 in both PDEAAm and PAAm gives p_{max} values only 0.23. The both main chain groups CH and CH_2 show rather more gradual increase of p-fraction with temperature. Signal D of PAAm CH group practically does not change with temperature which implies that virtually all AAm units show high mobil-

ity even at elevated temperatures. Similar dependences as shown in Fig. 8.4b were obtained for all SIPN A/D samples as well as for all IPN hydrogels as it is demonstrated for IPN D/A 37/64 in Fig. 8.4c.

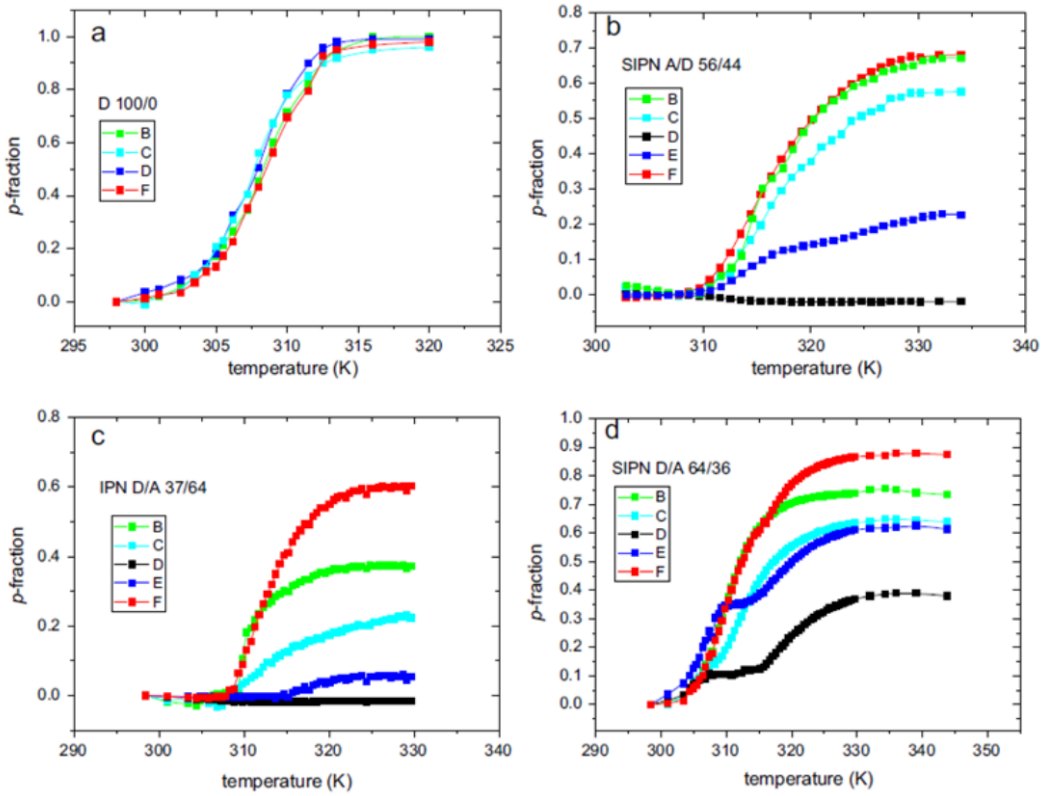

Figure 8.4: Temperature dependences of the p-fraction as determined from various PDEAAm and PAAm NMR signals for D (a), SIPN A/D 56/44 (b), IPN D/A 37/64 (c) and SIPN D/A 64/36 (d).

Evidently, the hydrophilic AAm units do not participate in collapse transition and moreover, they prevent DEAAm units to pack into globular structures and this results in smaller values of the p-fraction of PDEAAm proton groups. In this respect similar behavior was previously found for IPNs of PNIPAm and PAAm in chapter 7. Fig. 8.4d depicts temperature dependences of p-fraction typical for semi-interpenetrating networks SIPNs D/A. PDEAAm signals show p_{max} values lower than 1 as a result of the presence of AAm component in SIPN hydrogel. In contrast to SIPNs A/D, here PAAm signals decrease in their intensities and corresponding temperature dependences of p-fraction show rather gradual two-step character with value of $p_{max} \approx 0.39$ in the case of PAAm CH protons (signal D) and $p_{max} \approx 0.62$ in the case of mixed PAAm and PDEAAm CH_2 band. Obviously, shrinking of crosslinked PDEAAm chains in SIPNs D/A leads to the partial collapse of linear PAAm chains, but this process is slower than the initial process when PDEAAm chains are shrinked. This can indicate that in collapsed SIPN D/A hydrogels PAAm chains form small regions which are inside large regions (aggregates) preferably formed by chains of crosslinked PDEAAm.

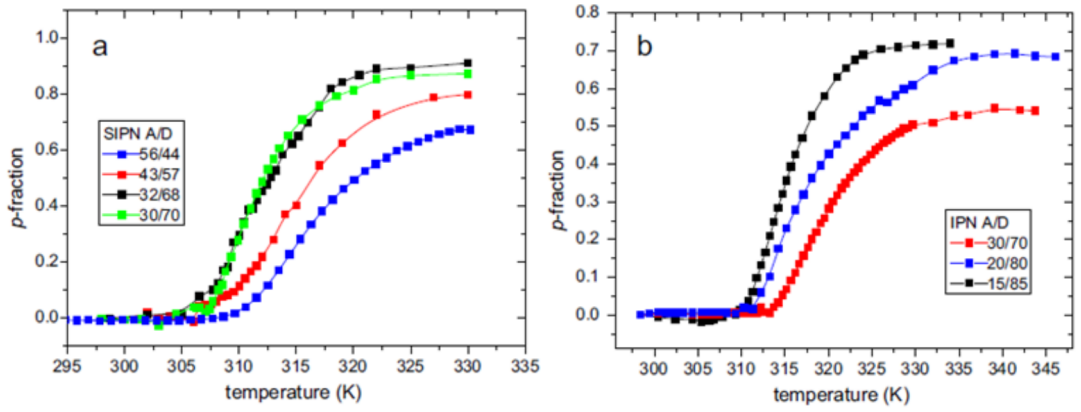

Figure 8.5: Temperature dependences of the p-fraction in hydrogels SIPN A/D (a) and IPN A/D (b) with various composition.

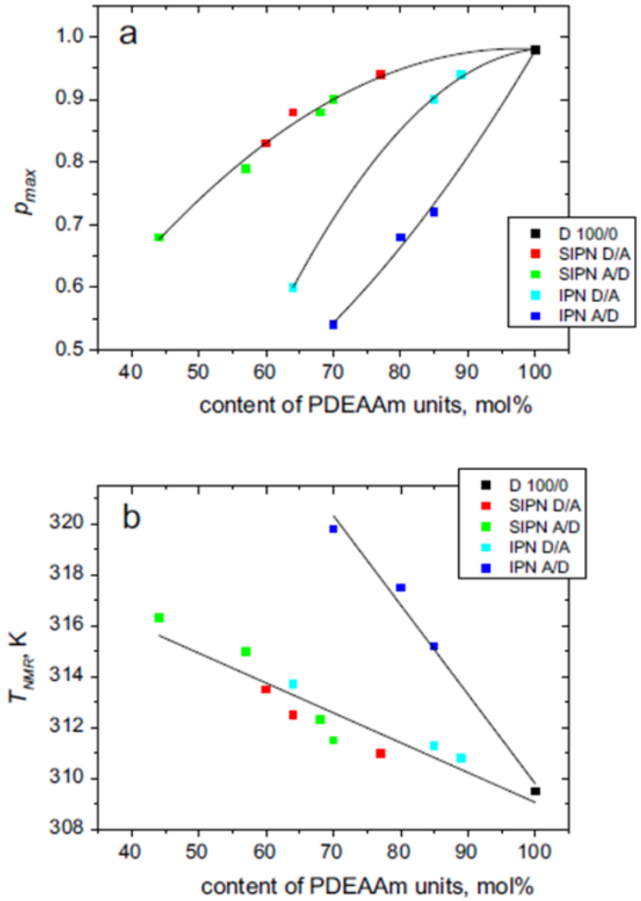

Figure 8.6: Dependences of maximum value p_{max} (a) and the critical temperatures T_{NMR} (b) on composition of SIPN and IPN hydrogels.

Fig. 8.5 illustrates the temperature dependences of the p-fraction determined from the integrated intensities of the methyl signal of PDEAAm (signal F) in PAAm/PDEAAm SIPN and IPN hydrogels with various compositions. The results are reasonably in accord with DSC results and transition temperatures determined by NMR, T_{NMR} (temperature in the middle of the transition corresponding

to $p_{max}/2$) agree rather well with T_{peak} values determined by DSC (cf. Table 8.2). Increasing content of PAAm component shifts VPTT to higher temperatures and maximum values of the p-fraction p_{max} are lower.

For all studied hydrogels, maximum values p_{max} and critical temperatures T_{NMR} were extracted from temperature dependences of the p-fractions, determined from PDEAAm methyl signal. Dependences of p_{max} and T_{NMR} on the composition of SIPN and IPN hydrogels are depicted in Fig. 8.6.

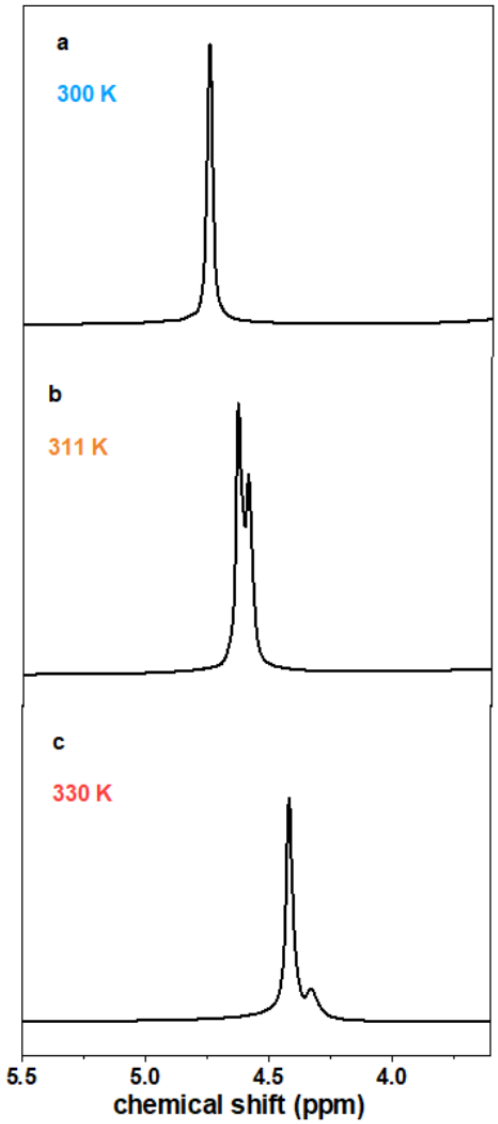

Figure 8.7: HDO signals in ^{1}H NMR spectra of SIPN D/A 64/36 hydrogel in D_2O measured at 300 K (a), 311 K (b) and 330 K (c).

It follows from Fig. 8.6a that the maximum value p_{max} of the neat PDEAAm hydrogel has reached almost 1 but it significantly decreases with increasing AAm content in SIPNs and IPNs. SIPN hydrogels show always higher values of p_{max} than those of IPN hydrogels, which could indicate that in interpenetrating networks, where both components are crosslinked, more DEAAm units remain sufficiently mobile above the transition as crosslinked structure hinders them to pack tightly into collapsed phase. Critical temperature T_{NMR} is proportional almost

linearly to the content of DEAAm units in SIPNs and IPNs (Fig. 8.6b). Such linear dependence of critical transition temperature on the composition was already observed in systems of linear random copolymers [111, 123, 124] and IPN hydrogels based on chemically modified poly(vinyl alcohol) and PNIPAm [125]. Surprisingly, all T_{NMR} values except critical temperatures corresponding to IPN A/D fit well to one linear dependence regardless of the preparation procedure. Much steeper dependence T_{NMR} vs. composition as detected for hydrogels of IPNs A/D could be eidently attributed to the substantially higher swelling ratios of these samples (Table 8.2). It was shown that the VPTT of polymer hydrogels having the same swelling ratio is equal, indicating that the VPTT is determined by the overall hydrophilicity of the polymer [123]. Presence of PAAm network prepared as the first component of IPNs A/D thus leads to higher hydrophilicity of hydrogel and tends to increase the value of the VPTT and to reduce enthalpies as detected by DSC.

Fig. 8.7 shows a part of ^{1}H NMR spectrum with signals of water (HDO) for SIPN D/A 64/36 at room temperature and at two elevated temperatures. From this figure it follows that a new signal of HDO with a smaller chemical shift of $\sim$0.03-0.09 ppm in comparison with the main HDO peak was detected at higher temperatures. This new HDO signal which appears in spectra of all the investigated SIPN and IPN hydrogels but only in the transition region and at temperatures above the phase transition evidently corresponds to water molecules bound in globular structures of the collapsed hydrogel. From the condition $1/\tau \ll \Delta\nu$, where τ is the residence time and $\Delta\nu$ is the difference of the respective chemical shifts in Hz, it follows that for the residence time of "bound" HDO molecules it holds $1/\tau \gg 20$ ms. Substantial differences between "bound" and "free" water were found from measurements of spin–spin relaxation time T_2 of HDO molecules. So in the collapsed hydrogel of SIPN D/A 64/36, T_2 value 0.024 s detected at 330 K for "bound" (confined) water was two orders of magnitude smaller in comparison with T_2 value 2.32 s of "free" water molecules.

It is clearly visible in Fig. 8.7 that during heating process, the intensity of the "bound" water signal is decreasing; fraction of "bound" water at 311 K and 330 K is 0.42 and 0.19, respectively. We attribute this effect to releasing of "bound" water from collapsed structures and besides increasing temperature this process is affected significantly by time as we found for IPN hydrogels PNIPAm/PAAm and PVCL/PNIPAm in chapter 7. Interestingly enough, it follows from Figs. 8.7 and 8.8 that the difference of chemical shifts between signals of the "free" and "bound" water increases with increasing temperature and this dependence has asymptotic behavior. Such observation was for the first time reported for methanol signals in microgels of NIPAm and DEAAm [118] and indicates changes in the polymer structure of the collapsed hydrogel which surrounds the restricted solvent (water) molecules. When hydrogel network begins to shrink, a part of water is entrapped into collapsed structures and its nearest environment is then different from bulk water. During subsequent heating, continuous shrinking is accompanied with releasing of the "bound" water and this leads to increasing difference in the environment surrounding restricted water molecules which remain in the collapsed globular structures. Consequently, chemical shift difference between signals of

the "free" water and "bound" water is increasing.

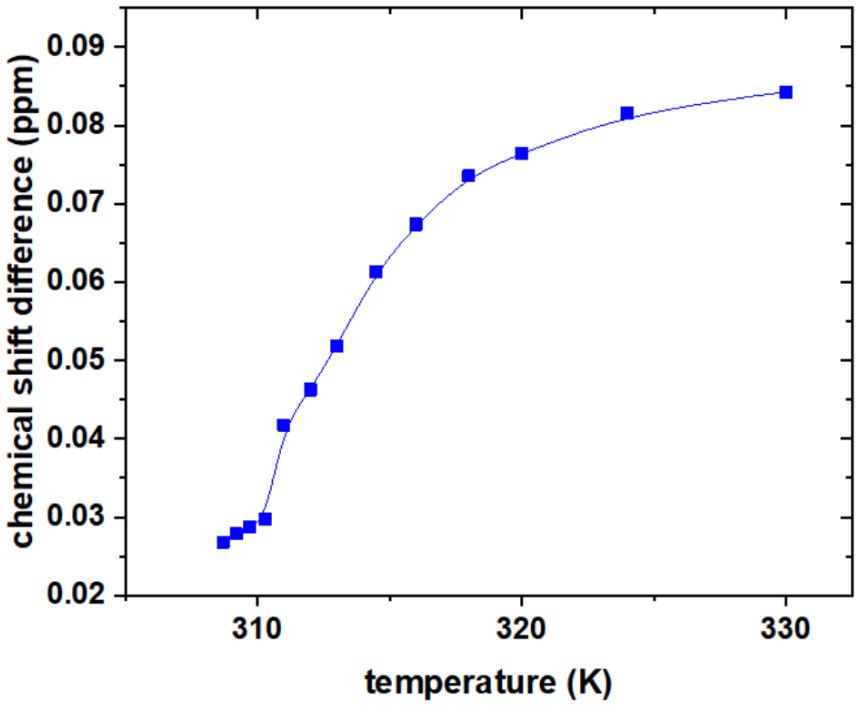

Figure 8.8: Temperature dependence of chemical shift difference between signals of the "free" and "bound" water measured for SIPN D/A 64/36 hydrogel.

Conclusion

Several types of thermoresponsive polymer systems – aqueous solutions of linear polymer and hydrogels of semi- and fully interpenetrating networks based on various thermoresponsive and hydrophilic polymers – were investigated in this thesis. The conclusions are as follows:

PVME/water solutions
The phase separation in aqueous solutions of PVME was examined NMR, DSC and OM methods. OM and DSC results showed that for polymer concentrations $30 - 50wt.\%$ the phase separation has non-reversible character, particularly as a consequence of different dynamical and structural changes during formation and dissolving of mesoglobules. NMR data were used to construct van't Hoff plots and changes of the enthalpy and entropy characterizing the phase transition were determined. As it follows from comparison of NMR and DSC thermodynamical parameters, for solutions with $c = 1 - 30wt.\%$, the size of the cooperative units (domains) undergoing the transition corresponds to the whole polymer chain; for higher polymer concentrations the size of domain decreases.

PVME/water solutions with additives
Temperature-induced phase separation of PVME/water solutions in the presence of small additives was investigated by NMR, DSC and OM methods. The dynamics during the phase transition as well as interactions between the water and the polymer are significantly influenced by the chemical structure of small additive molecules. The influence of the additive presence on the size of the cooperative units was found out.

Hydrophobic additives like TBME and TBMK more strongly affect polymer transition than additives with hydrophilic character – TBOH and TBAm. Hydrophilic additives act with a slight stabilizing effect of hydrogen bonding. It was manifested by the shift of the transition region towards higher temperatures in PVME solution and by a decrease of the fraction of PVME monomer units involved in globular structures. On the other hand, the effect of hydrophobic additives is much stronger with significant shift of the transition temperatures to lower values.

From comparison of thermodynamical parameters as obtained from NMR and DSC, the size of the cooperative units undergoing the transition as a whole was determined. Cooperative domains in PVME/TBOH and PVME/TBMK solutions are about twice smaller in comparison with those formed in other solutions and this is macroscopically manifested in smaller polymer aggregations. NMR relaxation experiments confirmed that a certain portion of water and additive molecules remained bound in PVME globules in the solutions with TBOH and TBMK. The incorporation of water and additive molecules into the globules thus leads to reduced cooperativity of the transition and influences the size of polymer aggregations formed above LCST.

IPNs of PNIPAm and PAAm
The temperature-induced phase transition in hydrogels of IPNs with various

compositions of PNIPAm/PAAm and PAAm/PNIPAm was detected by NMR spectroscopy, swelling and DSC methods. The increasing content of hydrophilic PAAm component in IPNs shifts the transition toward higher temperatures and the fraction p_{max} of polymer units with significantly reduced mobility detected by NMR, as well as the enthalpy change, are reduced. No phase transition was detected for IPN hydrogels containing at least $40 mol.\%$ of PAAm units.

Different order of components during IPNs preparation significantly affects the parameters of their transition. IPN PAAm/PNIPAm 42/58 shows substantially reduced enthalpy values in comparison with IPNs PNIPAm/PAAm prepared in a reversed order.

For all collapsed hydrogels of PNIPAm/PAAm and of the neat PNIPAm, measurements of the ^{1}H NMR spectra and spin-spin relaxation times T_2 revealed certain portion of water (HDO) bound in globular structures, while no bound water was detected for PAAm/PNIPAm hydrogel. Bound water could be distinguished even already at temperatures when polymer segments begin to form collapsed structures. Spin-spin relaxation times T_2 for "bound" HDO were up to one order of magnitude smaller in comparison with "free" HDO which was excluded from collapsed hydrogel structures. Slow exchange regime between free water and bound water was shown in most cases and the residence time of bound HDO was $\tau \gg 70\,\mathrm{ms}$. With time, water molecules bound in collapsed structures are released within tens of hours.

IPNs of PVCL/PNIPAm

The phase transition of IPNs PVCL/PNIPAm where both components are thermoresponsive was studied. Transition temperatures of PVCL and PNIPAm differ by $\sim 2\,\mathrm{K}$ and both transitions were found out by NMR, but only a single one was detected by DSC. We assume that both transitions can merge in one DSC peak in connection with fast heat flow and such a small difference in the transition temperatures of neat components. Such behavior resembles the LCST behavior typical for mixtures of two thermoresponsive homopolymers.

IPNs and SIPNs of PDEAAm and PAAm

In this part we applied NMR spectroscopy, DSC and swelling techniques to describe temperature-induced phase transition in hydrogels of PDEAAm and PAAm with interpenetrating and semi-interpenetrating architecture, reverse sequence in the preparation and various hydrogel compositions. The increasing content of hydrophilic PAAm component in SIPNs and IPNs shifts the transition linearly toward higher temperatures but at the same time the value of VPTT is significantly influenced by swelling ratio of hydrogels. Exceptional behavior was found for IPNs where hydrophilic PAAm network was prepared as the first component. These networks showed in comparison with other hydrogels consequently higher transition temperatures and lower enthalpy values with higher swelling ratio.

NMR fraction p_{max} of polymer units with significantly reduced mobility in IPN hydrogels is lower in comparison with SIPNs. Further it was shown that individual polymer groups participate in the collapse to various extent in dependence on the type of hydrogel preparation. AAm units do not participate in collapse transition in SIPN A/D and all IPN hydrogels and they prevent DEAAm units to pack into globular structures; this leads to smaller values of the p-fraction of

PDEAAm protons. On the other hand, in SIPNs D/A hydrogels, linear PAAm chains partially participate in collapse as a consequence of shrinking of crosslinked PDEAAm chains.

All SIPNs and IPNs hydrogels also report a certain portion of water (HDO) bound in globular structures from measurements of ^{1}H NMR spectra with a slow exchange regime residence time $\tau \gg 20\,\mathrm{ms}$. Releasing of the water molecules from the collapsed structures during subsequent heating leads to more different environment surrounding the rest of restricted water molecules which remain in the collapsed structures.

Bibliography

[1] Bryan Quintero and JJ Trujillo. Natural rubber: Overview and history. `http://www.warco.com/articles/natural-rubber/`. Accessed: 2018-07-26.

[2] PennState College of Earth and Mineral Sciences. Brief history of polymers. `https://www.e-education.psu.edu/matse202/node/4`. Accessed: 2018-07-25.

[3] C. Hofmann and M. Schonhoff. Do additives shift the lcst of poly(N–isopropylacrylamide) by solvent quality changes or by direct interactions? *Colloid Polym. Sci.*, 287:1369–1376, 2009.

[4] M. Ebara et al. *Smart Biomaterials*. Springer Japan, Tsukuba, 2014.

[5] W. E. Hennink and C. F. van Nostrum. Novel crosslinking methods to design hydrogels. *Adv. Drug Del. Rev.*, 54:13–36, 2002.

[6] A.C. Jen, M. C. Wake, and A. G. Mikos. Review: hydrogels for cell immobilization. *Biotechnol Bioeng*, 50:357–364, 1996.

[7] K. Y. Lee and D. J. Mooney. Hydrogels for tissue engineering. *Chem. Rev.*, 101:1869–1880, 2001.

[8] O. Wichterle and D. Lim. Hydrophilic gels for biological use. *Nature*, 185:117–118, 1960.

[9] J. Chen, H. Park, and K. Park. Synthesis of superporous hydrogels: hydrogels with fast swelling and superabsorbent properties. *J. Biomed. Mater. Res.*, 44:53–62, 1999.

[10] A. K. A. Silva, C. Richard, M. Bessodes, D. Scherman, and O-W. Merten. Growth factor delivery approaches in hydrogels. *Biomacromolecules*, 10:9–18, 2008.

[11] T-A. Asoh, M. Matsusaki, T. Kaneko, and M. Akashi. Fabrication of temperature-responsive bending hydrogels with a nanostructured gradient. *Adv. Mater*, 20:2080–2083, 2008.

[12] D. J. Beebe, J. S. Moore, J. M. Bauer, Q. Yu, R. H. Liu, C. Devadoss, and B. H. Jo. Functional hydrogel structures for autonomous flow control inside microfluidic channels. *Nature*, 404:588–590, 2000.

[13] A. Matsumoto, T. Ishii, J. Nishida, H. Matsumoto, K. Kataoka, and Y. Miyahara. A synthetic approach toward a self-regulated insulin delivery system. *Angew. Chem. Int. Ed.*, 51:2124–2128, 2012.

[14] T. Miyata, T. Uragam, and K. Nakamae. Biomolecule-sensitive hydrogels. *Adv. Drug. Del. Rev.*, 54:79–98, 2002.

[15] H. Feil, Y. H. Bae, J. Feijen, and S. W. Kim. Molecular separation by thermosensitive hydrogel membranes. *J. Membr. Sci.*, 64:283–294, 1991.

[16] T. Tanaka. Collapse of gels and the critical endpoint. *Phys. Rev. Lett.*, 40:820–823, 1978.

[17] Dušek K. Responsive gels: Volume transition i, ii. *J. of Adv. Polym. Sci.*, 109:110, 1993.

[18] M. Ilavský. Effect on phase transition on swelling and mechanical behavior of synthetic hydrogels. *J. of Adv. Polym. Sci.*, 109:173–206, 1993.

[19] S. Hirotsu. Coexistence of phases and the nature of first-order phase transition in poly–*N*–isopropylacrylamide gels. *Adv. Polym. Sci.*, 110:1–26, 1993.

[20] S. Fujishige, K. Kubota, and I. Ando. Phase transition of aqueous solutions of poly(*N*–isopropylacrylamide) and poly(*N*–isopropylmethacrylamide). *J. Phys. Chem.*, 93:3311–3313, 1989.

[21] H. G. Schild. Poly(*N*–isopropylacrylamide): experiment, theory and application. *Prog. Polym. Sci.*, 17:163–249, 1992.

[22] M. Ilavský, J. Hrouz, and I. Havlíček. Research article phase transition in swollen gels: 7. effect of charge concentration on the temperature collapse of poly(*N,N*–diethylacrylamide) networks in water. *Polymer*, 26:1514–1518, 1985.

[23] R. Tirumala, J. Ilavský, and M. Ilavský. Effect of chemical structure on the volume–phase transition in neutral and weakly charged poly(*N*–alkyl-(meth)acrylamide) hydrogels studied by ultrasmall–angle x–ray scattering. *J. Chem. Phys.*, 124:234911, 2006.

[24] R. Moerkerke et al. Phase transitions in swollen networks. 3. swelling behavior of radiation cross-linked poly(vinyl methyl ether) in water. *Macromolecules*, 31:2223–2229, 1998.

[25] E. Nies et al. Composition fluctuation, phase behavior, and complex formation in poly(vinyl methyl ether)/D_2O investigated by small–angle neutron scattering. *Macromolecules*, 38:915–924, 2005.

[26] F. Meeussen et al. Phase behaviour of poly(*N*–vinyl caprolactam) in water. *Polymer*, 41:8597–8602, 2000.

[27] V. O. Aseyev, H. Tenhu, and F. M. Winnik. Temperature dependence of the colloidal stability of neutral amphiphilic polymers in water. *Adv. Polym. Sci.*, 196:1–85, 2006.

[28] G. Mamytbekov, K. Bouchal, and M. Ilavský. Phase transition in swollen gels 26. effect of charge concentration on tempereture dependence of swelling and mechanical behaviour of poly(*N*–vinylcaprolactam). *Eur. Polym. J.*, 35:1925, 1999.

[29] V. O. Aseyev, H. Tenhu, and F. M. Winnik. Non-ionic thermoresponsive polymers in water. *Adv. Polym. Sci.*, 242:29–89, 2011.

[30] Wikipedia. Upper critical solution temperature. `https://en.wikipedia.org/wiki/Upper_critical_solution_temperature`. Accessed: 2018-07-26.

[31] T. Tanaka. Phase transitions in gels and a single polymer. *Polymer*, 20:1404–1412, 1979.

[32] J. Stejskal, M. Gordon, and J. A. Torkington. Collapse of polyacrylamide gels. *Polym. Bull.*, 3:621–625, 1980.

[33] A. Yu. Grosberg and A. R. Khokhlov. *Giant Molecules: Here, There and Everywhere...* Academic Press, San Diego, 1997.

[34] K. Dušek and D. J. Patterson. Transition in swollen polymer networks induced by intramolecular condensation. *J. Polym. Sci.*, 6:1209–1216, 1968.

[35] K. Dušek and W. Prins. Structure and elasticity of non-crystalline polymer networks. *Adv. Polym. Sci.*, 6:1–102, 1969.

[36] C. Cuniberti and U. Bianchi. Dilute solution behaviour of polymers near the phase separation temperature. *Polymer*, 15:346–350, 1974.

[37] P.J. Flory. *Principles of Polymer Chemistry*. Cornell University Press, New York, 1954.

[38] O. V. Ptitsyn, A. K. Kron, and Y. Y. Eizner. The models of the denaturation of globular proteins. I. theory of globul–coil transitions in macromolecules. *J. Polym. Sci. Part C*, 16:3509, 1968.

[39] I. M. Lifshitz, A. Y. Grosberg, and A. R. Khokhlov. Some problems of the statistical physics of polymer chains with volume interaction. *Rev. Mod. Phys.*, 50:683–713, 1978.

[40] J. K. M. Sanders and B. K. Hunter. *Modern NMR Spectroscopy – A Guide for Chemists*. Oxford Uni. Press Inc., Oxford, 1993.

[41] H. Günter. *NMR Spectroscopy: Basic Principles, Concepts, and Applications in Chemistry*. John Wiley and Sons, Chichester, 1995.

[42] F. Bloch. Nuclear induction. *Phys. Rev.*, 70:460–474, 1946.

[43] R. A. Horne, J. P. Almeida, A. F. Day, and N. T. Yu. Macromolecule hydration and the effect of solutes on the cloud point of aqueous solutions of polyvinyl methyl ether: A possible model for protein denaturation and temperature control in homeothermic animals. *J. Colloid Interface Sci.*, 35:78–84, 1971.

[44] H. Schafer-Soenen et al. Zero and off-zero critical concentrations in systems containing polydisperse polymers with very high molar masses. 2. the system water–poly(vinyl methyl ether). *Macromolecules*, 30:410–416, 1997.

[45] H. Maeda. Interaction of water with poly(vinyl methyl ether) in aqueous solution. *J. Polym. Sci. Part B*, 32:91–97, 1994.

[46] Y. Maeda. IR spectroscopic study on the hydration and the phase transition of poly(vinyl methyl ether) in water. *Langmuir*, 17:1737–1742, 2001.

[47] V. Aseyev et al. Mesoglobules of thermoresponsive polymers in dilute aqueous solutions above the LCST. *Polymer*, 46:7118–7131, 2005.

[48] S. Swier, K. Van Durme, and B. Van Mele. Modulated–temperature differential scanning calorimetry study of temperature–induced mixing and demixing in poly(vinylmethylether)/water. *J. Polym. Sci. Part B: Polym Phys.*, 41:1824–1836, 2003.

[49] K. Van Durme, E. Loozen, E. Nies, and B. Van Mele. Phase behavior of poly(vinyl methyl ether) in deuterium oxide. *Macromolecules*, 38:10234–10243, 2005.

[50] J. Zhang, H. Teng, X. Zhou, and D. Shen. Frozen bound water melting induced cooperative hydration of poly(vinyl methyl ether) in aqueous solution. *Polym. Bull.*, 48:277–282, 2002.

[51] E. Nies, T. Li, H. Berghmans, R. Heenan, and S. M. King. Upper critical solution temperature phase behavior, composition fluctuations, and complex formation in poly (vinyl methyl ether)/D_2O solutions: small–angle neutron–scattering experiments and wertheim lattice thermodynamic perturbation theory predictions. *J. Phys. Chem. B*, 110:5321–5329, 2006.

[52] J. Labuta et al. Probing the micro-phase separation of thermo-responsive amphiphilic polymer in water/ethanol solution. *J. Nanosci. Nanotech.*, 10:8408–8416, 2010.

[53] J. Spěváček, L. Hanyková, and M. Ilavský. Polymer-solvent interactions during phase transition in poly(vinyl methyl ether)/D_2O solutions as studied by NMR methods. *Macromol. Symp.*, 166:231–236, 2001.

[54] L. Hanyková and J. Spěváček. ^{1}H NMR study of thermotropic phase transition of linear and crosslinked poly(vinyl methyl ether) in D_2O. *Polymer*, 42:8607–8612, 2001.

[55] J. Spěváček and L. Hanyková. ^{1}H NMR relaxation study of polymer-solvent interactions during thermotropic phase transition in aqueous solutions. *Macromol. Symp.*, 203:229–238, 2003.

[56] J. Spěváček and L. Hanyková. ^{1}H NMR study on the hydration during temperature–induced phase separation in concentrated poly(vinyl methyl ether)/D_2O solutions. *Macromolecules*, 38:9187–9191, 2005.

[57] J. Spěváček and L. Hanyková. NMR study on polymer–solvent interactions during temperature–induced phase separation in aqueous polymer solutions. *Macromol. Symp.*, 251:72–80, 2007.

[58] J. Spěváček, L. Hanyková, and J. Labuta. Behavior of water during temperature-induced phase separation in poly(vinyl methyl ether) aqueous solutions. NMR and optical microscopy study. *Macromolecules*, 44:2149–2153, 2011.

[59] J. Spěváček. Ordered structures of stereoregular poly(methyl methacrylates). *Makromol. Chem. Macromol. Symp.*, 39:71–83, 1990.

[60] C. V. Rice. Phase-transition thermodynamics of *N*–isopropylacrylamide hydrogels. *Biomacromolecules*, 7:2923–2925, 2006.

[61] J. Spěváček. NMR investigations of temperature-induced phase transition in aqueous polymer solutions. *Macromol. Symp.*, 305:18–25, 2011.

[62] E. T. Tiktopulo et al. Cooperativity of the coil-globule transition in a homopolymer: Microcalorimetric study of poly(*N*–isopropylacrylamide). *Macromolecules*, 27:2879–2882, 1994.

[63] A. Housni and R. Narain. Aqueous solution behavior of poly(*N*–isopropylacrylamide) in the presence of water-soluble macromolecular species. *Eur. Polym. J.*, 43:4344–4354, 2007.

[64] C. Hofmann and M. Schonhoff. Dynamics and distribution of aromatic model drugs in the phase transition of thermoreversible poly(*N*–isopropylacrylamide) in solution. *Colloid Polym. Sci.*, 290:689–698, 2012.

[65] L. Starovoytova and J. Spěváček. Effect of time on the hydration and temperature-induced phase separation in aqueous polymer solutions. ^{1}H NMR study. *Polymer*, 47:7329–7334, 2006.

[66] R. Costa and R. Freitas. Phase behavior of poly(*N*–isopropylacrylamide) in binary aqueous solutions. *Polymer*, 43:5879–5885, 2002.

[67] Ikeda I. Maeda Y., Yamamoto H. Micro-Raman spectroscopic investigation on the phase separation of poly(vinyl methyl ether)/alcohol/water ternary mixtures. *Langmuir*, 20:7339–7341, 2004.

[68] C. Wu and S. Zhou. Internal motions of both poly(*N*–isopropylacrylamide) linear chains and spherical microgel particles in water. *Macromolecules*, 29:1574–1578, 1996.

[69] M. Shibayama, S. Mizutani, and S. Nomura. Thermal properties of copolymer gels containing *N*–isopropylacrylamide. *Macromolecules*, 29:2019–2024, 1996.

[70] E. C. Muniz and G. Geuskens. Compressive elastic modulus of polyacrylamide hydrogels and semi-IPNs with poly(*N*–isopropylacrylamide). *Macromolecules*, 34:4480–4484, 2001.

[71] H. Ohta et al. C-13 PST/MAS NMR-study of poly(*N*–isopropylacrylamide) in solution and in the gel phase. *J. Mol. Struct.*, 245:391–397, 1991.

[72] M. Andersson and S. L. Maunu. Volume phase transition and structure of poly(*N*–isopropylacrylamide) microgels studied with ^{1}H NMR spectroscopy in D_2O. *Colloid Polym. Sci.*, 285:293–303, 2006.

[73] K. E. Uhrich. Polymeric systems for controlled drug release. *Chem. Rev.*, 99:3181–3198, 1999.

[74] C. Park and I. Orozco-Avila. Concentrating cellulases from fermented broth using a temperature-sensitive hydrogel. *Biotechnol. Prog.*, 8:521–526, 1992.

[75] K. Kajiwara and S. B. Ross-Murphy. Synthetic gels on the move. *Nature*, 355:208–209, 1992.

[76] H. A. von Recum. Growth factors and matrix molecules preserve cell function on thermally responsive culture surfaces. *Tissue Eng.*, 5:251–265, 1999.

[77] T. Miyata, N. Asami, and T. Uragami. A reversibly antigenresponsive hydrogel. *Nature*, 399:766–769, 1999.

[78] L. K. Kostanski et al. Biocompatible poly(*N*–vinyllactam)-based materials with environmentally-responsive permeability. *J. Biomater. Sci. Polym. Edn.*, 19:275–290, 2008.

[79] S. Q. Zhou and B. Chu. Synthesis and volume phase transition of poly(methacrylic acid–co–*N*–isopropylacrylamide) microgel particles in water. *J. Phys. Chem. B*, 102:1364–1371, 1998.

[80] M. K. Krusic and J. Filipovic. Copolymer hydrogels based on *N*–isopropylacrylamide and itaconic acid. *Polymer*, 47:148–155, 2006.

[81] L. H. Sperling. Interpenetrating polymer networks: an overview. *Adv. Chem. Ser.*, 239:3–38, 1994.

[82] J. W. Aylsworth. U.s. patent 1,111,284. Technical report, U. S. Patent Office, 1914.

[83] S. J. Kim et al. Swelling kinetics of modified poly(vinyl alcohol) hydrogels. *J. Appl. Polym. Sci.*, 90:3310–3313, 2003.

[84] S. J. Kim et al. Electroactive characteristics of interpenetrating polymer network hydrogels composed of poly(vinyl alcohol) and poly(*N*isopropylacrylamide). *J. Appl. Polym. Sci.*, 89:890–894, 2003.

[85] S. J. Kim et al. Thermal characteristics of interpenetrating polymer networks composed of poly(vinyl alcohol) and poly(*N*–isopropylacrylamide). *J. Appl. Polym. Sci.*, 90:881–885, 2003.

[86] A. Szilágyi and M. Zrínyi. Temperature induced phase transition of interpenetrating polymer networks composed of poly(vinyl alcohol) and copolymers of *N*–isopropylacrylamide with acrylamide or 2-acrylamido-2-methylpropyl-sulfonic acid. *Polymer*, 46:10011–10116, 2005.

[87] Y. H. Lim, D. Kim, and D. S. Lee. Drug releasing characteristics of thermo- and ph-sensitive interpenetrating polymer networks based on poly(*N*–isopropylacrylamide). *J. Applied Pol. Sci.*, 64:2647–2655, 1997.

[88] X. Z. Zhang, D. Q. Wu, and C.C. Chu. Synthesis, characterization and controlled drug release of thermosensitive IPN-PNIPAAM hydrogels. *Biomaterials*, 25:3793–3805, 2004.

[89] J. Šťastná et al. Temperature-induced phase transition in hydrogels of interpenetrating networks poly(*N*–isopropylmethacrylamide)/poly(*N*–isopropylacrylamide). *Colloid Polym Sci*, 291:2409–2417, 2013.

[90] A. Gutowska, Y. H. Bae, and H. Jacobs. Thermosensitive interpenetrating polymer networks: Synthesis, characterization, and macromolecular release. *Macromolecules*, 27:4167–4175, 1994.

[91] B. C. Shin, M. S. Jhon, H. B. Lee, and S. H. Yuk. Temperature induced phase transition of semi-interpenetration polymer networks composed of poly(*N*–isopropylacrylamide) and hydrophilic polymers. *Eur. Polym. J.*, 34:1675–1681, 1998.

[92] J. Djonlagic and Z. Petrovich. Semi-interpenetrating polymer networks composed of poly(*N*–isopropylacrylamide) and polyacrylamide hydrogels. *J. Polym. Sci., Part B: Polym. Phys.*, 42:3987–3999, 2004.

[93] T. Baltes, F. Garret-Flaudy, and R. Freitagh. Investigation of the lcst of polyacrylamides as a function of molecular parameters and the solvent composition. *Polym. Chem.*, 37:2977–2989, 1999.

[94] I. Idziak et al. Thermosensitivity of aqueous solutions of poly(*N,N*–diethylacrylamide). *Macromolecules*, 32:1260–1263, 1999.

[95] H. Y. Liu and X. X. Zhu. Lower critical solution temperatures of *N*–substituted acrylamide copolymers in aqueous solutions. *Polymer*, 40:6985–6990, 1999.

[96] K. Zhou et al. The coil-to-globule-to-coil transition of linear polymer chains in dilute aqueous solutions: Effect of intrachain hydrogen bonding. *Macromolecules*, 41:8927–8931, 2008.

[97] Y. Lu, X. Ye, K. Zhou, and W. J. Shi. A comparative study of urea-induced aggregation of collapsed poly(*N*–isopropylacrylamide) and poly(*N,N*–diethylacrylamide) chains in aqueous solutions. *J. Phys. Chem. B*, 117:7481–7488, 2013.

[98] M. Panayiotou et al. Synthesis and characterisation of thermo-responsive poly(*N,N*–diethylacrylamide) microgels. *React. Funct. Polym.*, 67:807–819, 2007.

[99] M. Panayiotou and R. Freitag. Synthesis and characterisation of stimuli-responsive poly(*N,N*–diethylacrylamide) hydrogels. *Polymer*, 46:615–621, 2005.

[100] Y. Maeda and M. Yamabe. A unique phase behavior of random copolymer of *N*–isopropylacrylamide and *N,N*–diethylacrylamide in water. *Polymer*, 50:519–523, 2009.

[101] J. I. Ngadaonye, L. M. Geever, M. O. Cloonan, and Higginbotham C. L. Photopolymerised thermo-responsive poly(*N,N*–diethylacrylamide)-based copolymer hydrogels for potential drug delivery applications. *J. Polym. Res.*, 19:9822, 2012.

[102] M. Keerl, V. Smirnovas, R. Winter, and W. Richtering. Interplay between hydrogen bonding and macromolecular architecture leading to unusual phase behavior in thermosensitive microgels. *Angew. Chem. Int. Ed.*, 47:338–341, 2008.

[103] N. Zhang et al. Preparation, properties, and drug release of thermo- and pH-sensitive poly((2-dimethylamino)ethyl methacrylate)/poly(*N,N*–diethylacrylamide) semi-IPN hydrogels. *J. Mater. Sci.*, 46:1523–1534, 2011.

[104] Y. Maeda, T. Nakamura, and I. Ikeda. Hydration and phase behavior of poly(*N*–vinylcaprolactam) and poly(*N*–vinylpyrrolidone) in water. *Macromolecules*, 35:217–222, 2002.

[105] J. Spěváček et al. Temperature-induced phase separation and hydration in poly(*N*–vinylcaprolactam) aqueous solutions: a study by nmr and ir spectroscopy, saxs, and quantum-chemical calculations. *Soft Matter*, 8:6110–6119, 2012.

[106] J. Spěváček and J. Dybal. Temperature-induced phase separation and hydration in aqueous polymer solutions studied by NMR and IR spectroscopy: comparison of poly(*N*–vinylcaprolactam) and acrylamide-based polymers. *Macromol. Symp.*, 336:39–46, 2014.

[107] S. Sun and P. Wu. Infrared spectroscopic insight into hydration behavior of poly(*N*–vinylcaprolactam) in water. *J Phys Chem B*, 115:11609–11618, 2011.

[108] E. E. Makhaeva, L.T. M. Thanh, S. G. Starodoubtsev, and A. R. Khokhlov. Thermoshrinking behavior of poly(vinylcaprolactam) gels. *Macromol. Chem. Phys.*, 197:1973–1982, 1996.

[109] L. M. Mikheeva et al. Microcalorimetric study of thermal cooperative transitions in poly(*N*–vinylcaprolactam) hydrogels. *Macromolecules*, 30:2693–2699, 1997.

[110] H. G. Schild and D. A. Tirrell. Microcalorimetric detection of lower critical solution temperatures in aqueous polymer solutions. *J. Phys. Chem.*, 94:4352–4356, 1990.

[111] L. Starovoytova, J. Spěváček, and M. Ilavský. ^{1}H NMR study of temperature-induced phase transitions in D_2O solutions of poly(*N*–isopropylmethacrylamide)/poly(*N*–isopropylacrylamide) mixtures and random copolymers. *Polymer*, 46:677–683, 2005.

[112] H. Kouřilová er al. ^{1}H NMR study of temperature-induced phase separation in solutions of poly(*N*–isopropylmethacrylamide-co-acrylamide) copolymers. *Eur. Polym. J.*, 46:1299–1306, 2010.

[113] J. Šťastná, L. Hanyková, and J. Spěváček. NMR and DSC study of temperature-induced phase transition in aqueous solutions of poly(*N*–isopropylmethacrylamide-co-acrylamide) copolymers. *Colloid Polym. Sci.*, 290:1811–1817, 2012.

[114] A. Laukkanen, L. Valtola, F.M. Winnik, and H. Tenhu. Formation of colloidally stable phase separated poly(*N*–vinylcaprolactam) in water: a study by dynamic light scattering, microcalorimetry, and pressure perturbation calorimetry. *Macromolecules*, 37:2268–2274, 2004.

[115] L. Hanyková, J. Labuta, and J. Spěváček. NMR study of temperature-induced phase separation and polymer–solvent interactions in poly(vinyl methyl ether)/D_2O/ethanol solutions. *Polymer*, 47:6107–6116, 2006.

[116] E. Díez-Peña et al. NMR studies of the structure and dynamics of polymers gels based on *N*–isopropylacrylamide (*N*–iPAAm) and methacrylic acid (MAA). *Macromol. Chem. Physh.*, 203:491–502, 2002.

[117] N. Wang, G. Ru, L. Wang, and J. Feng. ^{1}H MAS NMR studies of the phase separation of poly(*N*–isopropylacrylamide) gel in binary solvents. *Langmuir*, 25:5898–5902, 2009.

[118] CH. Hofmann et al. Cononsolvency revisited: solvent entrapment by *N*–isopropylacrylamide and *N,N*–diethylacrylamide microgels in different water/methanol mixtures. *Macromolecules*, 46:523–532, 2013.

[119] B. Sierra-Martin et al. Microscopic signature of a microgel volume phase transition. *Macromolecules*, 38:10782–10787, 205.

[120] P.A. Mirau. *A Practical Guide to Understanding the NMR of Polymers*. 1^{st} edition. Wiley-Interscience, New Jersey, 2004.

[121] L. H. Gan, C. Wensheng, and K. C. Tam. Studies of phase transition of aqueous solution of poly(*N,N*–diethylacrylamide-co-acrylic acid) by differential scanning calorimetry and spectrophotometry. *Eur. Polym. J.*, 37:1773–1778, 2001.

[122] J. Spěváček, D. Geschke, and M. Ilavský. ^{1}H NMR study of temperature collapse of linear and crosslinked poly(*N,N*–diethylacrylamide) in D_2O. *Polymer*, 42:463–468, 2001.

[123] H. Feil, Y. H. Bae, J. Feijen, and S. W. Kim. Effect of comonomer hydrophilicity and ionization on the lower critical solution temperature of *N*–isopropylacrylamide copolymers. *Macromolecules*, 26:2496–2500, 1993.

[124] E. Djokpé and W. Vogt. *N*–isopropylacrylamide and *N*–isopropylmethacrylamide: cloud points of mixtures and copolymers. *Macromol. Chem. Phys.*, 202:750–757, 2001.

[125] A. C. Wenceslau et al. Thermo- and pH-sensitive IPN hydrogels based on PNIPAAm and PVA-Ma networks with LCST tailored close to human body temperature. *Mat. Sci. and Eng. C*, 32:1259–1265, 2012.

List of Figures

List of Tables

List of publications

1. L. Hanyková, and M. Radecki. NMR and Thermodynamic Study of Phase Transition in Aqueous Solutions of Thermo-responsive Amphiphilic Polymer. *Chem. Lett.*, 41:1044–1046, 2012.

2. M. Radecki, and L. Hanyková. Spectroscopic Studies of Behaviour and Interactions in PVME/Water Mixtures. *WDS'12 Proceedings of Contributed Papers, Part III*, 40–45, 2012.

3. L. Hanyková, J. Spěváček, M. Radecki, A. Zhigunov, J. Šťastná, H. Valentová and Z. Sedláková. Structures and interactions in collapsed hydrogels of thermoresponsive interpenetrating polymer networks. *Colloid. Polym. Sci.*, 293:709–720, 2015.

4. M. Radecki, J. Spěváček, A. Zhigunov, Z. Sedláková and L. Hanyková. Temperature-induced phase transition in hydrogels of interpenetrating networks of poly(*N*–isopropylacrylamide) and polyacrylamide. *Eur. Polym. J.*, 68:68–79, 2015.

5. L. Starovoytova, J. Šťastná, A. Šturcová, R. Konefal, J. Dybal, N. Velychkivska, M. Radecki and L. Hanyková. Additive Effects on Phase Transition and Interactions in Poly(vinyl methyl ether) Solutions. *Polymers*, 7:2572–2583, 2015.

6. L. Hanyková, J. Spěváček, M. Radecki, A. Zhigunov, H. Kouřilová, Z. Sedláková. Phase transition in hydrogels of thermoresponsive semi-interpenetrating and interpenetrating networks of poly(*N,N*–diethylacrylamide) and polyacrylamide. *Eur. Polym. J.*, 85:1–13, 2016.

List of conference contributions

1. M. Radecki, L. Hanyková. Molecular dynamic behaviour in mixtures water/ethanol. NMR Valtice 2010, 25th Central European NMR Meeting, Valtice (talk).

2. M. Radecki, L. Hanyková. Molecular dynamic behaviour in mixtures water/ethanol. Week of Doctoral Students 2010, Prague (talk).

3. M. Radecki, L. Hanyková, M. S. Sánchez. NMR and DSC study on molecular interactions in water/ethanol mixtures. 18th European Symposium on Polymer Spectroscopy 2010, Zadar (poster).

4. M. Radecki, L. Hanyková. Spectroscopic Studies of Behaviour and Interactions in PVME/Water Mixtures. Week of Doctoral Students 2012, Prague (poster).

5. M. Radecki, L. Hanyková. Spectroscopic study of the phase separation in poly(vinyl methyl ether)/water mixtures. 19th European Symposium on Polymer Spectroscopy 2013, Prague (poster).

6. M. Radecki, L. Hanyková. Phase separation of PVME/Water Mixtures as studied by NMR and DSC. European Polymer Congres 2013, Pisa (poster).

7. M. Radecki, L. Hanyková, J. Šťastná, J. Spěváček. Temperature-induced phase transition in hydrogels of interpenetrating networks. MACRO 2014, Chiang Mai (poster).

8. M. Radecki, L. Hanyková, J. Šťastná, J. Spěváček. Temperature-sensitive interpenetrating networks based on PNIPAm and PAAm. European Polymer Federation Congress 2015, Dresden (talk).

9. M. Radecki, L. Hanyková, J. Šťastná, J. Spěváček. Hydrogels of Poly(*N,N*–Isopropylacrylamide)-Polyacrylamide Thermoresponsive Interepenetrating Networks. Euromar 2015, Prague (poster).

10. M. Radecki, L. Hanyková, J. Šťastná, J. Spěváček. Phase Trension in Poly(*N,N*–isopropylacrylamide) and Polyacrylamide Hydrogels. EMN Meeting On Hydrogel Materials 2016, Singapore (poster).